Quantification and characterization of entanglement and coherence

By

Chandan Datta

PHYS07201304002

Institute of Physics, Bhubaneswar

A thesis submitted to the

Board of Studies in Physical Sciences

In partial fulfillment of requirements

for the Degree of

DOCTOR OF PHILOSOPHY

of

HOMI BHABHA NATIONAL INSTITUTE

August, 2018

Homi Bhabha National Institute

Recommendations of the Viva Voce Committee

As members of the Viva Voce Committee, we certify that we have read the dissertation prepared by Mr *Chandan Datta* entitled "*Quantification and characterization of entanglement and coherence*", and recommend that it may be accepted as fulfilling the dissertation requirement for the Degree of Doctor of Philosophy.

Amjayannavar

Chairman - ***Prof. Arun M. Jayannavar*** Date: 12/11/2018

Guide *Convener* - ***Prof. Pankaj Agrawal*** Date: 12/11/2018

Co-guide (if any) Date: 12/11/2018

Prasanta K. Panigrahi

External Examiner - ***Prof. Prasanta K. Panigrahi*** Date: 12/11/2018

Ajit M. Srivastava

Member 1 - ***Prof. Ajit M. Srivastava*** Date: 12/11/2018

Member 2 - ***Prof. Suresh K. Patra*** Date: 12/11/2018

Final approval and acceptance of this thesis is contingent upon the candidate's submission of the final copies of the dissertation to HBNI.

I hereby certify that I have read this thesis prepared under my/our direction and recommend that it may be accepted as fulfilling the thesis requirement.

Date: 19-11-18

Place: Bhubaneswar

Guide

STATEMENT BY AUTHOR

This dissertation has been submitted in partial fulfillment of requirements for an advanced degree at Homi Bhabha National Institute (HBNI) and is deposited in the Library to be made available to borrowers under rules of the HBNI.

Brief quotations from this dissertation are allowable without special permission, provided that accurate acknowledgement of source is made. Requests for permission for extended quotation from or reproduction of this manuscript in whole or in part may be granted by the Competent Authority of HBNI when in his or her judgment the proposed use of the material is in the interests of scholarship. In all other instances, however, permission must be obtained from the author.

(Chandan Datta)

DECLARATION

I, hereby declare that the investigations presented in the thesis have been carried out by me. The work is original and has not been submitted earlier as a whole or in part for a degree/diploma at this or any other Institution/University.

(Chandan Datta)

List of Publications arising from the thesis

Journal

Published

1. "Measuring higher-dimensional Entanglement", **Chandan Datta**, Pankaj Agrawal and Sujit K. Choudhary, Physical Review A, **2017**, 95, 042323-1 – 042323-7.

2. "A few finite trigonometric sums", **Chandan Datta** and Pankaj Agrawal, Mathematics, **2017**, 5, 13-1 – 13-11.

3. "Distinguishing different classes of entanglement of three-qubit pure states", **Chandan Datta**, Satyabrata Adhikari, Arpan Das and Pankaj Agrawal, The European Physical Journal D, **2018**, 72, 157-1 – 157-7.

4. "Coherence of quantum channels", **Chandan Datta**, Sk. Sazim, Arun K. Pati and Pankaj Agrawal, Annals of Physics, **2018**, 397, 243-258.

Communicated

1. "Authentication protocol based on polygamous nature of quantum steering" by Debasis Mondal, **Chandan Datta**, Jaskaran Singh and Dagomir Kaszlikowski [Communicated to Physical Review Letters]†.

In preparation

1. "Optimal Bell-CHSH value and two-qubit state" by **Chandan Datta**, Arpan Das, Sumit Nandi and Pankaj Agrawal [In preparation].

Conferences

1. **Poster:** Bell-type Inequalities can act as a measure of Entanglement (Based on the paper Measuring higher-dimensional Entanglement), Young Quantum-2015, February 24-26, 2015, HRI, Allahabad, India.

2. **Talk:** Distinguishing different classes of entanglement of three-qubit pure states, Young Quantum-2017, February 27 - March 1, 2017, HRI, Allahabad, India.

3. **Talk:** Measuring higher-dimensional entanglement, Advanced School and Workshop on Quantum Science and Quantum Technologies, September 4-15, 2017, ICTP, Trieste, Italy.

4. **Poster:** Authentication protocol based on polygamous nature of quantum steering, Quantum Frontiers and Fundamentals, April 30-May 4, 2018, RRI, Bengaluru, India.

5. **Poster:** Authentication protocol based on polygamous nature of quantum steering, Multipartite Entanglement, May 20-26, 2018, Centro de ciencias de benasque pedro pascual, Benasque, Spain.

(Chandan Datta)

† A part of the paper will contribute to the thesis

Dedicated To My Beloved Parents & Wife

Acknowledgments

This thesis would not have been possible without the support of a lot of people who directly and indirectly helped me during my past five years at the Institute of Physics, Bhubaneswar. Now this is the perfect opportunity for me to express my gratitude and appreciation to them.

Let me begin by expressing my sincerest gratitude to my supervisor Prof. Pankaj Agrawal for his enormous support and guidance during my Ph.D years. He helped me a lot to enhance my understanding about the subject. I would like to acknowledge all my collaborators – Prof. Arun K. Pati, Prof. Dagomir Kaszlikowski, Dr. Satyabrata Adhikari, Dr. Sujit K. Choudhary, Dr. Sk. Sazim, Dr. Debasis Mondal, Arpan Das, Sumit Nandi, Debarshi Das, Dr. C. Jebaratnam, Jaskaran Singh and Shubhayan Sarkar. It is my great pleasure to work with them. I am thankful to my Ph.D committee members Prof. Arun M. Jayannavar, Prof. Ajit M. Srivastava and Prof. Suresh K. Patra for their valuable comments and suggestions during my Ph.D years. I would like to thank all the faculties of IOP for the valuable courses during my pre-doctoral course work. I express my thanks to all the academic and non-academic staff members for their help during my stay at IOP.

I am grateful to all my IOP mates for their wonderful company for the last five years. Without your company it would not be the same. I will cherish those beautiful memories for the rest of my life. I would like to thank my childhood friends Ujjwal Nandi, Ashis Kundu and Animesh Dutta.

I am extremely obliged to my beloved parents for their unconditional love, support and inspiration from my childhood. I would like to express my special thanks to my dear wife Rubina Datta for her love, companionship, trust and encouragement. She is standing right beside me throughout every ups and downs in my career. I dedicate this thesis to my parents and wife. I am also thankful to my in-laws, especially my parents-in-law for their love and support. Without their constant encouragement, this long journey would not have been possible.

Contents

Synopsis

In 1935 Einstein, Podolsky and Rosen [1] described a spooky feature of quantum mechanics in their famous EPR paper. Later Schrödinger [2] coined the name for this feature as entanglement. This feature restricts a global state of a composite system from being written as a product of the states of individual subsystems. In quantum mechanics entanglement is one of the key features which differentiates between quantum and classical world. Moreover, it has been found to be a very useful resource for many information processing tasks, such as teleportation, remote state preparation, quantum cryptography, superdense coding [19] etc. There also exist an extensive amount of literature on entanglement from the foundational perspective of quantum mechanics. Therefore, the quantification and characterization of entanglement is one of the interesting problems in quantum information theory. Quantification and characterization of entanglement is unambiguous for pure bipartite state, but not for the mixed states. Entanglement of any pure bipartite state is uniquely captured by the entropy of entanglement in the asymptotic limit [5]. But this is not true for mixed states. There is no unique quantification of entanglement for this case and a number of entanglement measures and monotones [19] have been constructed over the years. Situation gets worse for multipartite scenario, both for pure and mixed states. Even for pure multipartite states there is no unique quantification of entanglement. There exist infinitely many inequivalent entanglement classes. Therefore, the study on characterization and quantification of entanglement is of great importance.

Quantum coherence is also a fundamental concept in quantum mechanics. It is just the linear superposition of quantum states. Unlike entanglement, coherence can be defined for a single system. Interestingly in a multi-party system coherence is the indispensable part and is the essence of entanglement. Recent developments in the field of quantum information and computation suggest that coherence can be a very useful resource for quantum computing, quantum algorithm, quantum metrology, quantum thermodynamics [111]etc. Coherence also plays a very crucial role in the field of quantum biology [37]. Therefore, the study of quantum coherence is of immense importance. Recently, there has been a lot of research to understand the coherence from the resource theory perspective. Resource theory tells us what can be achieved from a system by using some allowed operations which can not create coherence. However, the concept of such allowed operations or incoherent operations is not unique. There exist many classes of incoherent operations in the literature. Therefore, a study of such incoherent operations will be very useful for the resource theory of coherence. Moreover, coherence like every other resource is very fragile to the effect of the environment. Therefore, it is important to characterize coherence in the presence of environment.

This thesis is mostly focused on the characterization and quantification of two main resources in quantum information processing – quantum entanglement and quantum coherence.

In 1964, Bell established that any realistic interpretation of quantum theory is bound to be nonlocal [7]. He established this by means of an inequality which is violated by the singlet state of a pair of qubits. Later it was shown that any entangled pure two-qubit state will violate this inequality [8]. From here we can draw two conclusions – that entanglement is the main ingredient for the nonlocal phenomena in quantum mechanics and Bell inequality can serve as one of the potential way to detect entanglement. However, the situation gets worse for mix states. As there exist mixed entangled states which do not violate this inequality. Therefore, violation of Bell inequality is sufficient criteria to detect entanglement but not a necessary one. The Bell violation of entangled two-qubit pure states only depends on the entanglement. But for a mixed state only entanglement and purity are not enough to characterize Bell violation. As a mixed state contains many other parameters. So a state with large entanglement and purity can have smaller optimal Bell value. Recently Mendonça et. al. [9] showed that the whole entanglement and purity region of two-qubit states can be covered by two-qubit X-states. Hence, to explore the Bell inequality violation for mixed states, we can consider the two-qubit X-states. We have showed that optimal Bell value increases monotonically with the increment of entanglement and purity. Moreover, we explicitly show that optimal Bell value changes monotonically with respect to other parameters even when the entanglement and the purity of the states remain fixed. From this we may conclude that these parameters reflects some nonlocal classical or quantum properties of the state.

Apart from qubits, entanglement in higher dimensional systems is important from both fundamental and practical point of view. Higher dimensional entanglement provides important advantages in quantum communication than the conventional qubit entanglement. It provides much better security against eavesdropping in cryptography [18]; it can be used to increase the channel-capacity via superdense-coding [11] and is more robust against environmental noise [12] than the conventional two-qubit entanglement. However, for practical applications of these protocols, experimental preparation, detection and quantification of higher dimensional entangled state is of crucial importance. The violation of Bell-type inequalities can detect the presence of entanglement in such systems. Hence, we study local-realistic inequalities, Bell-type inequalities, for bipartite pure states of finite dimensional quantum systems – qudits. There are a number of proposed Bell-type inequalities for such systems. Our interest is in relating the value of Bell-type inequality function with a measure of entanglement. Interestingly, we find that one of these inequalities, the Son-Lee-Kim (SLK) inequality [13], can be used to measure entanglement of a pure bipartite qudit state and a class of mixed two-qudit states. Unlike the majority of earlier schemes in this direction, where number of observables needed to measure the entanglement increases with the dimension of the subsystems [14], this method needs only four observables. We also discuss the experimental feasibility of this scheme. It turns out that current experimental set ups can be used to measure the entanglement using our scheme.

We have derived two finite trigonometric sums which are required to get a relation between Bell-SLK function and entanglement. To the best of our knowledge, these two sums do not exist in any mathematics handbook or literature. Later we computed many more trigonometric sums like these; it is an active research area in mathematics. These sums may contain various powers of one or more trigonometric functions. Sums with one trigonometric function are known, however sums with products of trigonometric functions can get complicated and may not have a simple expressions in a number of cases. We obtain a number of such sums using method of residues.

The characterization of entanglement in multipartite scenario is far complex than the bipartite case. We can not even define a unique maximally-entangled multipartite state and there exist many inequivalent forms of entanglement. From the resource theory point of view of entanglement, two entangled states are said to be equivalent if they can be obtained from each other with certainty with respect to LOCC (local operation and classical communication) [15]. For a single copy, two states are LOCC equivalent if and only if they are related by LU (local unitary) [16]. But in the single copy restriction, even two bipartite pure states are not typically related by LU. To evade this difficulty, the LOCC operation, through which the conversion of entangled states is considered is slightly loosened. One now considers the conversion of states through stochastic local operation and classical communication (SLOCC), i.e. two entangled states are converted to each other by means of LOCC but with a non-vanishing probability of success [16]. For three-qubit pure states, there exist a total of six SLOCC inequivalent classes: separable, three biseparable and two genuinely entangled (GHZ and W). In general it is very difficult to characterize and distinguish different classes from each other. Employing the Pauli matrices, we have constructed a set of operators, which can be used to distinguish six inequivalent classes of entanglement under SLOCC for three-qubit pure states [54]. These operators have very simple structure and can be implemented in an experiment to distinguish the types of entanglement present in a state. We show that the measurement of only one operator is sufficient to distinguish GHZ class from rest of the classes. It is also shown that it is possible to detect and classify other classes by performing a small number of measurements. We also show how to construct such observables in any basis. Furthermore, we consider a few mixed states to investigate the usefulness of our operators. Furthermore, we consider the teleportation scheme of Lee et. al. [18] and show that the partial tangles and hence teleportation fidelity can be measured. We have also shown that these partial tangles can also be used to classify genuinely entangled state, biseparable state and separable state.

Like quantum entanglement, as discussed above, coherence is also a very fundamental concept. The quantum coherence like other quantum resources is also fragile in the presence of noisy environment. The interaction of quantum systems with environment have been extensively studied using different models, in particular using noisy channels. Characterizing all these channels and their effect on various physical resources are vital. These channels are also important to construct resource theoretic aspect of coherence. Therefore, it would be really interesting to characterize the channels using the notion of coherence. We define the coherence of quantum channels using the Choi-Jamiołlkowski (C-J) isomorphism [19]. C-J isomorphism also known as channel state duality is the corresponds between a quantum channel and a quantum state. It says that for every quantum channel, there exists a unique quantum state. The relation between the coherence and the purity of the channel respects a duality relation. It characterizes the allowed values of coherence when the channel has certain purity. This duality has been depicted via the Coherence-Purity diagrams. In particular, we study the quantum coherence of the unital and non-unital qubit channels and find out the allowed region of coherence for a fixed purity. We also study coherence of different incoherent channels, namely, incoherent operation (IO), strictly incoherent operation (SIO), physical incoherent operation (PIO) etc. Interestingly, we find that the allowed region for different incoherent operations maintains the relation $PIO \subset SIO \subset IO$. Interestingly, different kinds of qubit channels can be distinguished using the Coherence-Purity diagram. We also prove a complementarity relation between the relative entropy of coherence [111] and the Holevo quantity [61] of the quantum channel. This suggests that the coherence and the Holevo quantity of the channels cannot be arbitrarily large at the same time.

To summarize, a two-qubit mixed state contains many parameters. We have shown that optimal Bell value not only depends on the purity and entanglement but also on other parameters. We have provided a scheme to measure higher dimensional entanglement. We have constructed some observable which can be useful to distinguish different classes of entanglement presents in a three qubit pure state. Using C-J isomorphism we have defined the coherence of the channels. Coherence-purity diagram can be useful to distinguish two different qubit channels.

Bibliography

[1] A. Einstein, B. Podolsky, and N. Rosen, *Phys. Rev.* **47**, 777 (1935).

[2] E. Schrödinger, in *Mathematical Proceedings of the Cambridge Philosophical Society*, Vol. **31** (Cambridge University Press, 1935) pp. 555–563.

[3] R. Horodecki, P. Horodecki, M. Horodecki, and K. Horodecki, Rev. Mod. Phys. **81**, 865 (2009).

[4] C. H. Bennett, H. J. Bernstein, S. Popescu, and B. Schumacher, *Phys. Rev. A* **53**, 2046 (1996).

[5] A. Streltsov, G. Adesso, and M. B. Plenio, Rev. Mod. Phys. **89**, 041003 (2017).

[6] M. B. Plenio, and S. F. Huelga, *New J. Phys.* **10**, 113019 (2008); F. Levi, and F. Mintert, *New J. Phys.* **16**, 033007 (2014).

[7] J. S. Bell, *Physics* **1**, 195 (1964); J. S. Bell, *Rev. Mod. Phys.* **38**, 447 (1966).

[8] J. F. Clauser, M. A. Horne, A. Shimony, and R. A. Holt, *Phys. Rev. Lett.* **23**, 880 (1969).

[9] P. E. M. F. Mendonça, M. A. Marchiolli, and D. Galetti, *Ann. Phys* **351**, 79 (2014).

[10] H. Bechmann-Pasquinucci, and A. Peres *Phys. Rev. Lett.* **85**, 3313 (2000); D. Bruß, and C. Macchiavello, *Phys. Rev. Lett.* **88**, 127901 (2002).

[11] C. Wang, F.-G. Deng, Y.-S. Li, X.-S. Liu, and G. L. Long, *Phys. Rev. A* **71**, 044305 (2005).

[12] M. L. Almeida, S. Pironio, J. Barrett, G. Toth, and A. Acin, *Phys. Rev. Lett.* **99**, 040403 (2007); L. Sheridan, and V. Scarani *Phys. Rev. A* **82**, 030301 (2010).

[13] W. Son, J. Lee, and M. S. Kim, *Phys. Rev. Lett.* **96**, 060406 (2006); S.-W. Lee, J. Ryu, and J. Lee, *Journal of the Korean Physical Society*, Vol.**48** No. 6, 1307 (2006).

[14] J. T. Barreiro et al. *Nat. Phys.* **9**, 559 (2013); F. Mintert, M. Kuś, and A. Buchleitner *Phys. Rev. Lett* **95**, 260502 (2005); D. Giovannini, J. Romero, J. Leach, A. Dudley, A. Forbes, and M. J. Padgett *Phys. Rev. Lett* **110**, 143601 (2013).

[15] V. Vedral and M. B. Plenio, *Phys. Rev. A* **57**, 1619 (1998).

[16] C. H. Bennett, S. Popescu, D. Rohrlich, J. A. Smolin, and A. V. Thapliyal, *arXiv:* quant-ph/9908073.

[17] W. Dür, G. Vidal, and J. I. Cirac, *Phys. Rev. A* **62**, 062314 (2000).

[18] S. Lee, J. Joo, and J. Kim, *Phys. Rev. A* **72**, 024302 (2005).

[19] A. S. Holevo, *Russ. Math. Surv.* **53**, 1295 (1998); M. B. Ruskai, S. Szarek, and E. Werner, *Linear Algebra Appl.* **347**, 159 (2002).

[20] M. A. Nielsen and I. L. Chuang, *Quantum Computation and Quantum Information* (Cambridge University Press, 2010).

List of Figures

List of Tables

Chapter 1

Introduction

Quantum entanglement is one of the most nonclassical manifestations of quantum mechanics. It was discovered after a few years of the birth of quantum mechanics. Since then it has been puzzling feature of quantum mechanics. In 1935, Einstein, Podolsky and Rosen illustrated a counter-intuitive prediction of quantum mechanics about composite systems in their famous thought experiment known as EPR paradox [1]. They showed that quantum mechanical description of the physical reality by the wave function is not complete. Surprised by this fact, Einstein called it a spooky feature of quantum mechanics. Later Schrödinger [2] used the term entanglement to describe this spooky feature of quantum mechanics. In the EPR paper, the authors invoked realism and assigned values to the physical quantities prior to the measurement. Later, in 1964 Bell [3] formalized the idea of the EPR paper in terms of local hidden variable model and showed that entanglement does not allow such possibility.

Apart from foundational importance of quantum entanglement, it has been considered as one of the most valuable resource in quantum information science. It plays a pivotal role in many interesting discoveries such as quantum cryptography [4], teleportation [5], superdense coding [6], quantum error correction codes [7, 8] etc. Recent developments in the field of quantum information science suggest that entanglement is a new quantum resource for those tasks which cannot be achieved by a classical resource. Therefore, quantification and characterization of quantum entanglement are the basic requirements in quantum information theory.

On the other side, quantum coherence is also at the heart of the quantum mechanics. Quantum coherence or the coherent superposition of states is one of the most fundamental features of quantum mechanics which differentiates quantum world from the classical world. Interestingly coherence is the main underlying notion of quantum interference and quantum entanglement. The early approach to quantify coherence came in 2006 by Åberg [9] who considered the superposition of orthogonal quantum states. After that an extensive amount of research have been carried out to quantify and characterize coherence [10]. Like entanglement, coherence is also a very crucial resource in quantum computing [11], quantum algorithm [12], quantum metrology [13], quantum thermodynamics [14] and even in quantum biology [15]. Therefore a study of characterization of quantum coherence is also very important in quantum information theory.

1.1 Entanglement

1.1.1 Bipartite Entanglement

In entanglement theory one of the most basic and important question is which states are entangled. We don't have a complete answer to that. However, we have the answer to this question up to some extent. As an example, any bipartite pure state $|\psi\rangle_{AB}$ in the Hilbert space $\mathcal{H} = \mathcal{H}_A \otimes \mathcal{H}_B$ is entangled iff it cannot be written as a product of the state of the two subsystems or mathematically

$$|\psi\rangle_{AB} \neq |\phi\rangle_A \otimes |\xi\rangle_B. \tag{1.1}$$

In general, $|\psi\rangle_{AB}$ can be written in a orthonormal product basis as follows

$$|\psi\rangle_{AB} = \sum_{i=1}^{d_A} \sum_{j=1}^{d_B} c_{ij} |a_i\rangle_A \otimes |b_j\rangle_B, \tag{1.2}$$

where d_A and d_B represents the dimension of the system A and B respectively, coefficients c_{ij} could be complex and are the elements of a matrix C. $|a_i\rangle_A$ and $|b_j\rangle_B$ correspond to the basises of the systems A and B respectively. The state $|\psi\rangle_{AB}$ will be product if the rank of the matrix C is 1. Singular value decomposition theorem assures that one can always diagonalize the matrix C by applying proper local unitary transformation. Hence, we can write

$$|\psi\rangle_{AB} = \sum_{i=1}^{r} c_i |e_i\rangle_A \otimes |f_i\rangle_B, \tag{1.3}$$

where $r = \min[d_A, d_B]$, c_i's are strictly positive and are known as Schmidt coefficients [16]. $|e_i\rangle_A$ and $|f_i\rangle_B$ are the Schmidt basis of the systems A and B respectively. The Schmidt rank r is equal to either of the ranks of the reduced density matrices $\rho_A = \mathrm{Tr}_B[|\psi\rangle_{AB}\langle\psi|]$, $\rho_B = \mathrm{Tr}_A[|\psi\rangle_{AB}\langle\psi|]$. The state $|\psi\rangle_{AB}$ will be entangled if $r > 1$, otherwise it is a product state. Thus, in a pure bipartite state, the rank of the reduced density matrices can tell us whether the state is entangled.

But in a real life experiment, we cannot avoid the noise and as a result, we deal with a mixed state rather than a pure state. A bipartite mixed state ρ_{AB} in Hilbert space $\mathcal{H} = \mathcal{H}_A \otimes \mathcal{H}_B$ is entangled if it cannot be written as

$$\rho_{AB} = \sum_i p_i \rho_i^A \otimes \rho_i^B, \tag{1.4}$$

where $p_i \geqslant 0$ and $\sum_i p_i = 1$. For a finite dimensional Hilbert space one can choose ρ_i^A and ρ_i^B to be pure. In general, it is a very difficult problem to decide whether a state ρ_{AB} is entangled or not. There exist many approaches to detect entanglement in literature [17]. In the subsection below, we will provide a very brief description about some of them.

1.1.1.1 Separability criteria

A. Positive partial transpose Positive partial transpose criteria (PPT) also known as Peres-Horodecki criteria [18, 19], is sufficient to detect entanglement. Any general state ρ_{AB} can be written as

$$\rho_{AB} = \sum_{i,j,k,l} p_{ijkl} |i\rangle\langle j| \otimes |k\rangle\langle l|. \tag{1.5}$$

Its partial transpose with respect to the subsystem B is

$$\rho_{AB}^{T_B} = \sum_{i,j,k,l} p_{ijkl} |i\rangle\langle j| \otimes (|k\rangle\langle l|)^T = \sum_{i,j,k,l} p_{ijkl} |i\rangle\langle j| \otimes |l\rangle\langle k|, \tag{1.6}$$

where T represents the transpose operation. If the matrix $\rho_{AB}^{T_B}$ is not positive then the state ρ_{AB} is entangled. For a $2 \otimes 2$ or $2 \otimes 3$ system, Horodecki et. al. [19] have shown that it is a necessary and sufficient criteria to detect entanglement. However, if the dimension of the composite system is more than six, then the positivity of $\rho_{AB}^{T_B}$ does not guarantee that the state is separable. As there exist some PPT states which are entangled [20, 21].

B. Positive but not completely positive maps A positive linear map Λ^p on a given Hilbert space $\mathcal{H}$ takes a positive operator to another positive operator and can be mathematically represented as

$$\Lambda^p : \mathcal{O}(\mathcal{H}) \to \mathcal{O}(\mathcal{H}), \Lambda^p(\rho) = \rho' \geqslant 0, \quad \text{for all} \quad \rho \geqslant 0. \tag{1.7}$$

But if the system ρ is statistically correlated to another system and we are applying positive map Λ^p on ρ then we must consider the action of the map $\mathbb{I}_n \otimes \Lambda^p$ on the composite system. Here $\mathbb{I}_n$ represents the nth dimensional identity operator. The action of the map $\mathbb{I}_n \otimes \Lambda^p$ is positive for all values of n if Λ^p is completely positive. Complete positivity is required for entangled bipartite states. If the system is separable then positive maps are enough. From here we can provide a necessary and sufficient condition of separability which state that a state ρ_{AB} is separable if $(\mathbb{I} \otimes \Lambda^p)\rho_{AB} \geqslant 0$ for all positive map Λ^p [19]. In the PPT criteria transpose map is positive map but not a completely positive map. Hence, positive maps are useful to detect entanglement.

C. Reduction criteria A reduction map Λ^r can be represented as

$$\Lambda^r(\rho) = \mathbb{I}(\text{Tr}\rho) - \rho. \tag{1.8}$$

It can be easily verified that reduction map is positive but not completely positive [17]. The reduction criteria for separability [22, 23] is a necessary condition and states that a state ρ_{AB} is separable if $(\mathbb{I}_A \otimes \Lambda_B^r)\rho_{AB} \geqslant 0$, i.e. following condition will be satisfied

$$\rho_A \otimes \mathbb{I}_B - \rho_{AB} \geqslant 0, \tag{1.9}$$

where ρ_A is the reduced density matrix of ρ_{AB}. The reduction criteria is weaker than the PPT criteria as reduction map is decomposable [23]. However, this map plays an important role in entanglement distillation [23].

D. Extended reduction criteria This criteria is a modification of the reduction criteria on the even dimensional Hilbert space. There exist antisymmetric unitary operations, $U^T = -U$, such that the corresponding antiunitary map $U(\cdot)^T U^\dagger$ maps any pure state to another state which is orthogonal to the previous one [24, 25]. Hence, the action of this map on ρ can be expressed as

$$\Lambda^{er}(\rho) = \Lambda^r(\rho) - U(\rho)^T U^\dagger. \tag{1.10}$$

This map is positive but not completely positive [24]. Separability criteria using this map can be stated as $(\mathbb{I} \otimes \Lambda_B^{er}) \geqslant 0$ if the state ρ_{AB} is separable. As it is a nondecomposable map, it can detect a very weak entangled state, so called PPT entangled state [26].

E. Range criteria Range criteria state that if a state ρ_{AB} is separable, then there exists a set of product vectors $\{|\phi_i^A\rangle \otimes |\psi_i^B\rangle\}$, which spans the range of ρ_{AB} and the set $\{|\phi_i^A\rangle \otimes |\psi_i^B\rangle^*\}$ spans the range of $\rho_{AB}^{T_B}$ [20]. Here the complex conjugation '$*$' is taken in the same basis in which the partial transpose operation has been performed. This criteria is useful to detect some of the PPT entangled states or bound entangled states [20]. Unextendible product basis (UPB) is an interesting example of range criteria to find PPT entangled states [27, 28]. A set $\mathcal{S}_{UPB}$ of orthonormal product vectors in $\mathcal{H} = \mathcal{H}_A \otimes \mathcal{H}_B$ form UPB if there exists no product vector which is orthogonal to all of them. Consider a subspace $\mathcal{V}_{UPB}$, which is spanned by the vectors in $\mathcal{S}_{UPB}$. As there are no orthogonal product vectors in $\mathcal{V}_{UPB}$, therefore, any vector in $\mathcal{V}_{UPB}^\perp$ is entangled. As a result, using range criteria, we can assert that any mixed state with a support in $\mathcal{V}_{UPB}^\perp$ is entangled. Therefore, the idea of UPB gives a procedure to construct PPT entangled states.

F. Matrix realignment criteria Matrix realignment criteria or computable cross norm criteria is another strong criteria which is based on a linear contraction on product states [29–31]. It has been shown useful in detecting some PPT entangled states [29, 30]. The matrix realignment map $\mathcal{R}$ on a state ρ_{AB} can be defined as $\langle m|\langle\mu|\mathcal{R}(\varrho_{AB})|n\rangle|\nu\rangle \equiv \langle m|\langle n|\varrho_{AB}|\nu\rangle|\mu\rangle$, where $\langle m|\langle\mu|\mathcal{R}(\varrho_{AB})|n\rangle|\nu\rangle$ represents the elements of the matrix $\mathcal{R}(\rho_{AB})$. If a state ρ_{AB} is separable then $\|\mathcal{R}(\rho_{AB})\|_1 \leqslant 1$, where $\|\cdot\|_1$ represents the trace norm and is defined as $\|X\|_1 = \mathrm{Tr}\sqrt{XX^\dagger}$. Matrix realignment criteria is a special case of linear contraction criteria. Linear contraction criteria states that if a map Λ^l satisfies $\|\Lambda^l[|\psi_A\rangle\langle\psi_A| \otimes |\phi_B\rangle\langle\phi_B|]\|_1 \leqslant 1$ for all product states $|\psi_A\rangle\langle\psi_A| \otimes |\phi_B\rangle\langle\phi_B|$, then we have $\|\Lambda^l(\rho_{AB})\|_1 \leqslant 1$ for any separable state ρ_{AB}.

G. Entanglement witness An entanglement witness operator is a bounded Hermitian operator which is designed to detect entanglement. For every entangled state σ_{AB}, there exists an entanglement witness operator $\mathcal{W}$ such that $\mathrm{Tr}(\mathcal{W}\sigma_{AB}) < 0$ and $\mathrm{Tr}(\mathcal{W}\rho_{AB}) \geqslant 0$ for all separable states ρ_{AB} [19,32]. We can state this other way as well – If $\mathrm{Tr}(\mathcal{W}\rho_{AB}) \geqslant 0$ for any entanglement witness operator $\mathcal{W}$ satisfying $\mathrm{Tr}(\mathcal{W}|\psi_A\rangle\langle\psi_A| \otimes |\phi_B\rangle\langle\phi_B|) \geqslant 0$ for all product states $|\psi_A\rangle\langle\psi_A| \otimes |\phi_B\rangle\langle\phi_B|$, then the state ρ_{AB} is separable.

H. Bell type inequalities Bell type inequalities [3] are one of the experimental way to detect entanglement. A connection between Bell type inequalities and entanglement witness operator was first considered by Tehral [33]. But in general the connection between them is very complex as Bell inequality not only detect entanglement but also nonlocality of the state. Later in this chapter, we will discuss about Bell type inequalities in more details.

1.1.1.2 Quantification of entanglement

The idea of quantifying entanglement came from quantum communication task such as teleportation [5]. With a two-qubit maximally entangled state we can teleport a single qubit state. However, if the two-qubit state is not maximally entangled, then faithful teleportation is not possible. Nevertheless, one can still do faithful teleportation if he/she possesses many copies of two-qubit non-maximally entangled states. The rate of this faithful teleportation will depend on how many maximally entangled states we can obtain from those copies of non-maximally entangled states. This idea introduces two measures of entanglement – entanglement cost and distillable entanglement.

A. Entanglement cost Entanglement cost quantifies the number of ebits (ebit corresponds to the amount of entanglement contained in a Bell state $|\phi^+\rangle = \frac{1}{\sqrt{2}}[|00\rangle + |11\rangle]$)

that are required to prepare a copy of state by local operation and classical communication (LOCC) [34, 35]. We will introduce LOCC in a greater detail later in this chapter. Let's say Alice and Bob start from m copies of Bell state ($|\phi^+\rangle^{\otimes m}$) and after applying LOCC operations get n copies of state ρ ($\rho^{\otimes n}$). Then the rate of this protocol is $r = \frac{m}{n}$. However, in general it is impossible to perform this protocol exactly. Therefore, we consider $|\phi^+\rangle^{\otimes m} \approx \rho^{\otimes n}$ and check the quality of this approximation by measuring trace distance. Finally the entanglement cost is the infimum of all possible rates such that the approximation is very good. The entanglement cost can be defined mathematically as [34, 35]

$$E_C(\rho) = \inf\{r : \lim_{n\to\infty}[\inf_{\Lambda} \|\rho^{\otimes n} - \Lambda(|\phi^+\rangle^{\otimes m})\|_1] = 0\}, \tag{1.11}$$

where Λ represents the LOCC operation.

B. Distillable entanglement Distillable entanglement [36, 37] is just the dual of the entanglement cost. It quantifies the number of ebits that can be obtained from a single copy of a state. The formal mathematical definition of distillable entanglement is [37]

$$E_D(\rho) = \sup\{r : \lim_{n\to\infty}[\inf_{\Lambda} \|\Lambda(\rho^{\otimes n}) - |\phi^+\rangle^{\otimes m}\|_1] = 0\}. \tag{1.12}$$

The two measures we have described above are task dependent. Hence, they require some optimization over some protocols. Generally these are very hard to perform. Therefore, it is always better to define measures which are independent of tasks. These measures are some function of states and must obey some basic postulates. A good entanglement measure must satisfy the following postulates [38–41]–

- For any separable state ρ_{AB}, we must have $E(\rho_{AB}) = 0$.
- The measure of entanglement remains invariant under any local unitary operation. Hence, $E(\sigma_{AB}) = E([U_A \otimes U_B]\sigma_{AB}[U_A^\dagger \otimes U_B^\dagger])$.
- E should not increase under LOCC. Therefore, $E(\Lambda(\sigma_{AB})) \leqslant E(\sigma_{AB})$, where Λ represents a LOCC operation.

- For pure state E gives the value of von-Neumann entropy of reduced density matrices. $E(|\psi_{AB}\rangle) = S(\text{Tr}_B|\psi_{AB}\rangle\langle\psi_{AB}|) = S(\text{Tr}_A|\psi_{AB}\rangle\langle\psi_{AB}|)$, where S represents the von-Neumann entropy.

- For a maximally entangled state $|\Phi\rangle^+_{AB}$, $E(|\Phi\rangle^+_{AB}) = \log_2(d)$, where d is the dimension of the Hilbert space.

- Entanglement measure is a convex function. Most known existing entanglement measures are convex.

The quantifiers that we will describe below may not satisfy all the conditions. But to be an entanglement quantifier, they must satisfy the first three postulates stated above.

C. Distance measure An entanglement measure based on distance quantifies the minimum possible distance between the entangled states and the set of separable states. Intuitively, the closer you go to the set of separable states, less entangled it will be. Mathematically it can be represented as [38, 39]

$$E_{\text{dis}}(\rho) = \inf_{\sigma \in \mathcal{S}} \mathcal{D}(\rho, \sigma), \tag{1.13}$$

where we are measuring the distance of the ρ from the set $(\mathcal{S})$ of separable states σ. Vedral and Plenio [39] showed that Bures distance and relative entropy of entanglement satisfy the necessary conditions (first three postulates) required to be an entanglement measure. Entanglement measure based on Bures distance can be written as

$$E_B(\rho) = \inf_{\sigma \in \mathcal{S}} \left[2 - 2\sqrt{F(\rho, \sigma)}\right], \tag{1.14}$$

where $F(\rho, \sigma) = [\text{Tr}(\sqrt{\sqrt{\rho}\sigma\sqrt{\rho}})]^2$, is the fidelity [42, 43]. On the other hand, the relative entropy of entanglement is defined as

$$E_R(\rho) = \inf_{\sigma \in \mathcal{S}} S(\rho|\sigma) = \inf_{\sigma \in \mathcal{S}} \text{Tr}\rho(\log_2 \rho - \log_2 \sigma). \tag{1.15}$$

D. Entanglement of formation Entanglement of formation (E_F) [44] is a convex roof measure, i.e., one first start with an entanglement measure for pure states and then extends it for mixed states by convex roof [45]. E_F can be defined as

$$E_F(\rho_{AB}) = \inf_{\{p_j, |\psi_j\rangle_{AB}\}} \sum_j p_j S\big(\mathrm{Tr}_B[|\psi_j\rangle_{AB}\langle\psi_j|]\big), \tag{1.16}$$

where S is the von-Neumann entropy and the infimum is taken over all the pure state decomposition $\{p_j, |\psi_j\rangle_{AB}\}$, such that $\rho_{AB} = \sum_j p_j |\psi_j\rangle_{AB}\langle\psi_j|$.

E. Schmidt number The Schmidt rank can also be extended to the mixed state case by convex roof extension and can be defined as [33, 46]

$$r(\rho_{AB}) = \min\{\max_j [r(|\psi_j\rangle_{AB})]\}, \tag{1.17}$$

where minimization is taken over all the pure state decompositions of ρ_{AB} and $r(|\psi_j\rangle_{AB})$ represents the Schmidt rank for the corresponding pure state.

F. Concurrence Concurrence was first introduced by Hill and Wootters [47] for two-qubit pure states. Later Wootters [48] extended it to two-qubit mixed states by convex roof extension. The compact definition of concurrence is

$$\mathcal{C}(\rho_{AB}) = \max(0, \lambda_1 - \lambda_2 - \lambda_3 - \lambda_4). \tag{1.18}$$

$\lambda_i's$ here are in descending order and the eigenvalues of the matrix $\sqrt{\sqrt{\rho_{AB}}\widetilde{\rho_{AB}}\sqrt{\rho_{AB}}}$, where $\widetilde{\rho_{AB}} = (\sigma_y \otimes \sigma_y)\rho^*_{AB}(\sigma_y \otimes \sigma_y)$. σ corresponds to the Pauli matrices and '$*$' denotes the conjugate. For a pure state $|\psi\rangle_{AB}$, the concurrence is $\mathcal{C}(|\psi\rangle_{AB}) = \sqrt{2(1 - \mathrm{Tr}\rho_A^2)}$, where ρ_A is the reduced density matrix of $|\psi\rangle_{AB}$. Concurrence can be extended for higher dimension as [49, 50]

$$\mathcal{C}(|\psi\rangle_{AB}) = \sqrt{\langle\psi|\psi\rangle_{AB} - \mathrm{Tr}\rho_A^2}, \tag{1.19}$$

where ρ_A is the subsystem density matrix. Mintert et. al. [51] has derived a strong lower bound for its convex roof extension.

G. Negativity Negativity [52, 53] is another measure of entanglement and is very easy to compute. Negativity of a two-qudit state ρ_{AB} is defined as

$$\mathcal{N}(\rho_{AB}) = \frac{\|\rho^{T_B}\|_1 - 1}{d - 1}, \tag{1.20}$$

where ρ^{T_B} is the partial transpose of the state ρ_{AB} with respect to the subsystem B and d represents the dimension of the system. Logarithmic negativity is another version of negativity and can be defined as [53]

$$E_N(\rho_{AB}) = \log_2 \|\rho^{T_B}\|_1. \tag{1.21}$$

It gives the upper bound for the distillable entanglement [53].

1.1.2 Multipartite entanglement

The entanglement is far richer and complex in multipartite system than the usual bipartite entanglement. Unlike bipartite entanglement, not only there exist fully separable states and fully entangled states, but also there exists the concept of many partial separable states.

1.1.2.1 Separability

A. Full separability A multipartite state $\rho_{A_1\cdots A_n}$ of n subsystems on the Hilbert space $\mathcal{H} = \mathcal{H}_{A_1} \otimes \cdots \mathcal{H}_{A_n}$ is fully separable iff it can be written as [17, 54]

$$\rho_{A_1\cdots A_n} = \sum_i p_i \rho^i_{A_1} \otimes \cdots \otimes \rho^i_{A_n}. \tag{1.22}$$

Like the bipartite case full separability remains preserved under the fully separable operation of the form $\sum_i \zeta^i_1 \otimes \cdots \otimes \zeta^i_n$, i.e.,

$$\rho_{A_1\cdots A_n} \rightarrow \frac{\sum_i \zeta^i_1 \otimes \cdots \otimes \zeta^i_n \rho_{A_1\cdots A_n} (\zeta^i_1 \otimes \cdots \otimes \zeta^i_n)^\dagger}{\text{Tr}\big[\sum_i \zeta^i_1 \otimes \cdots \otimes \zeta^i_n \rho_{A_1\cdots A_n} (\zeta^i_1 \otimes \cdots \otimes \zeta^i_n)^\dagger\big]}. \tag{1.23}$$

B. Partial separability As we have already mentioned above, there exists many forms of partial separability in the multipartite entangled system. Here we will discuss about them very briefly.

1. **Separability with respect to partitions:** In a n-partite system let's consider a partition $\{I_1, I_2, \cdots, I_k\}$, where I_i corresponds to the disjoint subsets of the set of indices $I = \{1, 2, \cdots, n\}$ ($\cup^k_{l=1} I_l = I$). Then the n-partite state is separable with respect to the above mentioned partition if and only if [17]

$$\rho_{A_1\cdots A_n} = \sum_i p_i \rho^i_1 \otimes \cdots \otimes \rho^i_k. \tag{1.24}$$

Therefore, there exists several separability condition with respect to many different partitions. To make it more simple, we arrange a n-partite system in $k \leqslant n$ groups, i.e., we choose a k-partition. If we now consider each group as a single party, then it may happen that the n-partite state is separable with respect to this partition. It is interesting to note that n-partite state is k-separable irrespective of the case that the individual group may be entangled.

2. **Semiseparability:** A state $\rho_{A_1 \cdots A_n}$ in Hibert space $\mathcal{H} = \mathcal{H}_{A_1} \otimes \cdots \mathcal{H}_{A_n}$ is semiseparable iff it is separable under all 1 versus $n-1$ partitions, i.e., $\{I_1 = \{k\}, I_2 = \{1, \cdots, k-1, k+1, \cdots, n\}\}$ where $1 \leqslant k \leqslant n$ [17].

3. **s-partite entanglement:** There also exists a notion of at most s-partite entanglement. It can be defined as follows: A multipartite state $\rho_{A_1 \cdots A_n}$ of n parties is at most s-partite entangled if it is a mixture of all such states which are separable with respect to some partition $\{I_1, \cdots, I_k\}$, such that the cardinality of all I_i is less than s [55].

1.1.2.2 Characterization of separability

A. Case of pure state A pure multipartite state $|\Psi\rangle_{A_1 \cdots A_n}$ of n subsystems is fully separable or n-partite separable if and only if

$$|\Psi\rangle_{A_1 \cdots A_n} = |\psi\rangle_{A_1} \otimes \cdots \otimes |\psi\rangle_{A_n}. \tag{1.25}$$

In bipartite case the entanglement of pure states can be characterized by the condition, whether the reduced density matrix is mixed or not. However, in this case the violation of this condition for one bipartite partition does not guarantee that the state is n-partite entangled or fully entangled or genuinely entangled. We need to consider all the bipartite partitions of the state $|\Psi\rangle_{A_1 \cdots A_n}$ and then check whether the reduced density matrices are mixed or not. If they are mixed for all the bipartite partitions then the state $|\Psi\rangle_{A_1 \cdots A_n}$ is genuinely entangled. Hence, there does not exist any cut in which the state is product. This difficulty of characterization arises due to the fact that a pure multipartite state admits Schmidt decomposition very rarely [56]. Furthermore, one can classify genuinely entangled pure states into different non-comparable entanglement classes by means of stochastic LOCC (SLOCC) [57, 58]. There also exist partially separable and partially entangled state [17].

B. Case of mixed state The full characterization of entanglement for multipartite states is much much complicated than the bipartite case. However, for some cases we do have a generalization of bipartite separability criteria to the multipartite scenario.

I. Positive but not completely positive maps The separability criteria for a bipartite system by positive but not completely positive maps can be generalized to a multipartite scenario in a very natural way [59]. Consider a positive but not completely positive map $\Lambda^p_{A_2\cdots A_n} : \mathcal{O}(\mathcal{H}_{A_2} \otimes \cdots \otimes \mathcal{H}_{A_n}) \to \mathcal{O}(\mathcal{H}_{A_1})$, such that they are positive on product state, i.e., $\Lambda^p_{A_2\cdots A_n}(|\psi\rangle_{A_2}\langle\psi| \otimes \cdots \otimes |\psi\rangle_{A_n}\langle\psi|) \geqslant 0$. Then a necessary and sufficient separability criteria for a multipartite state $\rho_{A_1\cdots A_n}$ is [59]

$$(\mathbb{I}_{A_1} \otimes \Lambda^p_{A_2\cdots A_n})\rho_{A_1\cdots A_n} \geqslant 0, \text{ for all } \Lambda^p_{A_2\cdots A_n} : \mathcal{O}(\mathcal{H}_{A_2} \otimes \cdots \otimes \mathcal{H}_{A_n}) \to \mathcal{O}(\mathcal{H}_{A_1}), \quad (1.26)$$

where $\mathbb{I}_{A_1}$ is the identity operator for the A_1 subsystem. This criteria provides a full separability of the multipartite system. A positive map which is positive on product states may be written as a product of positive maps [17]. However, there exists some positive maps which are positive on product state but cannot be written as a product of positive maps. It has been shown that these maps are useful to detect some semiseparable states [44, 59].

II Entanglement witness Choi-Jamiołlkowski isomorphism [60–62] gives us a way to connect a positive, but not completely positive maps to the entanglement witness in the bipartite case, i.e., $\mathcal{W} = (\mathbb{I} \otimes \Lambda^p)|\Phi^+\rangle\langle\Phi^+|$, where $|\Phi^+\rangle = \frac{1}{\sqrt{d}}\sum_i |i_A i_B\rangle$. This idea can also be generalized to the multipartite scenario as well [17]. Hence, we can state that a multipartite state $\rho_{A_1\cdots A_n}$ is separable if $\mathrm{Tr}(\mathcal{W}\rho_{A_1\cdots A_n}) \geqslant 0$ for all $\mathcal{W}$. This is also a full separability criteria for the multipartite state.

1.1.2.3 Entanglement quantification

Some entanglement measures from the bipartite scenario can be generalized to the multipartite case in a very natural way. As an example, relative entropy of entanglement can be generalized by taking a suitable set of separable states instead of set of bipartite separable states. For instance, if we consider the set of fully separable states, then it cannot distinguish between genuinely entangled states and several cases of bipartite entanglement. However, genuinely entanglement characterization is still possible if one considers the set of states which has no more than k-partite entanglement $(1 \leqslant k \leqslant n)$ [38]. As multipartite entanglement is far more complex than the bipartite entanglement, hence many more parameters are required to characterize it. Therefore, many new measures for pure multipartite states have been introduced recently [17].

A. Tangle Tangle was first introduced in [63], in the context of distributed entanglement, to quantify the amount of three-way entanglement in a three-qubit state. For a pure state it can be interpreted as residual entanglement, which is not captured by two-way entanglement between the qubits. It was also shown to be an entanglement monotone [57]. The tangle is defined as

$$\tau = C^2_{A(BC)} - C^2_{AB} - C^2_{AC}, \tag{1.27}$$

where C_{AB} and C_{AC} denote the concurrence [50] of the entangled state between the qubits A and B and between the qubits A and C respectively. The concurrence $C_{A(BC)}$ refers to the entanglement of qubit A with the joint state of qubits B and C. Tangle is nonzero only for the genuinely entangled state. However, there exists genuinely entangled states for which tangle is zero, in particular for W-class of states [17]. A possible generalization of tangle to the other multiparty scenarios has been defined by the method of hyperdeterminant [64] and also a possible extension to mixed state by convex roof has been considered by Lohmayer et. al. in [65].

B. Schmidt measure Schmidt measure was the first measure of multipartite entanglement introduced by Eisert and Briegel [66]. This measure quantifies the minimum number of product basis required to write a state and can be mathematically expressed as

$$E_S(|\psi\rangle_{A_1 \cdots A_n}) = \min_r \log_2 r, \tag{1.28}$$

where r is the number of terms in a particular expansion of the state $|\psi\rangle_{A_1 \cdots A_n}$ in terms of product basis. As an example, for three qubit GHZ state $|\psi\rangle_{GHZ} = \frac{1}{\sqrt{2}}(|000\rangle + |111\rangle)$, Schmidt measure gives 1 as minimum of r is 2. This measure is zero only for fully product state. Therefore, this measure cannot distinguish between genuine entanglement and bipartite entanglement.

C. Measure based on normal forms In the context of classification of multipartite entangled states, Verstraete et. al. [67] in 2003 introduced an interesting class of entanglement measure based on normal forms. They considered a homogeneous function of state f which is invariant under SLOCC of determinant 1, i.e.,

$$f(\Lambda_{A_1} \otimes \cdots \otimes \Lambda_{A_n} |\psi\rangle_{A_1 \cdots A_n}) = f(|\psi\rangle_{A_1 \cdots A_n}), \tag{1.29}$$

where $\det \Lambda_{A_i} = 1$. Then the measure based on the function f is an entanglement monotone.

D. Hyperdeterminant Miyake [64] was first to notice that hyperdeterminants can describe genuine multipartite entanglement and moreover they satisfy monotonicity [68]. Hyperdeterminant can be considered as the generalization of concurrence and tangle. For example, concurrence is the modulus of determinant which is hyperdeterminant of first order and tangle is a special case of second order hyperdeterminant. It has been shown that hyperdeterminant of higher orders are also entanglement monotone [68]. Recently Levay derived a compact form of hyperdeterminant for four qubit states [69].

E. Geometric measure Geometric measure was introduced by Barnum and Linden in 2001 and can be expressed as [70]

$$E_g^k(|\psi\rangle) = 1 - \Lambda^k(|\psi\rangle), \tag{1.30}$$

where $\Lambda^k(|\psi\rangle) = \sup_{|\phi\rangle \in \mathcal{S}_k} |\langle\phi|\psi\rangle|^2$. Here $\mathcal{S}_k$ represents the set of k-separable states.

F. Concurrence type measure In literature there exists many attempts to generalize concurrence to multipartite states. A significant generalization to the even number of qubits has been derived by Wong and Christensen [71]. Their concurrence measure is represented by $\langle\psi^*|\sigma_y^{\otimes n}|\psi\rangle$, where '$*$' denotes the complex conjugate. This approach was generalized further by Osterloh and Siewert [72] using antilinear operations.

1.1.3 LOCC and SLOCC

In an entanglement theory, we mainly deal with three basic points –

1. Characterization: Decide which states are entangled.
2. Manipulation : Which kind of operations are allowed.
3. Quantify : Order the states according to their entanglement.

The most successful approach to describe the entanglement properties of bipartite and multipartite pure states is concerned with the study of equivalence relations under certain classes of allowed operations, for example local unitaries (LU), local operations and classical communication (LOCC) [8, 17] or stochastic local operations and classical communication (SLOCC) [17, 57]. The basic idea behind LOCC is that one party performs some local operation on his/her subsystem and communicates the outcome classically to other parties. In the next step, other parties perform some local operation depending on the measurement outcome of previous parties and the process will continue until the task they want to achieve. Suppose there are two states $|\psi\rangle$ and $|\phi\rangle$ such that we can obtain $|\phi\rangle$ from $|\psi\rangle$ by LOCC operation. Then we can say that $|\psi\rangle$ is as useful as $|\phi\rangle$ or in other way we can say that entanglement of $|\psi\rangle$ is equal or greater than that of $|\phi\rangle$. It provides an operational ordering on the set of entangled states. It is that entanglement cannot increase under LOCC. The study of deterministic state transformations under LOCC was started by Popescu and Lo [73]. A major approach to this deterministic LOCC convertibility uses the square of the Schmidt coefficients and is due to the work of Nielson [74]. Nielson majorization criteria provides the necessary and sufficient condition for deterministic LOCC inter-convertibility between two bipartite pure states. It states that a pure state $|\psi\rangle_{AB} = \sum_i \sqrt{p_i}|i_A i_B\rangle$ $\left(\sqrt{p_1} \geqslant \cdots \geqslant \sqrt{p_d}\right)$ can be deterministically converted to $|\phi\rangle_{AB} = \sum_i \sqrt{q_i}|i'_A i'_B\rangle$ $\left(\sqrt{q_1} \geqslant \cdots \geqslant \sqrt{q_d}\right)$, iff for all $k \in \{1, \cdots, d\}$

$$\sum_{i=1}^{k} p_i \leqslant \sum_{i=i}^{k} q_i, \tag{1.31}$$

where p_i and q_i are square of the Schmidt coefficients. Nielson majorization criteria only provides some partial ordering on the set of entangled states. The reversible conversion, i.e., $|\psi\rangle_{AB} \leftrightarrow |\phi\rangle_{AB}$ is possible iff the Schmidt coefficients of both states are equal. Moreover, there exist incomparable states (for $d > 2$), neither of which can be considered as more entangled than another. This irreversibility can be overcome if we consider many copies of state (asymptotic limit) instead of a single copy [75]. However, the situation gets worse in multipartite case as in general there is no Schmidt decomposition of states. Moreover, LOCC operation does not provide us a crystal clear picture about the different types of entanglement in a multipartite state. Further more, in a single copy restriction, two pure states can be transformed into each other under LOCC if and only if they are connected by LU [76]. However, even in a bipartite case two pure states are not typically related by LU. To overcome this difficulty, the LOCC operation, through which the conversion of entangled states is considered is slightly loosened. One now considers the conversion of states through stochastic LOCC (SLOCC), i.e. two entangled states are converted to each other by means of LOCC but with a non-vanishing probability of success [57]. Since, all bipartite pure states are SLOCC equivalent, there exists only a single class. But in a multipartite state, there exists infinitely many inequivalent SLOCC classes. The entanglement is not comparable in two different SLOCC inequivalent classes [57, 58].

1.2 Bell inequality

Bell inequality or Bell nonlocality is considered as one of the most profound discovery in the history of physics. In 1964, Bell discussed the famous EPR paradox in [1] and showed that the predictions of quantum mechanics are not compatible with the theory of local hidden variable [3]. The discovery of Bell opened a new direction in the field of quantum information science. Ever since the discovery of Bell's theorem, a zoo of Bell inequalities have been proposed [77]. In this section, we will provide a very brief overview of some of them. In a typical Bell test, a source prepares two particles and sends to two distant observers Alice and Bob. Alice and Bob may randomly perform some measurement on their system from a set of possible measurements $\{x\}$ and $\{y\}$ respectively. After the measurement, they find outcomes $\{a\}$ and $\{b\}$ respectively. The occurrence of these outcomes for a specific measurement setting can be described by a probability distribution $p(ab|xy)$. If our theory is described by a local hidden variable model, then [3, 77]

$$p(ab|xy) = \int \mathrm{d}\lambda q(\lambda) p(a|x, \lambda) p(b|y, \lambda), \tag{1.32}$$

where λ represents some hidden variable with the distribution $q(\lambda)$. Now let's consider an experiment, where Alice and Bob are measuring two dichotomic observables, i.e., $x, y \in \{0, 1\}$ and $a, b \in \{0, 1\}$. Then the correlation $\langle a_x b_y \rangle = \sum_{a,b} (-1)^{ab} p(ab|xy)$. If our theory satisfy local hidden variable model described in Eq. (1.32), then we must have

$$\langle a_0 b_0 \rangle + \langle a_0 b_1 \rangle + \langle a_1 b_0 \rangle - \langle a_1 b_1 \rangle \leqslant 2. \tag{1.33}$$

This is known as CHSH inequality [78] which is another version of the original Bell inequality [3]. Now one can verify that the prediction of quantum mechanics for some experiments involving entangled particles is inconsistent with the decomposition given in Eq. (1.32). As an example, a singlet pair of spin half particles violates this inequality. The violation of this inequality guarantees the presence of entanglement. It can be shown in a very simple way. A two-qubit separable state can be written as

$$\rho_{AB} = \sum_{\lambda} p_\lambda \rho_\lambda^A \otimes \rho_\lambda^B. \tag{1.34}$$

Now the correlations obtained after performing local measurements on A and B can be expressed as

$$\begin{aligned} p(ab|xy) &= \text{Tr}\big[\sum_{\lambda} p_\lambda (\rho_\lambda^A \otimes \rho_\lambda^B)(\Pi_{a|x} \otimes \Pi_{b|y})\big] \\ &= \sum_{\lambda} p_\lambda \text{Tr}[\rho_\lambda^A \Pi_{a|x}] \text{Tr}[\rho_\lambda^B \Pi_{b|y}] \\ &= \sum_{\lambda} p_\lambda p(a|x, \lambda) p(b|y, \lambda), \end{aligned} \tag{1.35}$$

which is exactly same as the local hidden variable model we have described in Eq. (1.32). Therefore, we can see the fact that the presence of nonlocal correlations in the system implies the presence of entanglement. Since the discovery of Bell's theorem, many Bell test experiments have been carried out and they supported the predictions of quantum mechanics over local hidden variable model. The first experiment in this direction was performed by Freedman and Clauser in 1972 [79]. They showed violation of CH type inequality (another version of CHSH inequality proposed by Clauser and Horne [80]), using the polarisation of photon pairs. After that a series of experiment have been conducted on CHSH inequality by Aspect et al. [81], Tittel et al. [82], etc. Although these experiments validate the fact that quantum mechanics is incompatible with any local hidden variable model, still there exists a lot of conceptual difficulties (loophole in Bell test) [77] about the implementation of the Bell type experiment. Very recently some experiments has been carried out which closes all the loopholes in a Bell test [83–85]. But here we are not going to discuss about that.

Bell's inequality can also be described by the space constructed by the vectors of the measurement outcomes [77, 86]. In a local hidden variable model the set of outcomes for different measurements are predetermined and form a convex polytope as shown in Fig. 1.1. In the polytope, the extremal points represents the predetermined measurement outcome. The convex combination of these points constructs a polytope. The region inside the polytope corresponds to the validity of local hidden variable model. Every facet of the polytope corresponds to a boundary that divides the probability space in two halves and can be represented as an inequality. Most of the facets are the positivity of the probabilities and are trivial. Some nontrivial facets correspond to the tight Bell inequalities. The language of polytope gives us a way to draw a line between local hidden variable theory and quantum correlations. In chapter 2, we will discuss in a greater detail about the construction of polytope for the CHSH case.

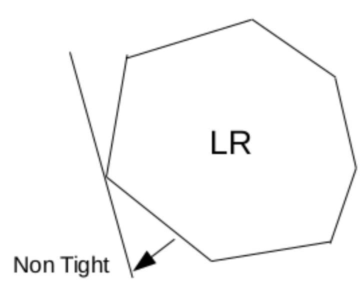

Figure 1.1: A schematic diagram of Bell polytope. The inside region corresponds to local realistic (LR) model.

After the discovery of Bell's theorem, there has been many generalization of Bell inequality in different directions, like two-qudit, multi-qubit etc. There exist many inequalities for a two-qudit system in the literature. Among them the most well known inequality is the Collins-Gisin-Linden-Massar-Popescu (CGLMP) inequality [87], which is in some sense the generalization of the CHSH inequality to two-qudit case. In CGLMP test, two distant parties may choose from two measurements with d outcomes. CGLMP inequality can be expressed as

$$\begin{aligned} I_C &= \sum_{\alpha=0}^{[d/2]-1} \left(1 - \frac{2\alpha}{d-1}\right) \Big[P(A_1 = B_1 + \alpha) + P(B_1 = A_2 + \alpha + 1) + \\ &\qquad P(A_2 = B_2 + \alpha) + P(B_2 = A_1 + \alpha) - \\ &\qquad P(A_1 = B_1 - \alpha - 1) - P(B_1 = A_2 - \alpha) - \\ &\qquad P(A_2 = B_2 - \alpha - 1) - P(B_2 = A_1 - \alpha - 1) \Big] \\ &\leqslant 2, \end{aligned} \tag{1.36}$$

where $P(A_a = B_b + \alpha) = \sum_{k=0}^{d-1} P(A_a = j, B_b = j + \alpha \bmod d)$, represents the joint probability of measurements A_a and B_b with outcomes that differ by α. Masanes showed that CGLMP inequality is also a tight Bell inequality [88]. However, it does not show maximum violation for a maximally entangled state [89]. Recently, Son et al. proposed a generic Bell inequality and its variant for two-qudit systems which is known as SLK inequality [90]. Unlike CGLMP inequality, SLK inequality gives maximum violation for a maximally entangled state [91]. However, this inequality is not tight [91]. We will discuss SLK inequality in detail in chapter 3.

1.3 Quantum steering

In 1935, Schrödinger [2] introduced the idea of quantum steering in order to describe the incompleteness of quantum mechanics in the EPR paper [1]. He described it as an ability of Alice to affect the state of Bob's by applying suitable local measurements on her system. Recently, the concept of steering has been properly formulated in terms of some task by Wiseman et al. [92]. Quantum steering can be observed when one of the party does some suitable local measurements on a part of entangled system. In this sense steering scenario can be considered as somehow in between a Bell test [3, 77] and standard entanglement test [17]. Now we will describe the bipartite steering scenario as introduced by Wiseman et al. [92]. Consider a bipartite state ρ_{AB} shared between two distant observers Alice and Bob. Alice performs a set of measurements (denoted by $x \in \{0, 1, \cdots, m-1\}$) on her local subsystem and obtain an outcome from the set $a \in \{0, 1, \cdots, n-1\}$. As a result, Bob's state will collapse to $\rho_{a|x}$ with probability $p(a|x)$ if Alice performs the measurement x and obtain an outcome a. One can completely characterize this steering scenario by the set of unnormalized conditional states on Bob's side $\{\sigma_{a|x}\}$, where $\sigma_{a|x} = p(a|x)\rho_{a|x}$, often called an unnormalized assemblage. According to quantum mechanics, each elements of the assemblage can be obtained as

$$\sigma_{a|x} = \text{Tr}[(M_{a|x} \otimes I)\rho_{AB}], \tag{1.37}$$

where $\sum_a M_{a|x} = \mathbb{I}$ for all x and $M_{a|x} \geqslant 0$ for all a, x. Now the state ρ_{AB} is steerable from Alice to Bob if the assemblage $\{\sigma_{a|x}\}$ does not have a local hidden state (LHS) model [92]. A LHS model can be described as following – A source (let's say Alice) sends a state ρ_λ corresponding to a classical variable λ to another party, let's say Bob. Depending on the classical random variable λ, Alice decides to perform measurement x. Then, the variable λ instructs Alice's measurement device to give an output a with probability $p(a|x, \lambda)$. Further, we consider the random classical variable λ which follows a distribution $\mu(\lambda)$. So, the final assemblage on Bob's side can be written as [92]

$$\sigma_{a|x} = \sum_\lambda \mu(\lambda)p(a|x, \lambda)\rho_\lambda. \tag{1.38}$$

Therefore, in the above scenario an assemblage will demonstrate steering if it cannot be described in terms of a LHS model as given in Eq. (1.38). Wiseman et al. showed that the steerable states are a strict subset of the entangled states and a superset of Bell nonlocal states [92]. Hence, the steerability of a state confirms the presence of entanglement in the system. For a pure two-qubit state these three sets are same [92]. It is important to note that quantum steering is asymmetric in nature. It means there exists some entangled state for which the state is steerable from Alice to Bob, but not steerable from Bob to Alice [93,94]. Since the formulation of quantum steering by Wiseman et al., many steering criteria have been introduced [95–100]. But most of them are not necessary and sufficient criteria for steering. Recently, Cavalcanti et al. proposed a steering inequality which is necessary and sufficient condition for steering [97]. Alice and Bob both can perform two dichotomic measurements A_1, A_2 and B_1, B_2 on their respective subsystems. Moreover, the measurements of the steered party (in this case Bob) are mutually unbiased. In this scenario they proposed a inequality [97]

$$\sqrt{\langle (A_1 + A_2)B_1\rangle^2 + \langle (A_1 + A_2)B_2\rangle^2} + \sqrt{\langle (A_1 - A_2)B_1\rangle^2 + \langle (A_1 - A_2)B_2\rangle^2} \leqslant 2. \tag{1.39}$$

The violation of this inequality suggest that the state is steerable form Alice to Bob. This inequality is analogues to the CHSH inequality [78]. Apart from this, there exist several linear steering inequalities in the literature [100] and some of them have been tested recently in the experiment.

Conventional bipartite steering have also been extended to the multipartite scenario [100–102]. Here we will discuss steering scenarios in tripartite case. Consider a tripartite state ρ_{ABC} shared among Alice, Bob and Charlie. In this case, we can generalize the bipartite steering in this two following ways –

- Let's say Alice on her local subsystem performs some measurements x and obtains an outcome a. As a result of that the joint system of Bob and Charlie will collapse to some conditional state. In this scenario the unnormalized assemblage $\{\sigma^{BC}_{a|x}\}$ possessed by Bob and Charlie can be written as

  $$\sigma^{BC}_{a|x} = \text{Tr}[(M_{a|x} \otimes \mathbb{I} \otimes \mathbb{I})\rho_{ABC}]. \tag{1.40}$$

  In this steering scenario one can analyze $\{\sigma^{BC}_{a|x}\}$ whether it can be decomposed in terms of any LHS model.

- Another possible generalization is that Alice and Bob both perform some measurements on their respective subsystems. Then, one can analyze the unnormalized assemblage jointly prepare by Alice and Bob for Charlie. In this case the unnormalized assemblage can be obtain as

  $$\sigma^{C}_{ab|xy} = \text{Tr}[(M_{a|x} \otimes M_{b|y} \otimes \mathbb{I})\rho_{ABC}]. \tag{1.41}$$

Similarly, one can generalize the steering scenario for more than three parties by considering all such asymmetric network scenarios.

1.4 Quantum channel

The most general quantum operation Ω which maps a density matrix ρ to another density matrix ρ' can be represented as

$$\rho' = \frac{\Omega(\rho)}{\mathrm{Tr}[\Omega(\rho)]}, \tag{1.42}$$

where $\mathrm{Tr}[\Omega(\rho)] \leqslant 1$. The action of such trace non-increasing completely positive operation can also be represented as [103]

$$\Lambda(\rho) = \sum_i K_i \rho K_i^\dagger, \tag{1.43}$$

where K_i's are the Kraus operators and satisfies $\sum_i K_i^\dagger K_i \leqslant 1$. If the operation Ω is trace preserving, i.e., $\sum_i K_i^\dagger K_i = 1$, then Ω represents a quantum channel. We denote this representation as the Kraus representation of the channel (KROC).

For the qubit case, the action of a qubit channel Ω can also be completely characterized by a 3×3 real matrix M and a 3-dimensional vector $\vec{\tau}$ [62, 104, 105]. An arbitrary qubit is expressed as $\rho = \frac{1}{2}(\mathbb{I} + \vec{r} \cdot \vec{\sigma})$, where $\vec{r}$ is the 3-dimensional Bloch vector. The action of qubit channel Ω on ρ is described in following way:

$$(1, \vec{r}')^T = \Lambda_\Omega (1, \vec{r})^T, \tag{1.44}$$

where Λ_Ω represents a real 4×4 matrix and T denotes transposition. The most general form of Λ_Ω for complete positivity can be written as

$$\Lambda_\Omega = \begin{pmatrix} 1 & 0_{1\times 3} \\ \vec{\tau} & M \end{pmatrix}. \tag{1.45}$$

where, $\vec{\tau} \in \mathbb{R}$ is a vector and M is a 3×3 a real matrix. It leads to the affine transformation of the Bloch vector, i.e., $\vec{r}' = M\vec{r} + \vec{\tau}$. Up to some local unitary equivalence, any qubit channel can be written as

$$\Lambda_\Omega = \begin{pmatrix} 1 & 0 & 0 & 0 \\ \tau_x & \lambda_x & 0 & 0 \\ \tau_y & 0 & \lambda_y & 0 \\ \tau_z & 0 & 0 & \lambda_z \end{pmatrix}, \tag{1.46}$$

where λ's are the (signed) singular values of the matrix M and τ's represents the shift of the coordinates [62, 104]. The above representation of a qubit channel Ω is known as the affine representation of the channel (AROC).

1.5 Choi-Jamiołlkowski

Choi-Jamiołkowski isomorphism [60–62] permits one to associate a complete positive and trace preserving (CPTP) map Ω to a density matrix of composite system AB with B being the auxiliary system of same dimension as A. The prescription is:

$$\rho_{AB} = \Omega \otimes \mathbb{I}_B(|\Psi\rangle_{AB}\langle\Psi|), \tag{1.47}$$

where $|\Psi\rangle_{AB}$ is a maximally entangled state. It states that for every quantum state there is a unique quantum operation. It is also known as the channel-state duality.

1.6 Coherence

Quantum coherence is a fundamental concept in quantum mechanics. It arises due to the superposition principle [9]. Recently, much attention has been paid to define a proper measure of quantum coherence [106–109]. As coherence is a basis dependent quantity, we should first fix a particular basis. Let $\{|i\rangle\}$ ($i = 1 \ldots d$) be a basis in a d-dimensional Hilbert space $\mathcal{H}_d$. The density matrices which are diagonal in this basis are called incoherent states. The structure of these density matrices are as follows

$$\delta = \sum_{i=1}^{d} \delta_i |i\rangle\langle i|, \tag{1.48}$$

where $\sum_{i=1}^{d} \delta_i = 1$. For more than one party, the coherence can be studied in a basis which is the tensor product of local basis states of each subsystem and then a multipartite incoherent state is defined as the convex combination of those incoherent product states [110, 111].

1.6.1 Incoherent operation

Resource theory of coherence tells us what can be achieved from a system by using some allowed operations which cannot create coherence from an incoherent state. However, the concept of such allowed operations or incoherent operations are not unique. There exist many classes of incoherent operations in the literature [10]. Here we will briefly discuss about some important incoherent operations which have been introduced in the different resource theoretic perspectives of the quantum coherence.

A. Maximally Incoherent operation (MIO) An incoherent operation Φ is MIO iff $\Phi[\delta] \in \mathcal{I}$, for all incoherent states δ, i.e., MIO preserves the set of incoherent states. This is the largest set of operations which preserve incoherence [9].

B. Incoherent operation (IO) In Ref. [106], a smaller and relevant class of incoherent operations was introduced. An incoherent operation or quantum channel Φ with Kraus decomposition $\{K_i\}$ is IO iff $\frac{K_i \delta K_i^\dagger}{\mathrm{Tr}[K_i \delta K_i^\dagger]} \in \mathcal{I}$ for all i and $\delta \in \mathcal{I}$. Here, the Kraus operators of IO may be expressed as

$$K_i = \sum_{j=0}^{d-1} c_{ij} |f_i(j)\rangle\langle j|, \tag{1.49}$$

where $f_i : \{0, 1, .., d-1\} \mapsto \{0, 1, .., d-1\}$ and d is the dimension of the Hilbert space. Note that coherence cannot be generated, even probabilistically, from incoherent states due to the action of this quantum channel.

The above two incoherent operations are defined in terms of their inability to create coherence. One can add further desirable restriction to the set of free operations. One such constraint is that the operations will be unable to use the coherence of the input state.

C. Strictly Incoherent operation (SIO) A quantum channel Φ is SIO iff its Kraus operators $\{K_i\}$ individually commutes with dephasing, i.e., $\triangle(K_i \delta K_i^\dagger) = K_i \triangle(\delta) K_i^\dagger$, where $\triangle$ is dephasing operation [114, 117] defined as $\triangle(\rho) = \sum_i \langle i|\rho|i\rangle |i\rangle\langle i|$. This condition makes f_i one-to-one, i.e., f_i becomes permutation, π_i in Eq.(1.49). Thus, SIO admits the set $\{K_i\}$ as well as $K_i^\dagger$ are also incoherent. This indicates that the SIOs are not capable of using coherence of initial input states [117]. However, the above mentioned operations cannot be implemented by introducing an incoherent environment and a global unitary operation. This observation led one to introduce physically motivated incoherent operations [107, 118].

D. Physical Incoherent operation (PIO) A PIO is obtained through a class of noncoherence generating operations on a primary (A) and an ancillary system (B) [107,118]. A general PIO operation consist of an unitary operation U_{AB} on the state ρ_A of system A and the incoherent state ρ_B of system B, followed by a general incoherent projective measurement on system B. The PIO admits following Kraus decomposition $K_i = \sum_j e^{\mathrm{i}\theta_j}|\pi_i(j)\rangle\langle j|P_i$ and their convex combinations. The π_i are permutations and $\{P_i\}$ is an complete set of orthogonal incoherent projectors [107]. Orthogonal incoherent projectors are those which does not introduce any coherence in the system after measurement. The PIOs are implementable using the aforementioned method and additionally it allows incoherent measurements in environment and classical post-selection on the outcomes.

It is evident now that the MIO is the largest set of incoherent operations, and others are strict subset of it. The nontrivial relationship can be depicted in the following way [107, 109, 118, 119]

$$PIO \subset SIO \subset IO \subset MIO. \tag{1.50}$$

A special subset of PIO is considered and discussed in [120]. These are very important in the sense that they preserve coherence of the input states.

E. Coherence preserving operation (CPO) A quantum channel Φ is CPO [120] iff it keeps the coherence of a state invariant, i.e., $C(\Phi[\rho]) = C(\rho)$, where C is an arbitrary coherence measure. The Kraus operator of CPO is expressed as $K = \sum_i e^{\mathrm{i}\theta_i}|\pi(i)\rangle\langle i|$.

F. Genuinely Incoherent operation (GIO) A quantum channel Φ is GIO [109] iff $\Phi[\delta] = \delta$, i.e., all incoherent states are fixed points for the channel. Therefore, GIO does not allow transformation between any incoherent states. All Kraus operators for this operation are diagonal in the incoherent basis.

G. Fully Incoherent operation (FIO) A quantum operation is fully incoherent if and only if all Kraus operators are incoherent and have the same form [109]. Kraus operators are incoherent means, $K_i\delta K_i^\dagger$ is an incoherent state as well for all i. This means that only pure incoherent states are free in this resource theory.

1.6.2 Quantification of coherence

The very first approach to quantify coherence came in 2006 by Åberg [9]. Very recently considering coherence as a resource Baumgratz et. al. have provided a rigorous framework to quantify coherence [106]. Any proper quantifier of the coherence must satisfy the following conditions [9, 106, 112]

(A1) $C(\delta) = 0$, where $\delta \in \mathcal{I}$ and $\mathcal{I}$ is the set of incoherent states. Hence, for any quantum state $C(\rho) \geqslant 0$.

(A2) It should not increase under any incoherent operation, i.e., $C(\rho) \geqslant C(\Phi[\rho])$, where $\Phi[\rho]$ is any incoherent operation.

(A3) $C(\rho)$ is nonincreasing under selective measurements on average, $C(\rho) \geqslant \sum_i q_i C(\rho_i)$, where $q_i = \mathrm{Tr}(K_i\rho K_i^\dagger)$ and $\rho_i = K_i\rho K_i^\dagger/q_i$ for all i with $\sum_i K_i^\dagger K_i = \mathbb{I}$ and $K_i\mathcal{I}K_i^\dagger \in \mathcal{I}$. K_i's are the Kraus operators.

(A4) $C(\rho)$ does not increase under mixing of quantum states, $\sum_i p_i C(\rho_i) \geqslant C(\sum_i p_i\rho_i)$, with $\rho = \sum_i p_i\rho_i$.

Now we will introduce some relevant coherence quantifier which has been introduced in the literature very recently.

A. Distillable coherence Distillable coherence borrows the same idea as used to quantify distillable entanglement. It quantifies the number of maximally coherent state $|\Psi\rangle$ can be obtained from a copy of a given state ρ via incoherent operations. In the asymptotic limit it can be expressed as [113, 114]

$$C_d(\rho) = \sup\{r : \lim_{n\to\infty} (\inf_{\Lambda} \|\Lambda(\rho^{\otimes n}) - |\Psi\rangle\langle\Psi|^{\otimes m}\|_1) = 0\}, \tag{1.51}$$

where Λ corresponds to incoherent operation, $r = \frac{m}{n}$ is the rate of getting m copies of maximally coherent state from n copies of a given state ρ via incoherent operation and supremum is taken over all such possible r.

B. Coherence cost Coherence cost quantifies the number of maximally coherent state $|\Psi\rangle$ are required to prepare a copy of a state and can be expressed mathematically as [113, 114]

$$C_c(\rho) = \inf\{r : \lim_{n\to\infty} (\inf_{\Lambda} \|\rho^{\otimes n} - \Lambda(|\Psi\rangle\langle\Psi|^{\otimes m})\|_1) = 0\}, \tag{1.52}$$

where infimum is taken over all possible r and Λ represents the incoherent operation.

C. Distance based quantifier A distance based quantifier can be defined as the minimum distance between the given state ρ and the set of incoherent states σ. It can be expressed as [106]

$$C_D(\rho) = \min_{\sigma\in\mathcal{I}} \mathcal{D}(\rho, \sigma), \tag{1.53}$$

where $\mathcal{D}$ is the distance. In the following we will introduce some quantifier based on distance.

1. l_1-norm of coherence: For l_1-norm of coherence the distance is measured using the concept of matrix norm (in a vector space of matrices, vector norm corresponds to matrix norm). l_1-norm of coherence can be defined as [106]

$$C_{l_1}(\rho) = \min_{\sigma\in\mathcal{I}} \|\rho - \sigma\|_{l_1} = \sum_{i\neq j} |\rho_{i,j}|, \tag{1.54}$$

   where $\rho_{i,j} = \langle i|\rho|j\rangle$.

2. Relative entropy of coherence: In this case the distance is defined by the relative entropy between two states. It can be expressed as [106]

$$C_r(\rho) = \min_{\sigma\in\mathcal{I}} S(\rho|\sigma) = \min_{\sigma\in\mathcal{I}} \mathrm{Tr}\rho(\log_2 \rho - \log_2 \sigma). \tag{1.55}$$

Moreover, the relative entropy of coherence is equal to the distillable coherence [106, 114, 115]. Therefore, both of them can be expressed as a very simple compact expression

$$C_r(\rho) = C_d(\rho) = S(\rho^D) - S(\rho), \tag{1.56}$$

where ρ^D is the matrix constructed from ρ by removing all the off-diagonal elements

3. Geometric coherence: Geometric coherence is defined as [111]

$$C_g(\rho) = 1 - \max_{\sigma \in \mathcal{I}} F(\rho, \sigma) = \min_{\sigma \in \mathcal{I}} [1 - F(\rho, \sigma)], \tag{1.57}$$

where $F(\rho, \sigma) = [\mathrm{Tr}(\sqrt{\sqrt{\rho}\sigma\sqrt{\rho}})]^2$, is the fidelity [42, 43] between the states ρ and σ.

D. Coherence of formation Coherence of formation is a convex roof measure, i.e., given a coherence quantifier for all pure states one can extend it for mixed states by means of convex roof extension. Coherence of formation comes from the convex roof extension of distillable coherence for pure states. It can be expressed as [113, 114]

$$C_f(\rho) = \inf_{\{p_i, |\psi_i\rangle\}} p_i S\big(\Delta(|\psi_i\rangle\langle\psi_i|)\big) \tag{1.58}$$

where Δ is the dephasing operator which removes all the off-diagonal elements in a density matrix and infimum is taken over all the pure state ensembles $\{p_i, |\psi_i\rangle\}$ of $\rho = \sum_i p_i |\psi_i\rangle\langle\psi_i|$.

E. Coherence concurrence Coherence concurrence is another convex roof extension of l_1-norm of coherence. It can be expressed as [116]

$$C_{co}(\rho) = \inf_{\{p_i, |\psi_i\rangle\}} p_i C_{l_1}(|\psi_i\rangle\langle\psi_i|), \tag{1.59}$$

where infimum is taken over all the pure state decompositions of $\rho = \sum_i p_i |\psi_i\rangle\langle\psi_i|$.

1.7 Outline of the thesis

In this thesis, we have mainly discussed the characterization of two main resources in quantum information theory – entanglement and coherence. In this section, we give a very brief overview of our findings.

In the second chapter, we consider the characterization of the non-local properties of two-qubit states. Firstly, we discuss Bell-CHSH violation and its dependence on entanglement for pure states. For pure two-qubit states Bell-CHSH violation only depends on entanglement. However, for a mixed two-qubit states the situation is rather complex, as a mixed two-qubit state can be characterized by many parameters. Taking a two-qubit X-state, we show that non-local properties not only depends on purity and concurrence, but also depends on other functions of state parameters.

In the third chapter, we give an experimental scheme to measure entanglement (as characterized by negativity) for a two-qudit system. For this purpose, we use SLK-Bell inequality. For a particular measurement setting, we obtain a relation between Bell-SLK function and negativity for two-qudit pure states. It provides an operational way to detect and measure entanglement. Furthermore, we discuss our scheme for some classes of mixed states. We also discuss experimental feasibility of our scheme.

In the fourth chapter, we provide a way to completely characterize six SLOCC classes of three-qubit pure states. We construct a few observables to separate these classes from one another. We will show that the measurement of only one observable is enough to separate the GHZ class from rest of the classes. Taking a few classes of mixed states, we also discuss the usefulness of these observables. Furthermore, we discuss a teleportation protocol and show that these observables can be related to the teleportation fidelity.

In the fifth chapter, we discuss a possible connection between coherence and steering for three-qubit states. In this chapter, we discuss a steering scenario where the state of one party, Alice, can be steered only by the joint effort of the two other parties, Bob and Charlie. Moreover, we construct some coherence steerability criteria to detect these kind of states.

In the final chapter, we have characterized the coherence of quantum channels using C-J isomorphism. For a fixed purity, we find out the allowed range of coherence and depict them in coherence-purity diagrams. We characterize coherence of unital, non-unital, incoherent and other well-known qubit channels. Coherence-purity diagrams may be useful to distinguish different qubit channels, like unital and non-unital. Furthermore, we discuss a complementarity relation between Holevo quantity and coherence of channels. Finally, we summarize.

Chapter 2

Two-qubit entanglement and optimal Bell-CHSH value

In 1964, Bell formulated the idea of EPR paper in terms of local hidden variable model and proved that quantum mechanics cannot be described by any local hidden variable model [3]. Bell established this by means of an inequality, famously known as Bell inequality, which shows violation for a singlet state of two qubits [3, 78]. Later, it was shown that some other states also violate this inequality and thus forbid a local-realistic description for them. All these led to a very natural question – whether this contradiction between quantum theory and local realism is typical or it is restricted to some very special cases. The answer to this question came in 1991 when Gisin [121] showed that any pure entangled state of a bipartite system violates a version of Bell's inequality, popularly known as the Clauser-Horne-Shimony-Holt (CHSH) inequality [78]. From here we can highlight that entanglement is the main essence of nonlocality in quantum mechanics and Bell inequality serves as an operational way to detect it. However, the situation is far from simple for a mixed two-qubit state. Since there exist entangled states which do not violate Bell-CHSH inequality [77]. Hence, Bell inequality is a sufficient condition for entanglement detection, but not a necessary one.

2.1 Bell-CHSH Inequality

In a typical Bell experiment, a source prepares an entangled state of two particles and send them to two spatially separated distant observers Alice and Bob. Alice and Bob both can measure two dichotomic observables $X \in \{1,2\}$ and $Y \in \{1,2\}$ with outcomes $A \in \{0,1\}$ and $B \in \{0,1\}$ respectively. The values assigned to X, Y, A and B are required to distinguish different possibilities and are purely conventional. For many runs of this experiment we will get a probability distribution $P(AB|XY)$ and from that we can calculate the expectation value $\langle A_X B_Y \rangle = \sum_{A,B} (-1)^{AB} P(AB|XY)$, for a given measurement choice of X and Y. Now if this probability distribution satisfies a local hidden variable model then one can show that

$$I_B = |\langle A_1 B_1 \rangle + \langle A_1 B_2 \rangle + \langle A_2 B_1 \rangle - \langle A_2 B_2 \rangle| \leqslant 2, \tag{2.1}$$

which is known as Bell-CHSH inequality [78].

2.1.1 Bell-CHSH Polytope

Mathematically, a polytope consist of some facets and some vertices. In fact the facets of a certain polytope corresponds to Bell inequalities [86]. A polytope can be represented uniquely by providing either the vertices or facets. In usual Bell-CHSH scenario, we have two parties, two measurements and two outcomes, illustrated as $(2,2,2)$ scenario. In a Bell experiment, we measure the joint outcome probabilities $P(AB|XY)$. The whole scenario can be characterized by sixteen joint probabilities. These probabilities satisfy normalization condition

$$\sum_{A,B=0,1} P(AB|XY) = 1 \qquad \text{for all} \quad X, Y = 1, 2, \tag{2.2}$$

and no-signalling condition

$$\begin{aligned} P(A|X) &\equiv \sum_{B=0,1} P(AB|XY) = 1 \qquad \text{for all} \quad A = 0,1 \,\text{and}\, X, Y = 1, 2, \\ P(B|Y) &\equiv \sum_{A=0,1} P(AB|XY) = 1 \qquad \text{for all} \quad B = 0,1 \,\text{and}\, X, Y = 1, 2. \end{aligned} \tag{2.3}$$

There are four normalization constraints and twelve no-signaling constraints. However, these constraints are not all independent. Using normalization constraints we can reduce the no-signaling conditions by four. Therefore, there will be a total of eight independent constraints. These eight constraints will reduce the joint probabilities space to eight from sixteen. This probability space can be represented as

$$P = [P(A_1), P(A_2), P(B_1), P(B_2), P(A_1B_1), P(A_1B_2), P(A_2B_1), P(A_2B_2)], \quad (2.4)$$

where $P(A_X) = P(0|X)$, $P(B_Y) = P(0|Y)$ and $P(A_XB_Y) = P(00|XY)$. As A_1, A_2, B_1 and B_2 can take two different values 0 and 1, there will be sixteen different points in the above said probability space. By connecting these points we can construct a local polytope, known as Bell-CHSH polytope [86]. The Bell-CHSH polytope is eight dimensional and described by sixteen vertices. Description of polytope in terms of vertices known as V-representation. One can find the facets of this polytope from V-representation by using a standard algorithm [122]. There will be twenty four facets as follows,

$$P(A_iB_j) \geqslant 0, \quad i = 1,2 \quad \text{and} \quad j = 1,2, \quad (2.5)$$

$$-P(A_i) + P(A_iB_j) \leqslant 0, \quad i = 1,2 \quad \text{and} \quad j = 1,2, \quad (2.6)$$

$$-P(B_j) + P(A_iB_j) \leqslant 0, \quad i = 1,2 \quad \text{and} \quad j = 1,2, \quad (2.7)$$

$$P(A_i) + P(B_j) - P(A_iB_j) \leqslant 1, \quad i = 1,2 \quad \text{and} \quad j = 1,2, \quad (2.8)$$

$$P(A_1) + P(B_2) - P(A_1B_1) - P(A_1B_2) + P(A_2B_1) - P(A_2B_2) \leqslant 1, \quad (2.9)$$

$$P(A_1) + P(B_1) - P(A_1B_1) - P(A_1B_2) - P(A_2B_1) + P(A_2B_2) \leqslant 1, \quad (2.10)$$

$$P(A_2) + P(B_2) + P(A_1B_1) - P(A_1B_2) - P(A_2B_1) - P(A_2B_2) \leqslant 1, \quad (2.11)$$

$$P(A_2) + P(B_1) - P(A_1B_1) + P(A_1B_2) - P(A_2B_1) - P(A_2B_2) \leqslant 1, \quad (2.12)$$

$$-P(A_1) - P(B_2) + P(A_1B_1) + P(A_1B_2) - P(A_2B_1) + P(A_2B_2) \leqslant 0, \quad (2.13)$$

$$-P(A_1) - P(B_1) + P(A_1B_1) + P(A_1B_2) + P(A_2B_1) - P(A_2B_2) \leqslant 0, \quad (2.14)$$

$$-P(A_2) - P(B_2) - P(A_1B_1) + P(A_1B_2) + P(A_2B_1) + P(A_2B_2) \leqslant 0, \quad (2.15)$$

$$-P(A_2) - P(B_1) + P(A_1B_1) - P(A_1B_2) + P(A_2B_1) + P(A_2B_2) \leqslant 0. \quad (2.16)$$

First sixteen inequalities are trivial, as they are the positivity condition of probabilities. The last eight inequalities are the famous CH inequalities [80] and are equivalent to Bell-CHSH inequalities [78]. Furthermore, these eight inequalities can be combined to a single inequality. If we interchange indices $B_1 \leftrightarrow B_2$ then we can get Eq. (2.9) and Eq. (2.13) from Eq. (2.10) and Eq. (2.14) respectively. Similarly we can get others from Eq. (2.10) and Eq. (2.14). Therefore, we can write these eight inequalities as a single inequality

$$1 \geqslant P(A_1) + P(B_1) - P(A_1B_1) - P(A_1B_2) - P(A_2B_1) + P(A_2B_2) \geqslant 0. \tag{2.17}$$

In the next subsection we will show the equivalency between Bell-CHSH inequality and CH inequality.

2.1.2 Equivalency of Bell-CHSH and CH

Let's consider the Bell-CHSH inequality [78]

$$-2 \leqslant \langle A_1B_1\rangle + \langle A_1B_2\rangle + \langle A_2B_1\rangle - \langle A_2B_2\rangle \leqslant 2. \tag{2.18}$$

The expectation value of A_1B_1 is

$$\langle A_1B_1\rangle = P(00|A_1B_1) - P(01|A_1B_1) - P(10|A_1B_1) + P(11|A_1B_1). \tag{2.19}$$

We can write $P(01|A_1B_1)$ as

$$\begin{aligned} P(01|A_1B_1) &= P(00|A_1B_1) + P(01|A_1B_1) - P(00|A_1B_1) \\ &= P(0|A_1) - P(00|A_1B_1). \end{aligned} \tag{2.20}$$

Similarly

$$P(10|A_1B_1) = P(0|B_1) - P(00|A_1B_1). \tag{2.21}$$

$$\begin{aligned} P(11|A_1B_1) &= 1 - \Big(P(00|A_1B_1) + P(01|A_1B_1) + P(10|A_1B_1)\Big) \\ &= 1 - P(00|A_1B_1) - P(0|A_1) + P(00|A_1B_1) - P(0|B_1) \\ &\quad + P(00|A_1B_1) \\ &= 1 - P(0|A_1) - P(0|B_1) + P(00|A_1B_1). \end{aligned} \tag{2.22}$$

Using (2.20), (2.21) and (2.22) in (2.19) we get,

$$\langle A_1B_1\rangle = 4P(00|A_1B_1) - 2P(0|A_1) - 2P(0|B_1) + 1. \tag{2.23}$$

Similarly we can find

$$\langle A_1B_2\rangle = 4P(00|A_1B_2) - 2P(0|A_1) - 2P(0|B_2) + 1, \tag{2.24}$$

$$\langle A_2B_1\rangle = 4P(00|A_2B_1) - 2P(0|A_2) - 2P(0|B_1) + 1 \text{ and} \tag{2.25}$$

$$\langle A_2B_2\rangle = 4P(00|A_2B_2) - 2P(0|A_2) - 2P(0|B_2) + 1. \tag{2.26}$$

Bell-CHSH inequality given in Eq. (2.18) can be written as

$$\begin{aligned}
-2 &\leqslant \langle A_1B_1\rangle + \langle A_1B_2\rangle + \langle A_2B_1\rangle - \langle A_2B_2\rangle \leqslant 2\\
-2 &\leqslant 4\Big[P(00|A_1B_1) + P(00|A_1B_2) + P(00|A_2B_1) - P(00|A_2B_2)\Big]\\
&\quad -4P(0|A_1) - 4P(0|B_1) + 2 \leqslant 2\\
-4 &\leqslant 4\Big[P(00|A_1B_1) + P(00|A_1B_2) + P(00|A_2B_1) - P(00|A_2B_2)\Big]\\
&\quad -4P(0|A_1) - 4P(0|B_1) \leqslant 0\\
1 &\geqslant P(0|A_1) + P(0|B_1) - P(00|A_1B_1) - P(00|A_1B_2)\\
&\quad -P(00|A_2B_1) + P(00|A_2B_2) \geqslant 0.
\end{aligned} \tag{2.27}$$

Equation (2.27) is same as given in (2.17). Hence, we proved the equivalency of Bell-CHSH inequality and CH inequality.

2.1.3 Tsirelson Bound

Bell-CHSH inequality implies that a value of I_B more than two corresponds to violation of local-realism. Now one may ask: is there any upper limit to the correlations between distant events imposed by quantum mechanics? Tsirelson showed that indeed there is an upper limit of $2\sqrt{2}$ imposed by quantum mechanics [123]. We can see this as follows. Squaring the Bell-CHSH operator in (2.1) we get

$$I_B^2 = 4 + [A_1, A_2][B_1, B_2]. \tag{2.28}$$

For any bounded operator the following relation will hold

$$||[A, B]|| \leqslant ||AB|| + ||BA|| \leqslant 2||A||||B||, \tag{2.29}$$

where $||\cdot||$ represents the trace norm. As $||A|| \leqslant 1$ and $||B|| \leqslant 1$, we find

$$|I_B| \leqslant 2\sqrt{2}. \tag{2.30}$$

Quantum mechanics does not allow any larger violation than this. However, Popesu and Rohrlich formulated a correlation, known as PR box which can give $|I_B| = 4$ [124]. It demonstrates that we can construct a theory which respect no-signalling principle but violates quantum mechanics. But till now we have not seen this kind of correlation in nature.

2.2 Measurement settings and Bell-CHSH operator value

In this section, we will discuss the importance of measurement settings for the violation of Bell-CHSH inequality. As we will see at the end of the section, if we do not choose wisely the measurement settings then even a maximally entangled state leads to no violation. In the following subsections, we will consider a few measurement settings and the corresponding Bell-CHSH value.

2.2.1 Setting 1

The Bell-CHSH function is

$$I_B = A_1B_1 + A_1B_2 + A_2B_1 - A_2B_2. \tag{2.31}$$

Let's consider the measurement settings $A_1 = \sigma_x$, $A_2 = \sigma_y$, $B_1 = \frac{1}{\sqrt{2}}(\sigma_x + \sigma_y)$ and $B_2 = \frac{1}{\sqrt{2}}(\sigma_x - \sigma_y)$. We will calculate the Bell-CHSH operator for a non maximally entangled state

$$|\psi\rangle = c_0|00\rangle + c_1|11\rangle, \tag{2.32}$$

where c_i's are the Schmidt coefficients and $\sum_i c_i^2 = 1$. Bell-CHSH value for this state is

$$\langle\psi|I_B|\psi\rangle = \langle I_B\rangle_{|\psi\rangle} = 2\sqrt{2}\mathcal{C}, \tag{2.33}$$

where $\mathcal{C} = 2c_0c_1$ is the concurrence [47, 48] of the state. One can always get this result if the measurement settings are chosen perpendicular to the basis of the state. To verify this we take a state in arbitrary direction as $|\psi_n\rangle = c_0|\hat{n}_+\hat{n}_+\rangle + c_1|\hat{n}_-\hat{n}_-\rangle$, where $\hat{n} = \sin\theta\cos\phi\hat{i} + \sin\theta\sin\phi\hat{j} + \cos\theta\hat{k}$. $|\hat{n}_+\rangle$ and $|\hat{n}_-\rangle$ are defined as follows

$$|\hat{n}_+\rangle = \begin{pmatrix} \cos\frac{\theta}{2} \\ e^{i\phi}\sin\frac{\theta}{2} \end{pmatrix} \quad \text{and} \quad |\hat{n}_-\rangle = \begin{pmatrix} e^{-i\phi}\sin\frac{\theta}{2} \\ -\cos\frac{\theta}{2} \end{pmatrix}. \tag{2.34}$$

As the measurement plane must be perpendicular to the state we choose two other unit vectors $\hat{m}_1 = \cos\theta\cos\phi\hat{i} + \cos\theta\sin\phi\hat{j} - \sin\theta\hat{k}$ and $\hat{m}_2 = -\sin\phi\hat{i} + \cos\phi\hat{j}$, such that $\hat{n}$, $\hat{m}_1$ and $\hat{m}_2$ are perpendicular to each other. We consider the measurement settings as

$$A_1 = \hat{m}_1 \cdot \vec{\sigma}, \;\; A_2 = \hat{m}_2 \cdot \vec{\sigma}, \tag{2.35}$$

$$B_1 = \frac{1}{\sqrt{2}}(\hat{m}_1 \cdot \vec{\sigma} + \hat{m}_2 \cdot \vec{\sigma}) \quad \text{and} \tag{2.36}$$

$$B_2 = \frac{1}{\sqrt{2}}(\hat{m}_1 \cdot \vec{\sigma} - \hat{m}_2 \cdot \vec{\sigma}). \tag{2.37}$$

The effect of the operators $\hat{n} \cdot \vec{\sigma}$, $\hat{m}_1 \cdot \vec{\sigma}$ and $\hat{m}_2 \cdot \vec{\sigma}$ on the basis state $|\hat{n}_+\rangle$ and $|\hat{n}_-\rangle$ can be described as

$$\hat{n} \cdot \vec{\sigma}|\hat{n}_+\rangle = |\hat{n}_+\rangle, \quad \hat{n} \cdot \vec{\sigma}|\hat{n}_-\rangle = |\hat{n}_-\rangle, \tag{2.38}$$

$$\hat{m}_1 \cdot \vec{\sigma}|\hat{n}_+\rangle = |\hat{n}_-\rangle, \quad \hat{m}_1 \cdot \vec{\sigma}|\hat{n}_-\rangle = |\hat{n}_+\rangle, \tag{2.39}$$

$$\hat{m}_2 \cdot \vec{\sigma}|\hat{n}_+\rangle = i|\hat{n}_-\rangle, \quad \hat{m}_2 \cdot \vec{\sigma}|\hat{n}_-\rangle = -i|\hat{n}_+\rangle. \tag{2.40}$$

Using (2.38-2.40) we obtain the expectation value of the Bell-CHSH operator for the state $|\psi_n\rangle$ as

$$\langle I_B\rangle_{|\psi_n\rangle} = 4\sqrt{2}c_0c_1 = 2\sqrt{2}\mathcal{C}. \tag{2.41}$$

Therefore, for two-qubit pure states, we will always obtained maximum violation for maximally entangled state if the measurement settings are perpendicular to the state vector. But this result is not optimal. As we can see the state which have $\mathcal{C} < \frac{1}{\sqrt{2}}$ will not show any violation. Although this kind of measurement setting does not give optimal violation of CHSH inequality, but is useful to measure entanglement of the state.

2.2.2 Setting 2

Now consider another measurement settings as follows

$$A_1 = \sigma_z, \;\; A_2 = \sigma_x, B_1 = \frac{1}{\sqrt{2}}(\sigma_z + \sigma_x) \text{ and } B_2 = \frac{1}{\sqrt{2}}(\sigma_z - \sigma_x). \tag{2.42}$$

For these measurement setting the expectation value of the Bell-CHSH operator for the state $|\psi\rangle$ given in Eq. (2.32) is

$$\langle I_B \rangle_{|\psi\rangle} = \sqrt{2}(1+\mathcal{C}). \tag{2.43}$$

Similarly as in the previous case we can find this relation for an arbitrary state $|\psi_n\rangle = c_0|\hat{n}_+\hat{n}_+\rangle + c_1|\hat{n}_-\hat{n}_-\rangle$. Here we have to use the measurement settings in the following way

$$A_1 = \hat{n}\cdot\vec{\sigma}, \;\; A_2 = \hat{m}\cdot\vec{\sigma}, \tag{2.44}$$

$$B_1 = \frac{1}{\sqrt{2}}(\hat{n}\cdot\vec{\sigma} + \hat{m}\cdot\vec{\sigma}) \quad \text{and} \tag{2.45}$$

$$B_2 = \frac{1}{\sqrt{2}}(\hat{n}\cdot\vec{\sigma} - \hat{m}\cdot\vec{\sigma}), \tag{2.46}$$

where $\hat{n}$ and $\hat{m}$ are perpendicular to each other. Again doing similar kind of calculation one can check that the expectation value of Bell-CHSH operator for these measurement settings with $|\psi_n\rangle$ is

$$\langle I_B \rangle_{|\psi_n\rangle} = \sqrt{2}(1+\mathcal{C}). \tag{2.47}$$

In this case also maximally entangled state gives maximum violation. However, this is not an optimal settings for any non maximally entangle state. Since we will not find violation until $\mathcal{C} > \sqrt{2}-1$. Here also one can easily find the entanglement of state experimentally.

2.2.3 Setting 3

Let's consider another measurement settings

$$A_1 = \sigma_z, \;\; A_2 = \sigma_x, B_1 = \cos\chi\sigma_z + \sin\chi\sigma_x \text{ and } B_2 = \cos\chi\sigma_z - \sin\chi\sigma_x, \tag{2.48}$$

where $\cos\chi = \frac{1}{\sqrt{1+\mathcal{C}^2}}$. The expectation value of the Bell-CHSH operator for these settings is

$$\langle I_B \rangle_{|\psi\rangle} = 2\sqrt{1+\mathcal{C}^2}. \tag{2.49}$$

We can easily generalize this as done in the previous cases. In this case we have to consider the measurement settings as follows [125]

$$A_1 = \hat{n}\cdot\vec{\sigma}, \;\; A_2 = \hat{m}\cdot\vec{\sigma}, \tag{2.50}$$

$$B_1 = \cos\chi\hat{n}\cdot\vec{\sigma} + \sin\chi\hat{m}\cdot\vec{\sigma} \quad \text{and} \tag{2.51}$$

$$B_2 = \cos\chi\hat{n}\cdot\vec{\sigma} - \sin\chi\hat{m}\cdot\vec{\sigma}, \tag{2.52}$$

where $\hat{n}$ and $\hat{m}$ are perpendicular to each other. After doing a similar kind of calculation we find

$$\langle I_B \rangle_{|\psi_n\rangle} = 2\sqrt{1+\mathcal{C}^2}. \tag{2.53}$$

From Eq. (2.53) it is clear that we will get violation as soon as $\mathcal{C} \neq 0$. $\mathcal{C} = 0$ means the state is not entangled. For this measurement settings any entangled two-qubit pure state will show violation. These settings are useful to get optimal violation for any non maximally entangled pure state. But these are not experimentally realizable, as you need to know the χ which depends on the state parameter. From an experimental point of view these settings are not useful to measure the entanglement of an unknown state.

2.2.4 Most General Setting

So far we have seen that the measurement setting are in the plane or perpendicular plane of the state vector. Here we will consider a most general measurement setting as follows $A_1 = \sigma_x \sin\theta_1 \cos\phi_1 + \sigma_y \sin\theta_1 \sin\phi_1 + \sigma_z \cos\theta_1$, $A_2 = \sigma_x \sin\theta_2 \cos\phi_2 + \sigma_y \sin\theta_2 \sin\phi_2 + \sigma_z \cos\theta_2$ and $B_1 = \sigma_x \sin\theta_3 \cos\phi_3 + \sigma_y \sin\theta_3 \sin\phi_3 + \sigma_z \cos\theta_3$, $B_2 = \sigma_x \sin\theta_4 \cos\phi_4 + \sigma_y \sin\theta_4 \sin\phi_4 + \sigma_z \cos\theta_4$. For this measurement setting the expectation value of the Bell-CHSH operator for the state $|\psi\rangle = c_0|00\rangle + c_1|11\rangle$ is

$$\begin{aligned}\langle I_B \rangle_{|\psi\rangle} \;&=\; \cos\theta_1(\cos\theta_2 + \cos\theta_4) + \cos\theta_3(\cos\theta_2 - \cos\theta_4) + \\ &\quad\; \mathcal{C}\Big[\sin\theta_1\big(\sin\theta_2\cos(\phi_1+\phi_2) + \sin\theta_4\cos(\phi_1+\phi_4)\big) \\ &\quad\; + \sin\theta_3\big(\sin\theta_2\cos(\phi_2+\phi_3) - \sin\theta_4\cos(\phi_3+\phi_4)\big)\Big].\end{aligned} \tag{2.54}$$

We rewrite Eq. (2.54) as $\langle I_B \rangle_{|\psi\rangle} = K + \mathcal{C}G$, where

$$K = \cos\theta_1(\cos\theta_2 + \cos\theta_4) + \cos\theta_3(\cos\theta_2 - \cos\theta_4) \quad \text{and} \tag{2.55}$$

$$\begin{aligned}G &= \sin\theta_1\big(\sin\theta_2\cos(\phi_1+\phi_2) + \sin\theta_4\cos(\phi_1+\phi_4)\big) \\ &\quad + \sin\theta_3\big(\sin\theta_2\cos(\phi_2+\phi_3) - \sin\theta_4\cos(\phi_3+\phi_4)\big).\end{aligned} \tag{2.56}$$

One can check that K is always less than or equal to 2. We will see violation only if the term G contribute. Hence, it means that a product state will not show any violation. Interestingly we can always measure entanglement from these kind of measurement settings. We see that for a pure state the Bell-CHSH operator value only depend on the entanglement of the state. However, since the value of Bell-CHSH operator depends on the measurement settings, we would be able to find settings for which even a less entangled state would show a greater violation than a maximal entangled state. Lets take a entangled state of concurrence $\mathcal{C} = 0.5$. For this state we get $\langle I_B \rangle_{|\psi\rangle} \approx 2.234$ for the measurement settings $\theta_1 = \frac{\pi}{18}$, $\theta_2 = \frac{\pi}{18}$, $\theta_3 = \frac{5\pi}{18}$, $\theta_4 = \frac{5\pi}{18}$, $\phi_1 = 0$, $\phi_2 = \pi$, $\phi_3 = \pi$ and $\phi_4 = 0$. We can find a measurement settings for which a maximally entangled state i.e., $\mathcal{C} = 1$ will give less violation. As an example for the measurement settings $\theta_1 = \frac{4\pi}{9}$, $\theta_2 = \frac{17\pi}{18}$, $\theta_3 = \frac{16\pi}{18}$, $\theta_4 = \frac{\pi}{18}$, $\phi_1 = 0$, $\phi_2 = 0$, $\phi_3 = \frac{\pi}{18}$ and $\phi_4 = \frac{13\pi}{9}$ we get $\langle I_B \rangle_{|\psi\rangle} \approx 2.05$, which is very less than the previous example. It is interesting to note that we can even find measurement settings for which a maximally entangled state will not show any violation. We are providing two examples here. i) We will get $I = 0.5$ for the measurement settings $\theta_1 = \frac{5\pi}{6}, \theta_2 = \frac{4\pi}{9}, \theta_3 = \frac{4\pi}{9}, \theta_4 = \frac{17\pi}{18}, \phi_1 = 0, \phi_2 = \frac{\pi}{9}, \phi_3 = \pi$ and $\phi_4 = \frac{14\pi}{9}$. ii) $I = 1.1$ for the measurement settings $\theta_1 = \frac{8\pi}{9}, \theta_2 = \frac{7\pi}{9}, \theta_3 = \frac{13\pi}{18}, \theta_4 = \frac{8\pi}{9}, \phi_1 = 0, \phi_2 = 0, \phi_3 = \frac{8\pi}{9}$ and $\phi_4 = \frac{13\pi}{9}$. We can find many measurement settings for which maximally entangled state will not show any violation. Hence, to show Bell-CHSH violation entanglement as well as measurement settings are both very important.

2.3 Optimal Bell-CHSH violation

In the previous subsection we have discussed the importance of measurement settings for the Bell-CHSH operator value. However, given a state what is the maximum value of the Bell-CHSH operator and which measurement settings will provide that optimal value is an important question. Horodecki et. al. [126] in 1995 provided the answer to this question. In this section we will give a derivation of their proof for the maximum Bell-CHSH operator value for a two-qubit state ρ and the corresponding measurement settings. A two-qubit state ρ can be represented in Hilbert-Schmidt basis as

$$\rho = \frac{1}{4}\Big(I \otimes I + \mathbf{r} \cdot \boldsymbol{\sigma} \otimes I + I \otimes \mathbf{s} \cdot \boldsymbol{\sigma} + \sum_{n,m=1}^{3} t_{nm} \sigma_n \otimes \sigma_m\Big), \tag{2.57}$$

where I stands for identity operator, σ_n are the Pauli matrices, $\mathbf{r}$ and $\mathbf{s}$ are vectors in three dimension. $t_{nm} = \text{Tr}(\rho\sigma_n \otimes \sigma_m)$ form a real matrix which is denoted by T_ρ. Using $\text{Tr}(\rho^2)$, one can get

$$\sum_{i=1}^{3}\left(r_i^2 + s_i^2\right) + \sum_{n,m=1}^{3} t_{nm}^2 \leq 3, \tag{2.58}$$

where the equality is achieved for pure states. The operator associated with the Bell-CHSH inequality can be written as

$$I_B = \mathbf{a}\cdot\boldsymbol{\sigma}\otimes(\mathbf{b}+\mathbf{b}')\cdot\boldsymbol{\sigma} + \mathbf{a}'\cdot\boldsymbol{\sigma}\otimes(\mathbf{b}-\mathbf{b}')\cdot\boldsymbol{\sigma}, \tag{2.59}$$

where $\mathbf{a}, \mathbf{a}', \mathbf{b}, \mathbf{b}'$ are unit vectors in R^3. As $\text{Tr}(\sigma_i) = 0$, we get

$$\begin{aligned} \langle I\rangle_\rho &= \text{Tr}(\rho S) \qquad (2.60)\\ &= \frac{1}{4}\text{Tr}\Big[\big(\sum_{n,m} t_{nm}\sigma_n\otimes\sigma_m\big)\big(\mathbf{a}\cdot\boldsymbol{\sigma}\otimes(\mathbf{b}+\mathbf{b}')\cdot\boldsymbol{\sigma} + \mathbf{a}'\cdot\boldsymbol{\sigma}\otimes(\mathbf{b}-\mathbf{b}')\cdot\boldsymbol{\sigma}\big)\Big]. \end{aligned}$$

After doing a few step of calculation and using $\text{Tr}(\sigma_i^2) = 2$, we find

$$\begin{aligned} \langle I\rangle_\rho &= \sum_{n,m=1}^{3} t_{nm}a_n(b+b')_m + \sum_{n,m=1}^{3} t_{nm}a_n{}'(b-b')_m \\ &= \Big(\mathbf{a}, T_\rho(\mathbf{b}+\mathbf{b}')\Big) + \Big(\mathbf{a}', T_\rho(\mathbf{b}-\mathbf{b}')\Big). \end{aligned} \tag{2.61}$$

We introduce a pair of mutual orthogonal vector such as

$$\mathbf{b}+\mathbf{b}' = 2\cos\chi\mathbf{c}; \quad \mathbf{b}-\mathbf{b}' = 2\sin\chi\mathbf{c}', \tag{2.62}$$

where $\chi \in [0, \frac{\pi}{2}]$ and $\mathbf{c}$, $\mathbf{c}'$ are the unit vectors. Hence, $\max\langle I\rangle_\rho$ will take the form

$$\max\langle I\rangle_\rho = \max\ 2\big[(\mathbf{a}, T_\rho\mathbf{c})\cos\chi + (\mathbf{a}', T_\rho\mathbf{c}')\sin\chi\big]. \tag{2.63}$$

The maximal value of $(\mathbf{a}, T_\rho\mathbf{c})$ is $\parallel T_\rho\mathbf{c} \parallel$ obtained when $\mathbf{a}$ is chosen parallel to $T_\rho\mathbf{c}$. Similarly for the second term. By choosing $\mathbf{a}$ and $\mathbf{a}'$ in this way, we get

$$\max\langle I\rangle_\rho = \max\ 2\big(\cos\chi \parallel T_\rho\mathbf{c} \parallel + \sin\chi \parallel T_\rho\mathbf{c}' \parallel\big). \tag{2.64}$$

As, $\max(\cos\chi x + \sin\chi y) = \sqrt{x^2+y^2}$ when we choose $\cos\chi = \dfrac{x}{\sqrt{x^2+y^2}}$ and $\sin\chi = \dfrac{y}{\sqrt{x^2+y^2}}$, we obtain

$$\max\langle I\rangle_\rho = \max\ 2\sqrt{\parallel T_\rho\mathbf{c} \parallel^2 + \parallel T_\rho\mathbf{c}' \parallel^2}, \tag{2.65}$$

where, $\parallel T_\rho \mathbf{c} \parallel^2 = \left(\mathbf{c}, {T_\rho}^t T_\rho \mathbf{c}\right)$ and ${T_\rho}^t T_\rho$ is a positive orthogonal matrix. Here t represents transposition. We can maximize Eq. (2.65) by choosing $\mathbf{c}$ and $\mathbf{c}'$ as the two eigenvectors corresponding to two largest eigenvalues of the matrix ${T_\rho}^t T_\rho$. Therefore, the maximum value of Bell-CHSH operator with von-Neumann measurements on a generic two-qubit state ρ is

$$\max\langle I\rangle_\rho = 2\sqrt{\lambda_1 + \lambda_2}, \tag{2.66}$$

where λ_1 and λ_2 are the two largest eigenvalues of the orthogonal matrix ${T_\rho}^t T_\rho$ [126].

2.4 Mixed state

So far we have seen that the optimal Bell-CHSH value (expectation value of Bell-CHSH operator) for pure state just depend on a single parameter concurrence which is a measure of entanglement. But for mixed state the situation is not that simple. There are many parameters which characterize a mixed state. It is a general consensus that the nonlocal feature of a mixed state can be characterized by purity and entanglement. But here in this section we will show that not only these two are required but also it depends on other functions of state parameters as well. Recently Mendonça et. al. have shown that a two-qubit X-state can cover all purity and concurrence region in a concurrence-purity diagram of two-qubit state [127]. So rather than taking a most general mix state we choose X-state to characterize its optimal Bell-CHSH value with purity, concurrence and other functions of state parameters of X-state. Recently in [128], author have studied teleportation fidelity with respect to purity, concurrence and other functions of state parameters of two-qubit X-state.

X-state	
Rank 1	$(x = \mathcal{H}, y = 0, \mathcal{A} = 0)$ or $(x = 0, y = \mathcal{G}, \mathcal{B} = 0)$
Rank 2	$(x < \mathcal{H}, y = 0, \mathcal{A} = 0)$ or $(x = 0, y < \mathcal{G}, \mathcal{B} = 0)$ or $(x = \mathcal{H}, y = \mathcal{G}, \mathcal{AB} > 0)$
Rank 3	$(x < \mathcal{H}, y = \mathcal{G}, \mathcal{A} > 0)$ or $(x = \mathcal{H}, y < \mathcal{G}, \mathcal{B} > 0)$
Rank 4	$(x < \mathcal{H}, y < \mathcal{G}, \mathcal{AB} > 0)$

Table 2.1: Parameterization of two-qubit X-state for different rank

2.4.1 Two-qubit X-state

In [127], Mendonça et. al. proposed a parametric from of two-qubit X-state which can be represented as

$$\rho_{AB} = \begin{pmatrix} \cos^2\theta & 0 & 0 & \sqrt{x}e^{i\mu} \\ 0 & \sin^2\theta\cos^2\phi & \sqrt{y}e^{i\nu} & 0 \\ 0 & \sqrt{y}e^{-i\nu} & \sin^2\theta\sin^2\phi\cos^2\psi & 0 \\ \sqrt{x}e^{-i\mu} & 0 & 0 & \sin^2\theta\sin^2\phi\sin^2\psi \end{pmatrix}. \tag{2.67}$$

Here $x, y \geq 0$, $\mu, \nu \in [0, 2\pi]$ and $\theta, \phi, \psi \in [0, \frac{\pi}{2}]$. However, we need two further conditions to make it a valid density matrix. Eq. (2.67) will be a valid density matrix if $x \in [0, \mathcal{H}]$ and $y \in [0, \mathcal{G}]$, where $\mathcal{H} = \sin^2\theta\cos^2\theta\sin^2\phi\sin^2\psi$ and $\mathcal{G} = \sin^4\theta\cos^2\phi\sin^2\phi\cos^2\psi$. These two condition will make sure that the matrix in Eq. (2.67) is positive semidefinite. The rank of X-state depends on the restriction on these parameters as specified in [127]. Table (1.1) gives the parameter specification for different rank of two-qubit X-state.

Here the definition of $\mathcal{A}$ and $\mathcal{B}$ are as follows $\mathcal{A} = \sin^2\theta(1 - \sin^2\phi\sin^2\psi)$ and $\mathcal{B} = 1 - \mathcal{A}$. The purity and concurrence of a two-qubit X-state given in Eq. (2.67) are [127]

$$\mathcal{P} = 1 - 2\big(\mathcal{AB} + \mathcal{G} - y + \mathcal{H} - x\big) \quad \text{and} \tag{2.68}$$

$$\mathcal{C} = 2 \max\left[\sqrt{x} - \sqrt{\mathcal{G}}, \sqrt{y} - \sqrt{\mathcal{H}}\right]. \tag{2.69}$$

Now one can find out the optimal Bell-CHSH value by finding the eigenvalues of the orthogonal matrix $(T_{\rho_{AB}})^t T_{\rho_{AB}}$. For our future convenience we will represent this orthogonal matrix by $\mathcal{T}$. The eigenvalues of $\mathcal{T}$ are $4(\sqrt{x}-\sqrt{y})^2$, $4(\sqrt{x}+\sqrt{y})^2$ and $(\cos^2\theta - e\sin^2\theta)^2$, where $e = \cos^2\phi + \cos 2\psi \sin^2\phi$. The largest between first and third eigenvalue will decide the optimal Bell-CHSH value of the X-state. The details characterization of optimal Bell-CHSH value for two-qubit X-state of different ranks are as follows. Note that rank-one state corresponds to pure state. As we have already discussed about pure state scenario in a greater detail, we will start with rank-two X-state.

2.4.1.1 Rank-two X-state

First kind Rank-two X-state of first kind can be parameterized by $(x < \mathcal{H}, y = 0, \mathcal{A} = 0)$. $\mathcal{A} = 0$ corresponds to two solution as follows, $\theta = 0$ or $\phi = \psi = \frac{\pi}{2}$. But the first one is not possible due to the following fact. For $\theta = 0$, $\mathcal{H} = 0$ and hence $x < \mathcal{H} = 0$. But by definition x is positive. So this is not a valid solution. Now for the other solution, we have

$$\mathcal{P} = 1 + 2x - 2\sin^2\theta + 2\sin^4\theta \quad \text{and} \tag{2.70}$$

$$\mathcal{C} = 2\sqrt{x}. \tag{2.71}$$

Eigenvalues of the $\mathcal{T}$ matrix are 1, $4x$ and $4x$. As $x < \mathcal{H} = \sin^2\theta\cos^2\theta \leq \frac{1}{4}$. So the optimal Bell-CHSH value is

$$\mathcal{B} = 2\sqrt{\mathcal{M}}, \tag{2.72}$$

where $\mathcal{M} = 1 + 4x$ is the sum of the two largest eigenvalues of the matrix $\mathcal{T}$. Using Eq. (2.71) one can show that $\mathcal{B} = 2\sqrt{1+\mathcal{C}^2}$. Hence, as soon as the state is entangled, we will get Bell-CHSH violation. This relation is similar to the optimal Bell-CHSH violation of a pure state as given in Eq. (2.53).

Second kind $(x = 0, y < \mathcal{G}, \mathcal{B} = 0)$ represents the rank-two X-state of second kind. Here $\mathcal{B} = 0$ also provides two solution, $\theta = \frac{\pi}{2}$, $\phi = 0$ and $\theta = \frac{\pi}{2}$, $\psi = 0$. But again the following argument will show that the first solution is not possible. For $\theta = \frac{\pi}{2}$ and $\phi = 0$ $\mathcal{G} = 0$, which makes y negative. This is not possible as by definition y is positive. Using the other solution we find

$$\mathcal{P} = 1 + 2y - 2\sin^2\phi\cos^2\phi \quad \text{and} \tag{2.73}$$

$$\mathcal{C} = 2\sqrt{y}. \tag{2.74}$$

The eigenvalues of the $\mathcal{T}$ matrix are 1, $4y$ and $4y$. Again one can easily check that the maximum value of $\mathcal{G}$ is $\frac{1}{4}$ and hence, $y < \frac{1}{4}$. Therefore, optimal Bell-CHSH value is

$$\mathcal{B} = 2\sqrt{\mathcal{M}}, \tag{2.75}$$

where $\mathcal{M} = 1 + 4y$. Eq. (2.75) can be written as $\mathcal{B} = 2\sqrt{1 + \mathcal{C}^2}$ and this is similar to the first kind.

Third kind Rank-two X-state of third kind can be represented as $(x = \mathcal{H}, y = \mathcal{G}, \mathcal{AB} > 0)$. If we choose $x > y$ then

$$\mathcal{P} = 1 + 2r\sin^2\theta + 2r^2\sin^4\theta \quad \text{and} \tag{2.76}$$

$$\mathcal{C} = 2\sqrt{x} - 2\sqrt{y}, \tag{2.77}$$

where $r = -1 + \sin^2\phi\sin^2\psi$. Here the eigenvalues of the matrix $\mathcal{T}$ are $4(\sqrt{x} - \sqrt{y})^2$, $4(\sqrt{x} + \sqrt{y})^2$ and $(\cos^2\theta - e\sin^2\theta)^2$. For this we will get two choices of optimal Bell value. For the first choice we choose $4(\sqrt{x} - \sqrt{y})^2 > (\cos^2\theta - e\sin^2\theta)^2$. For this choice $\mathcal{M} = 4(\sqrt{x} - \sqrt{y})^2 + 4(\sqrt{x} + \sqrt{y})^2$. Using Eq. (2.77) we can show that

$$\mathcal{B} = 2\sqrt{\mathcal{M}} = 2\sqrt{\mathcal{C}^2 + (\mathcal{C} + 4\sqrt{y})^2}. \tag{2.78}$$

For the other choice, i.e., $4(\sqrt{x} - \sqrt{y})^2 < (\cos^2\theta - e\sin^2\theta)^2$, we have

$$\mathcal{M} = 4(\sqrt{x} + \sqrt{y})^2 + (\cos^2\theta - e\sin^2\theta)^2. \tag{2.79}$$

We get $\sin^2\theta = \frac{-1\pm\sqrt{2\mathcal{P}-1}}{2r}$ by solving the Eq. (2.76) for $\sin^2\theta$. Using this and Eq. (2.77) in Eq. (2.79) we get

$$\mathcal{M} = (\mathcal{C} + 4\sqrt{y})^2 + \left(1 - (1+e)\frac{-1 \pm \sqrt{2\mathcal{P} - 1}}{2r}\right)^2. \tag{2.80}$$

As $2r = -(1+e)$ we obtain

$$\mathcal{B} = 2\sqrt{\mathcal{M}} = 2\sqrt{(\mathcal{C} + 4\sqrt{y})^2 + 2\mathcal{P} - 1}. \tag{2.81}$$

From this expression it is clear that by keeping $\mathcal{C}$ and y fixed one can increase $\mathcal{B}$ with purity. For the other case i.e., by keeping $\mathcal{P}$ and y fixed one can increase $\mathcal{B}$ with $\mathcal{C}$ as well. This can be easily verified by looking at the Fig.4.2 and Fig.4.3. In this regard it is different from the pure state case. There optimal Bell-CHSH value only depend on the entanglement. But here it depends not only on entanglement but also on other function of state parameters. Here we will provide one interesting example. Consider a state with $y = 0.001$, $\mathcal{P} = 0.7$ and $\mathcal{C} = 0.65$. For this state we get maximum optimal Bell-CHSH value $\mathcal{B} \approx 2.03014$, with $\theta \approx 0.67795$, $\phi \approx 0.84216$ and $\psi \approx 1.36286$. Now lets consider another state with $y = 0.001$, $\mathcal{P} = 0.8$ and $\mathcal{C} = 0.6$. This will give maximum optimal Bell-CHSH value $\mathcal{B} \approx 2.12395$ with $\theta \approx 0.53695$, $\phi \approx 0.89259$ and $\psi \approx 1.32081$. Hence a less entangled state with more purity can give more optimal Bell-CHSH value. Similar kind of situation has been discussed taking teleportation fidelity in [128]. Now, when $y > x$ then we will get a similar kind of trend only differences are $\mathcal{C} = 2\sqrt{y} - 2\sqrt{x}$ and in the expression of $\mathcal{B}$, y will be replaced by x.

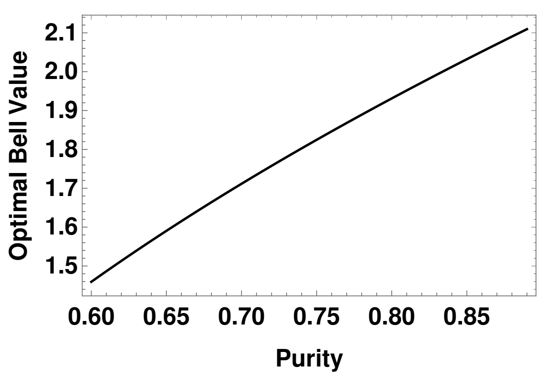

Figure 2.1: Variation of optimal Bell-CHSH value with purity for $\mathcal{C} = 0.45$ and $y = 0.001$ for rank-two X-state of third kind.

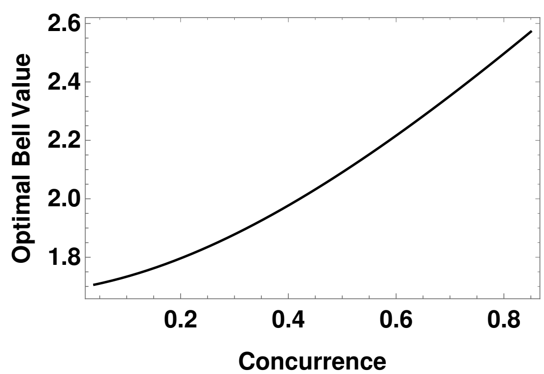

Figure 2.2: Variation of optimal Bell-CHSH value with concurrence for $\mathcal{P} = 0.85$ and $y = 0.001$ for rank-two X-state of third kind.

2.4.1.2 Rank-three X-state

First kind Rank-three X-state of first kind can be represented as $(x < \mathcal{H}, y = \mathcal{G}, \mathcal{A} > 0)$. The purity of this kind of X-state is

$$\mathcal{P} = 1 + 2x - 2\sin^2\theta + 2d\sin^4\theta, \tag{2.82}$$

where $d = 1 - \sin^2\phi\sin^2\psi + \sin^4\phi\sin^4\psi$. Now lets consider $x > y$. Hence, $\mathcal{H} > x > y = \mathcal{G}$. So the concurrence of this kind of state is

$$\mathcal{C} = 2(\sqrt{x} - \sqrt{\mathcal{G}}) = 2(\sqrt{x} - f\sin^2\theta), \tag{2.83}$$

where $f = \cos\phi\sin\phi\cos\psi$. Suppose $4(\sqrt{x}-\sqrt{y})^2 > (\cos^2\theta - e\sin^2\theta)^2$ then $\mathcal{M} = 4(\sqrt{x}+\sqrt{y})^2 + 4(\sqrt{x}-\sqrt{y})^2$ and $\mathcal{B} = 2\sqrt{\mathcal{M}} = 2\sqrt{\mathcal{C}^2 + (\mathcal{C}+4\sqrt{y})^2}$. Now for the other choice, i.e.,$4(\sqrt{x}-\sqrt{y})^2 < (\cos^2\theta - e\sin^2\theta)^2$, we have $\mathcal{M} = 4(\sqrt{x}+\sqrt{y})^2 + (\cos^2\theta - e\sin^2\theta)^2$. Now using $\mathcal{C} = 2(\sqrt{x} - f\sin^2\theta)$, we get

$$\mathcal{M} = (\mathcal{C} + 4f\sin^2\theta)^2 + (1-(1+e)\sin^2\theta)^2. \tag{2.84}$$

Replacing x by $(\frac{\mathcal{C}}{2} + f\sin^2\theta)^2$ in purity expression given in Eq. (2.82) and solving for $\sin^2\theta$ we get

$$\sin^2\theta = \mathcal{K}_1(\mathcal{C},\mathcal{P},d,f) = \frac{(1-\mathcal{C}f) \pm \sqrt{(1-\mathcal{C}f)^2 - (f^2+d)(\mathcal{C}^2+2-2\mathcal{P})}}{2(f^2+d)}. \tag{2.85}$$

As minimum value of $(1+e)$ is zero, so to achieve optimal Bell-CHSH value Eq. (2.84) suggest to take minus sign in the expression of $\sin^2\theta$. Finally we find

$$\mathcal{B} = 2\sqrt{\mathcal{M}} = 2\sqrt{\left[\mathcal{C} + 4f\mathcal{K}_1(\mathcal{C},\mathcal{P},d,f)\right]^2 + \left[1-(1+e)\mathcal{K}_1(\mathcal{C},\mathcal{P},d,f)\right]^2}. \tag{2.86}$$

From the above expression it is implicit that with fixed value of $\mathcal{C}$, d, e and f, $\mathcal{B}$ increases with $\mathcal{P}$, as $\mathcal{K}_1(\mathcal{C},\mathcal{P},d,f)$ decreases with $\mathcal{P}$. We will show this behavior graphically for a fixed value of $\phi = \frac{\pi}{3}$ and $\psi = \frac{\pi}{2}$. For this ϕ and ψ, $d = \frac{13}{16}$, $e = -\frac{1}{2}$ and $f = 0$. We plot $\mathcal{B}$ with purity for a fixed concurrence; it increases with purity as shown in Fig.2.3. Furthermore, if we plot $\mathcal{B}$ with concurrence for a fixed purity, we observe in Fig.2.4 that it increases with concurrence also. We see that Eq. (2.86) contains few more functions of state parameters except $\mathcal{P}$ and $\mathcal{C}$. In this regard we will describe an interesting example. Consider a state with $\mathcal{P} = 0.85$, $\mathcal{C} = 0.45$, $\phi = \frac{\pi}{3}$ and $\psi = \frac{\pi}{2}$ will give $\mathcal{B} \approx 2.06449$. This value of ϕ and ψ corresponds to $d = \frac{13}{16}$, $e = -\frac{1}{2}$ and $f = 0$. Now lets choose another state with $\mathcal{P} = 0.8$, $\mathcal{C} = 0.4$, $\phi = \frac{\pi}{2}$ and $\psi = \frac{11\pi}{25}$. For this state we get $d \approx 0.96612$, $e \approx -0.92978$, $f = 0$ and $\mathcal{B} \approx 2.13232$. From these two state we can conclude that the state with less entanglement and purity, still gives much better optimal Bell-CHSH value. The other state parameters ϕ and ψ or functions of state parameters d, e and f are also equally important for the optimal Bell-CHSH value. The ranges of d, e and f are as follows

$$\frac{3}{4} \leqslant d < 1, \tag{2.87}$$

$$-1 < e < 1, \text{ and} \tag{2.88}$$

$$0 \leqslant f < \frac{1}{2}. \tag{2.89}$$

Note that d, e and f are functions of state parameter ϕ and ψ. So they can not be varied independently. As the optimal Bell-CHSH value depends on these other functions of state parameters so we plot the variation of $\mathcal{B}$ with e and f in Fig.2.5 and Fig.2.6 respectively. Fig.2.5 and Fig.2.6 suggest that $\mathcal{B}$ decreases with e and increases with f respectively. From here we may say that the increment of e some how increases classicality in the system.

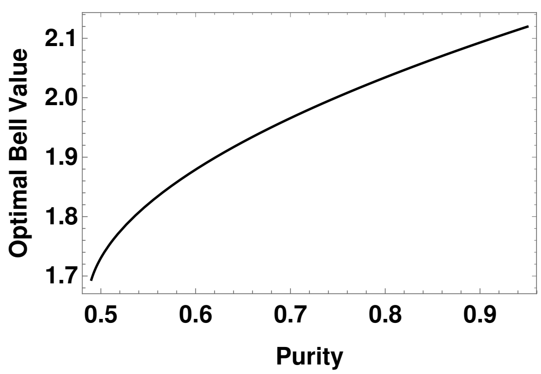

Figure 2.3: Variation of optimal Bell-CHSH value with purity for $\mathcal{C} = 0.45$, $d = \frac{13}{16}$, $e = -\frac{1}{2}$ and $f = 0$ for rank-three X-state of first kind.

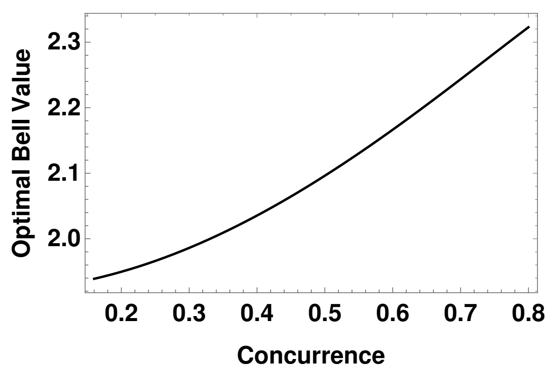

Figure 2.4: Variation of optimal Bell-CHSH value with concurrence for $\mathcal{P} = 0.85$, $d = \frac{13}{16}$, $e = -\frac{1}{2}$ and $f = 0$ for rank-three X-state of first kind.

Now when $y > x$, the concurrence will be

$$\mathcal{C} = 2(\sqrt{y} - \sqrt{\mathcal{H}}) = 2(\sqrt{y} - f' \sin\theta\cos\theta), \tag{2.90}$$

where $f' = \sin\phi\sin\psi$. If we choose $4(\sqrt{y} - \sqrt{x})^2 > (\cos^2\theta - e\sin^2\theta)^2$ then using Eq. (2.90) we get

$$\mathcal{B} = 2\sqrt{\mathcal{M}} = 2\sqrt{2\big[(\mathcal{C} + 2f' \sin\theta\cos\theta)^2 + 4x\big]}. \tag{2.91}$$

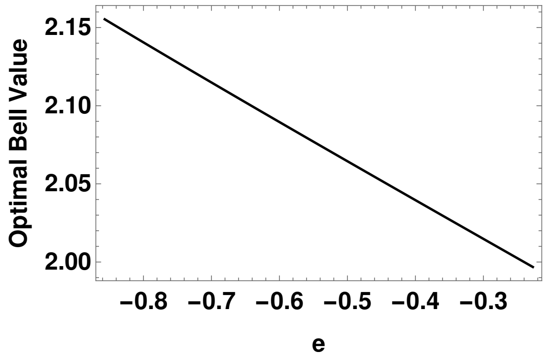

Figure 2.5: Variation of optimal Bell-CHSH value with e for $\mathcal{P} = 0.85, \mathcal{C} = 0.45$, and $f = 0$ for rank-three X-state of first kind.

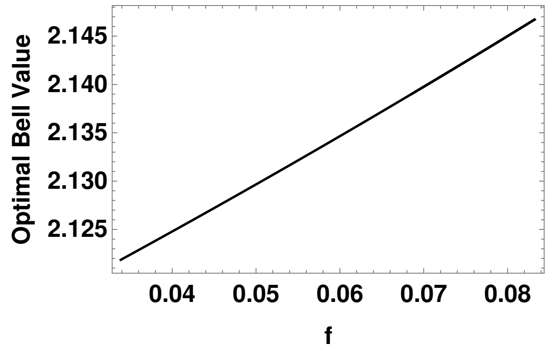

Figure 2.6: Variation of optimal Bell-CHSH value with f for $\mathcal{P} = 0.85$, $\mathcal{C} = 0.45$ and $e = -\frac{2}{3}$ for rank-three X-state of first kind.

In the other situation i.e., when $4(\sqrt{y} - \sqrt{x})^2 < (\cos^2\theta - e\sin^2\theta)^2$, we have

$$\mathcal{M} = (\mathcal{C} + 2f'\sin\theta\cos\theta + 2\sqrt{x})^2 + (1 - (1+e)\sin^2\theta)^2. \tag{2.92}$$

Now solving Eq. (2.82) for $\sin^2\theta$ we get

$$\sin^2\theta = \mathcal{K}_2(\mathcal{P}, x, d) = \frac{1 \pm \sqrt{1 - 2d(1 + 2x - \mathcal{P})}}{2d}. \tag{2.93}$$

Finally we get

$$\begin{aligned}\mathcal{B} &= 2\sqrt{\mathcal{M}}\\ &= 2\Big[\big(\mathcal{C} + 2f'\sqrt{\mathcal{K}_2(\mathcal{P}, x, d)}\sqrt{1 - \mathcal{K}_2(\mathcal{P}, x, d)} + 2\sqrt{x}\big)^2 + \\ &\qquad \big[1 - (1+e)\mathcal{K}_2(\mathcal{P}, x, d)\big]^2\Big]^{\frac{1}{2}}.\end{aligned} \tag{2.94}$$

Here also for optimal Bell-CHSH value we will again take minus sign in the expression of $\mathcal{K}_2(\mathcal{P}, x, d)$. For both these above cases we will get similar kind of trend as we have already shown graphically before for third-rank X-state of first kind.

Second kind Rank-three second kind two-qubit X-state can be represented by $(x = \mathcal{H}, y < \mathcal{G}, \mathcal{B} > 0)$. Purity of the state is

$$\mathcal{P} = 1 + 2y - 2t\sin^2\theta + 2u\sin^4\theta, \tag{2.95}$$

where $t = 1 - \sin^2\phi\sin^2\psi$ and $u = 1 + \sin^4\phi\sin^4\psi - \cos^2\phi\cos^2\psi\sin^2\phi - 2\sin^2\phi\sin^2\psi$. Let's consider the situation $x > y$. As $x = \mathcal{H} > y$, concurrence should be

$$\mathcal{C} = 2(\sqrt{x} - \sqrt{\mathcal{G}}) = 2(\sqrt{x} - f\sin^2\theta). \tag{2.96}$$

Again if we consider $4(\sqrt{x} - \sqrt{y})^2 > (\cos^2\theta - e\sin^2\theta)^2$ and using Eq. (2.96) we have

$$\begin{aligned} \mathcal{M} &= 4(\sqrt{x} + \sqrt{y})^2 + 4(\sqrt{x} - \sqrt{y})^2 \\ &= (\mathcal{C} + 2f\sin^2\theta + 2\sqrt{y})^2 + (\mathcal{C} + 2f\sin^2\theta - 2\sqrt{y})^2. \end{aligned} \tag{2.97}$$

Solving the Eq. (2.95) for $\sin^2\theta$ we get

$$\sin^2\theta = \mathcal{K}_3(\mathcal{P}, y, t, u) = \frac{t \pm \sqrt{t^2 - 2u(1 + 2y - \mathcal{P})}}{2u}. \tag{2.98}$$

Using this in Eq. (2.97), we get the optimal Bell-CHSH value (Again we have to choose minus sign in $\mathcal{K}_3(\mathcal{P}, y, t, u)$ for optimal Bell-CHSH value)

$$\mathcal{B} = 2\sqrt{\mathcal{M}} = 2\sqrt{2\Big(\big[\mathcal{C} + 2f\mathcal{K}_3(\mathcal{P}, y, t, u)\big]^2 + 4y\Big)}. \tag{2.99}$$

Now for the other case i.e., $4(\sqrt{x} - \sqrt{y})^2 < (\cos^2\theta - e\sin^2\theta)^2$, we have

$$\begin{aligned} \mathcal{M} &= 4(\sqrt{x} + \sqrt{y})^2 + \big(1 - (1+e)\sin^2\theta\big)^2 \\ &= (\mathcal{C} + 2f\sin^2\theta + 2\sqrt{y})^2 + \big(1 - (1+e)\sin^2\theta\big)^2. \end{aligned} \tag{2.100}$$

Finally we find

$$\begin{aligned} \mathcal{B} &= 2\sqrt{\mathcal{M}} \\ &= 2\sqrt{\big[\mathcal{C} + 2f\mathcal{K}_3(\mathcal{P}, y, t, u) + 2\sqrt{y}\big]^2 + \big[1 - (1+e)\mathcal{K}_3(\mathcal{P}, y, t, u)\big]^2}. \end{aligned} \tag{2.101}$$

Now let's consider the other situation when $y > x$. In this case we have $\mathcal{G} > y > x = \mathcal{H}$ and hence

$$\mathcal{C} = 2(\sqrt{y} - \sqrt{\mathcal{H}}) = 2(\sqrt{y} - \sqrt{x}) = 2(\sqrt{y} - f'\sin\theta\cos\theta). \tag{2.102}$$

Considering $4(\sqrt{y} - \sqrt{x})^2 > (\cos^2\theta - e\sin^2\theta)^2$, we have $\mathcal{M} = 4(\sqrt{y} - \sqrt{x})^2 + 4(\sqrt{y} + \sqrt{x})^2 = \mathcal{C}^2 + (\mathcal{C} + 4\sqrt{x})^2$. Optimal Bell-CHSH value is

$$\mathcal{B} = 2\sqrt{\mathcal{M}} = 2\sqrt{\mathcal{C}^2 + (\mathcal{C} + 4\sqrt{x})^2}. \tag{2.103}$$

Now if $4(\sqrt{y}-\sqrt{x})^2 < (\cos^2\theta - e\sin^2\theta)^2$ and using $2\sqrt{y} = \mathcal{C} + 2\sqrt{x}$ we get

$$\mathcal{M} = (\mathcal{C} + 4\sqrt{x})^2 + \left[1 - (1+e)\sin^2\theta\right]^2. \tag{2.104}$$

Replacing y by $(\frac{\mathcal{C}}{2} + \sqrt{x})^2$ in Eq. (2.95) and solving for $\sin^2\theta$ we find

$$\sin^2\theta = \mathcal{K}_4(\mathcal{P}, \mathcal{C}, x, t, u) = \frac{t \pm \sqrt{t^2 - u(2 + \mathcal{C}^2 + 4\mathcal{C}\sqrt{x} + 4x^2 - 2\mathcal{P})}}{2u}. \tag{2.105}$$

For optimal Bell-CHSH value again we have to take the minus sign in the above expression and the optimal Bell-CHSH value is

$$\mathcal{B} = 2\sqrt{\mathcal{M}} = 2\sqrt{(\mathcal{C} + 4\sqrt{x})^2 + \left[1 - (1+e)\mathcal{K}_4(\mathcal{P}, \mathcal{C}, x, t, u)\right]^2}. \tag{2.106}$$

2.4.1.3 Rank-four X-state

X-state of fourth rank can be parameterized by $(x < \mathcal{H}, y < \mathcal{G}, \mathcal{AB} > 0)$. Here purity is

$$\mathcal{P} = 1 + 2x + 2y - 2\sin^2\theta + 2g\sin^4\theta, \tag{2.107}$$

where $g = \frac{1}{64}(53 + 4\cos 2\phi + 7\cos 4\phi + 8\cos 4\psi \sin^4\phi)$. Now let's consider $x > y$ and $\sqrt{x} - \sqrt{\mathcal{G}} = \sqrt{x} - f\sin^2\theta > \sqrt{y} - \sqrt{\mathcal{H}} = \sqrt{y} - f'\sin\theta\cos\theta$. So in this situation concurrence is

$$\mathcal{C} = 2(\sqrt{x} - f\sin^2\theta). \tag{2.108}$$

Again among the three eigenvalues if we take $4(\sqrt{x}-\sqrt{y})^2 > (\cos^2\theta - e\sin^2\theta)^2$, then using Eq. (2.108) we get

$$\begin{aligned}\mathcal{M} &= 4(\sqrt{x}-\sqrt{y})^2 + 4(\sqrt{x}+\sqrt{y})^2 \\ &= (\mathcal{C} + 2f\sin^2\theta - 2\sqrt{y})^2 + (\mathcal{C} + 2f\sin^2\theta + 2\sqrt{y})^2.\end{aligned} \tag{2.109}$$

Replacing x in the purity equation given in Eq. (2.107) by $(\frac{\mathcal{C}}{2} + f\sin^2\theta)^2$ and solving for $\sin^2\theta$ we get

$$\begin{aligned}\sin^2\theta &= \mathcal{K}_5(\mathcal{P}, \mathcal{C}, y, g, f) \\ &= \frac{1 - \mathcal{C}f \pm \sqrt{(1-\mathcal{C}f)^2 - (g+f^2)(2 - 2\mathcal{P} + \mathcal{C}^2 + 4y)}}{2(g+f^2)}.\end{aligned} \tag{2.110}$$

Hence the optimal Bell-CHSH value is

$$\mathcal{B} = 2\sqrt{\mathcal{M}} = 2\sqrt{2\Big(\big[\mathcal{C} + 2f\mathcal{K}_5(\mathcal{P},\mathcal{C},y,g,f)\big]^2 + 4y\Big)}. \tag{2.111}$$

For optimal Bell-CHSH value again we have to choose minus sign in $\mathcal{K}_5(\mathcal{P},\mathcal{C},y,g,f)$. Now if we consider the other situation i.e., $4(\sqrt{x}-\sqrt{y})^2 < (\cos^2\theta - e\sin^2\theta)^2$, then by using Eq. (2.108) we get

$$\begin{aligned}\mathcal{M} &= 4(\sqrt{x}+\sqrt{y})^2 + \big(1-(1+e)\sin^2\theta\big)^2 \\ &= (\mathcal{C}+2f\sin^2\theta+2\sqrt{y})^2 + \big(1-(1+e)\sin^2\theta\big)^2.\end{aligned} \tag{2.112}$$

In this case optimal Bell-CHSH value is

$$\begin{aligned}\mathcal{B} &= 2\sqrt{\mathcal{M}} \\ &= 2\sqrt{\big[\mathcal{C}+2f\mathcal{K}_5(\mathcal{P},\mathcal{C},y,g,f)+2\sqrt{y}\big]^2 + \big[1-(1+e)\mathcal{K}_5(\mathcal{P},\mathcal{C},y,g,f)\big]^2}.\end{aligned} \tag{2.113}$$

For this case we have plotted optimal Bell-CHSH value with purity and concurrence keeping other parameters constant. Again Fig.2.7 and Fig.2.8 suggest that optimal Bell-CHSH value changes monotonically with purity and concurrence respectively. Now consider the

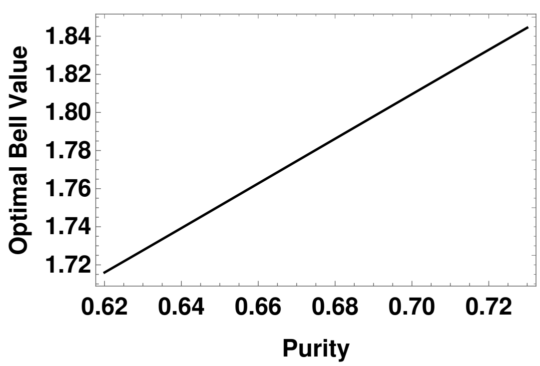

Figure 2.7: Variation of optimal Bell-CHSH value with purity for $\mathcal{C} = 0.4$, $y = 0.002$, $g = \frac{45}{64}$, $f = \frac{1}{4}$ and $e = \frac{1}{4}$ for rank-four X-state.

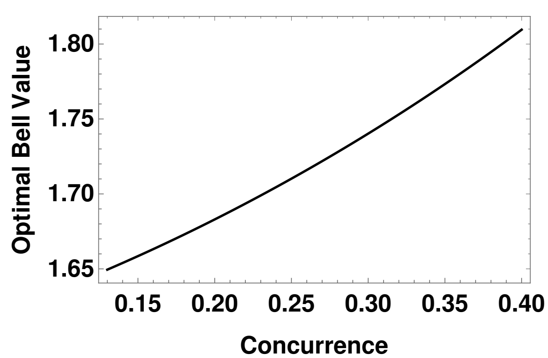

Figure 2.8: Variation of optimal Bell-CHSH value with concurrence for $\mathcal{P} = 0.7$, $y = 0.002$, $g = \frac{45}{64}$, $f = \frac{1}{4}$ and $e = \frac{1}{4}$ for rank-four X-state.

situation when $\sqrt{x}-\sqrt{\mathcal{G}} = \sqrt{x} - f\sin^2\theta < \sqrt{y}-\sqrt{\mathcal{H}} = \sqrt{y} - f'\sin\theta\cos\theta$. Here concurrence will be

$$\mathcal{C} = 2(\sqrt{y} - f' \sin\theta \cos\theta). \tag{2.114}$$

Again if we consider $4(\sqrt{x} - \sqrt{y})^2 > (\cos^2\theta - e\sin^2\theta)^2$ and using Eq. (2.114) we get

$$\begin{aligned} \mathcal{M} &= 4(\sqrt{x} - \sqrt{y})^2 + 4(\sqrt{x} + \sqrt{y})^2 \\ &= (\mathcal{C} + 2f' \sin\theta\cos\theta + 2\sqrt{x})^2 + (\mathcal{C} + 2f' \sin\theta\cos\theta - 2\sqrt{x})^2. \end{aligned} \tag{2.115}$$

Now substituting y from Eq. (2.114) in Eq. (2.107) we find

$$1 - \mathcal{P} + 2x + \frac{\mathcal{C}^2}{2} + 2\mathcal{C} f' \sin\theta\cos\theta + 2f'^2 \sin^2\theta\cos^2\theta - 2\sin^2\theta + 2g\sin^4\theta = 0 \tag{2.116}$$

As there is $\cos\theta$ terms present in the above equation so we will get a fourth order equation of $\sin^2\theta$. For now we are skipping this part, as we will tackle similar scenario in the next case when $y > x$.

Consider the situation $y > x$ and $\sqrt{x} - \sqrt{\mathcal{G}} = \sqrt{x} - f\sin^2\theta > \sqrt{y} - \sqrt{\mathcal{H}} = \sqrt{y} - f' \sin\theta\cos\theta$. So in this situation concurrence is

$$\mathcal{C} = 2(\sqrt{x} - f\sin^2\theta). \tag{2.117}$$

We have already discussed similar scenario in greater detail in the case of $x > y$. So we will just write the final optimal Bell-CHSH value for the two cases. In first case we consider $4(\sqrt{y} - \sqrt{x})^2 > (\cos^2\theta - e\sin^2\theta)^2$ and the optimal Bell-CHSH value is

$$\mathcal{B} = 2\sqrt{\mathcal{M}} = 2\sqrt{2\Big(\big[\mathcal{C} + 2f\mathcal{K}_5(\mathcal{P}, \mathcal{C}, y, g, f)\big]^2 + 4y\Big)}. \tag{2.118}$$

For the other case i.e., when $4(\sqrt{y} - \sqrt{x})^2 < (\cos^2\theta - e\sin^2\theta)^2$, we have

$$\begin{aligned} \mathcal{B} &= 2\sqrt{\mathcal{M}} \\ &= 2\sqrt{\big[\mathcal{C} + 2f\mathcal{K}_5(\mathcal{P}, \mathcal{C}, y, g, f) + 2\sqrt{y}\big]^2 + \big[1 - (1+e)\mathcal{K}_5(\mathcal{P}, \mathcal{C}, y, g, f)\big]^2}. \end{aligned} \tag{2.119}$$

Now we will consider the other value of concurrence that is

$$\mathcal{C} = 2(\sqrt{y} - f' \sin\theta\cos\theta). \tag{2.120}$$

In this situation if we replace y by $(\frac{\mathcal{C}}{2} + f' \sin\theta\cos\theta)$ in the purity equation given in Eq. (2.107) we will get a fourth order equation of $\sin^2\theta$ as follows

$$\alpha^2 \sin^8\theta + 2\alpha\beta\sin^6\theta + \Big(\beta^2 + 2\alpha\big(1 + 2x + \frac{\mathcal{C}^2}{2} - \mathcal{P}\big) + 4\mathcal{C}^2 f'^2\Big)\sin^4\theta$$
$$+\Big(2\beta\big(1 + 2x + \frac{\mathcal{C}^2}{2} - \mathcal{P}\big) - 4\mathcal{C}^2 f'^2\Big)\sin^2\theta + \big(1 + 2x + \frac{\mathcal{C}^2}{2} - \mathcal{P}\big)^2 = 0,$$

where $\alpha = 2g - 2f'^2$ and $\beta = 2f'^2 - 2$. In principle by solving the above equation we will get four solutions and from there we can find out optimal Bell-CHSH value. As the solution is very complicated, so we just plot Fig.2.9 and Fig.2.10 which shows that optimal Bell-CHSH value changes monotonically with purity and concurrence keeping other parameters fixed.

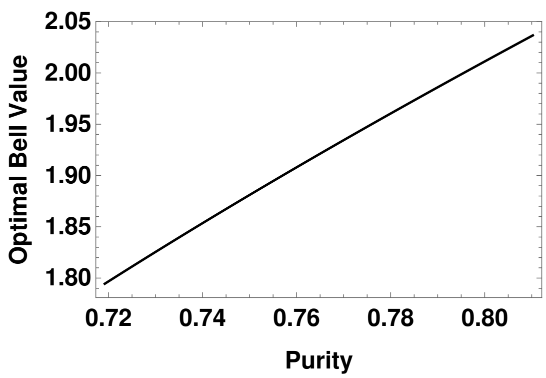

Figure 2.9: Variation of optimal Bell-CHSH value with purity for $\mathcal{C} = 0.4$, $x = 0.001$, $g = \frac{1}{128}(103 + 6\sqrt{2})$, $f' = \frac{1}{2}\sin\frac{\pi}{8}$ and $e = \frac{1}{8}(6 + \sqrt{2})$ for rank-four X-state.

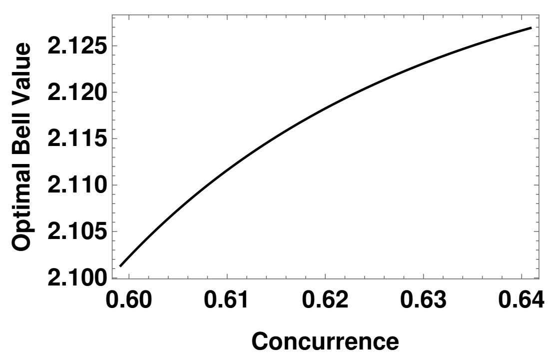

Figure 2.10: Variation of optimal Bell-CHSH value with concurrence for $\mathcal{P} = 0.65$, $x = 0.001$, $g = \frac{45}{64}$, $f' = \frac{1}{2\sqrt{2}}$ and $e = \frac{3}{4}$ for rank-four X-state.

2.5 Discussion

Bell-CHSH inequality is one of the operational ways to detect two-qubit entanglement. Not only entanglement, but measurement settings are equally important to show a violation of Bell-CHSH inequality. The Bell-CHSH value of a pure two-qubit state only depends on the entanglement. But for a mixed state the situation is far more complex. We have shown that purity and concurrence are not enough, but we also need other functions of state parameters to characterize the optimal Bell-CHSH value. We have shown that optimal Bell-CHSH value changes monotonically with these extra functions of state parameters. Hence, these functions may correspond to some nonlocal classical or quantum properties of the state.

Chapter 3

Higher-dimensional entanglement and Bell-SLK function

Entanglement in higher dimensional systems is important from both fundamental and practical point of view. Higher dimensional entanglement is much more propitious in quantum communication than the conventional two-qubit entanglement. It provides more security against eavesdropping in cryptography [129]; it can be used to increase the channel-capacity via superdense coding [130], and is more robust against environmental noise [131] than the conventional two-qubit entanglement. However, for practical applications of these protocols, experimental preparation, detection and quantification of higher dimensional entangled state is of crucial importance. The violation of Bell-type inequalities can detect the presence of entanglement in such systems. Therefore, Bell-type inequalities in higher dimensional system have generated much interest in recent years [87, 90, 132–137]. One of the approaches to obtain Bell-type inequality in higher dimension employs a projection of multilevel down to dichotomic one [121, 132]. But sometimes it is also important to know whether it enables to probe genuine high-dimensionality or not [87, 90, 138]. In 2002, Collins, Gisin, Linden, Massar, and Popescu introduced [87] an inequality (henceforth will be referred to as CGLMP inequality) which is known to be the only tight inequality [88] for higher dimensional systems. But, this inequality is not maximally violated by a maximally entangled state of such systems [89]. Interestingly, in 2006, Son, Lee and Kim introduced another set of Bell-type inequalities for qudit systems (hereafter, the SLK inequality) [90] which is maximally violated for a maximally entangled two-qudit state. In the case of two-qubit entangled states, as discussed in chapter 2, there exist measurement settings for which value of the Bell-CHSH operator increases with the entanglement of the state. In this chapter, we will show that for a particular measurement setting, the value of the Bell-SLK function increases with the entanglement of the pure bipartite entangled states. Therefore, Bell-SLK function gives us a way to quantify the amount of entanglement present in a two-qudit pure state. Moreover, we will show that it can also quantify entanglement for some classes of mixed states.

3.1 The Bell-SLK inequality and negativity

In the Bell-SLK test, two far separated observers Alice and Bob, can independently choose one of the two observables denoted by A_1, A_2 for Alice and B_1, B_2 for Bob. Note that with each hermitian observable H, we can associate a unitary operator U by the simple relation $U = \exp(iH)$. We take U as an unitary observable here. This simple correspondence will make mathematics simple rather than changing any physics. Measurement outcomes of the observables are elements of the set, $V = \{1, \omega, \cdots, \omega^{d-1}\}$, where $\omega = \exp(2\pi \mathrm{i}/d)$. In a variant of Bell-SLK inequality [133], the Bell-SLK function, I_{SLK}, is given by

$$I_{SLK} = \frac{1}{\sqrt{2}} \sum_{n=1}^{d-1} \left(\omega^{-n/4} C_{1,1}^n + \omega^{-3n/4} C_{2,1}^n + \omega^{n/4} C_{1,2}^n + \omega^{-n/4} C_{2,2}^n \right) + c.c., \tag{3.1}$$

$\omega = exp(2\pi \mathrm{i}/d)$, c.c. is for complex conjugate, $C_{a,b}^n = \langle A_a^n B_b^n \rangle$. The assumption of local-realism implies $I_{SLK} \leq I_{SLK}^{\max}(\mathrm{LR})$, where $I_{SLK}^{\max}(\mathrm{LR}) = \frac{1}{\sqrt{2}} \left(3 \cot \frac{\pi}{4d} - \cot \frac{3\pi}{4d} \right) - 2\sqrt{2}$ [133]. It is remarkable to note that we can write a Bell function either in correlation space or in joint probability space. Both forms are connected by a simple Fourier transform [91, 133]. As an example, we have a Bell function in correlation space

$$I_B = \sum_{a,b} \sum_{n=0}^{d-1} \zeta_{ab}(n) C_{a,b}^n, \tag{3.2}$$

where the zeroth order correlation has no meaning and we can choose $\sum_{a,b}\zeta_{ab}(0) = 0$. Then we can write Eq. (3.2) in joint probability space as

$$I_B = \sum_{a,b}\sum_{\alpha=0}^{d-1} f_{ab}(\alpha)P(A_a = B_b + \alpha), \tag{3.3}$$

where the sum inside the probability is modulo d sum and the coefficients $\zeta_{ab}(n)$ and $f_{ab}(\alpha)$ are connected by simple Fourier transform in the following way [91, 133]

$$f_{ab}(\alpha) = \frac{1}{d}\sum_{n=0}^{d-1}\zeta_{ab}(n)\omega^{n\alpha}, \quad \text{and} \tag{3.4}$$

$$\zeta_{ab}(n) = \frac{1}{d}\sum_{\alpha=0}^{d-1} f_{ab}(\alpha)\omega^{-n\alpha}. \tag{3.5}$$

By using above Fourier transformation, we write Bell-SLK function in joint probability space as [91, 133]

$$\begin{aligned} I_{SLK} \;=\; & \sum_{\alpha=0}^{d-1} f(\alpha)[P(A_1 = B_1 + \alpha) + P(B_1 = A_2 + \alpha + 1) + P(A_2 = B_2 + \alpha) \\ & + P(B_2 = A_1 + \alpha)], \end{aligned} \tag{3.6}$$

where sums inside the probabilities are modulo d sums, and

$$f(\alpha) = \frac{1}{\sqrt{2}}\Big(\cot[\frac{\pi}{d}(\alpha + \frac{1}{4})] - 1\Big). \tag{3.7}$$

We now calculate the value of the Bell-SLK function for an arbitrary pure two-qudit state $|\psi\rangle = \sum_i c_i|ii\rangle$ and for the measurement settings originally given in [139]. The nondegenerate eigenvectors of the operators $\hat{A}_a$, $a = 1, 2$, and $\hat{B}_b$, $b = 1, 2$, are respectively

$$|k\rangle_{A,a} = \frac{1}{\sqrt{d}}\sum_{j=0}^{d-1}\omega^{(k+\delta_a)j}|j\rangle \quad \text{and} \tag{3.8}$$

$$|l\rangle_{B,b} = \frac{1}{\sqrt{d}}\sum_{j=0}^{d-1}\omega^{(-l+\epsilon_b)j}|j\rangle, \tag{3.9}$$

where $\delta_1 = 0, \delta_2 = 1/2, \epsilon_1 = 1/4$ and $\epsilon_2 = -1/4$. The joint probabilities in (3.6) can be calculated as

$$P(A_1 = B_1 + \alpha) = \frac{1}{d}\sum_{p,q=0}^{d-1} c_p c_q \omega^{(\alpha+1/4)(p-q)}, \tag{3.10}$$

$$P(B_1 = A_2 + \alpha + 1) = \frac{1}{d}\sum_{p,q=0}^{d-1} c_p c_q \omega^{-(\alpha+1/4)(p-q)}, \tag{3.11}$$

$$P(A_2 = B_2 + \alpha) = \frac{1}{d}\sum_{p,q=0}^{d-1} c_p c_q \omega^{(\alpha+1/4)(p-q)} \quad \text{and} \tag{3.12}$$

$$P(B_2 = A_1 + \alpha) = \frac{1}{d}\sum_{p,q=0}^{d-1} c_p c_q \omega^{-(\alpha+1/4)(p-q)}. \tag{3.13}$$

Putting these probabilities in (3.6), we get

$$I_{SLK} = \frac{4}{d}\sum_{\alpha=0}^{d-1} f(\alpha) \sum_{p,q=0}^{d-1} c_p c_q \omega^{(\alpha+1/4)(p-q)}. \tag{3.14}$$

From the identity $\sum\limits_{k=0}^{d-1}(-1)^k \cot(\frac{2k+1}{4d})\pi = d$ [140], we can obtain another identity

$$\sum_{k=0}^{d-1} \cot(\frac{4k+1}{4d})\pi = d. \tag{3.15}$$

Therefore, we get $\sum\limits_{\alpha=0}^{d-1} f(\alpha) = 0$. We can then rewrite (3.14) as

$$\begin{aligned} I_{SLK} &= \frac{4}{d}\sum_{\alpha=0}^{d-1} f(\alpha) \sum_{\substack{p\neq q \\ p>q}} 2c_p c_q \cos\Big(\frac{2\pi}{d}(\alpha+\frac{1}{4})(p-q)\Big) \\ &= \frac{4}{d}\sum_{\alpha=0}^{d-1} \frac{1}{\sqrt{2}}\Big(\cot[\frac{\pi}{d}(\alpha+\frac{1}{4})] - 1\Big) \sum_{\substack{p\neq q \\ p>q}} 2c_p c_q \cos\Big(\frac{2\pi}{d}(\alpha+\frac{1}{4})(p-q)\Big) \end{aligned} \tag{3.16}$$

To evaluate it further, we now need to find following two sums

$$\sum_{\alpha=0}^{d-1} \cos\Big(\frac{2\pi m}{d}(\alpha+\frac{1}{4})\Big), \tag{3.17}$$

and

$$\sum_{\alpha=0}^{d-1} \cos\Big(\frac{2\pi m}{d}(\alpha+\frac{1}{4})\Big) \cot\Big(\frac{\pi}{d}(\alpha+\frac{1}{4})\Big), \tag{3.18}$$

where we have replaced $p-q$ by m (an integer). Using trigonometrical identity in [141], we obtain

$$\begin{aligned}
&\sum_{\alpha=0}^{d-1}\cos\Big(\frac{2\pi m}{d}(\alpha+\frac{1}{4})\Big)\\
&=\cos\Big(\frac{\pi m}{2d}+\frac{(d-1)\pi m}{d}\Big)\sin\pi m\operatorname{cosec}\frac{\pi m}{d}\\
&=0,
\end{aligned}\tag{3.19}$$

i.e, the first sum (3.17) is equal to zero. Now we will describe two theorems which will be required to calculate (3.18).

Before going to the theorems we will introduce some mathematical expansions, which will be useful to prove these two theorems. We will use the expansion

$$\frac{1}{\mathrm{t}e^{z}-1}=\sum_{\nu=0}^{\infty}\frac{A_\nu(t)}{\nu!}z^\nu,\tag{3.20}$$

where $A_\nu(t)$ is a function of t and $t\neq 1$. The functions $A_\nu(t)$ can be written in terms of the so-called "Apostol-Bernoulli numbers" $B_\nu(0,t)$ [142]. In fact

$$A_\nu(t)=\frac{B_{\nu+1}(0,t)}{\nu+1}.\tag{3.21}$$

The first few terms are $A_0(t)=\frac{1}{t-1}$, $A_1(t)=\frac{-t}{(t-1)^2}$, $A_2(t)=\frac{t+t^2}{(t-1)^3}$ and $A_3(t)=\frac{-(t+4t^2+t^3)}{(t-1)^4}$. We will also need to expand cotangent in a power series

$$\cot(\pi w)=\sum_{j=0}^{\infty}C_j\pi^{2j-1}w^{2j-1},\tag{3.22}$$

where w satisfies $0<|w|<\pi$ and

$$C_j=\frac{(-1)^j2^{2j}B_{2j}}{(2j)!},\tag{3.23}$$

where B_j are the well known "Bernoulli Numbers". The first few C_j are $C_0=1$, $C_1=-\frac{1}{3}$, $C_2=-\frac{1}{45}$ and $C_3=-\frac{2}{945}$. In our case, we need the expansion

$$\cot(\pi z+\pi b)=\sum_{j=0}^{\infty}C_j\pi^{2j-1}(z-1+b)^{2j-1},\tag{3.24}$$

with the condition $0 < |z-1+b| < \pi$. We will now give proof of two theorems.

Theorem 1: If m, n and d denote positive integers with $m < d$ and $b \notin \mathbb{Z}/d$, then

$$\begin{aligned} e_n(d,m) &= \sum_{j=0}^{d-1} \cos\left(\frac{2\pi m j}{d}\right) \cot^n\left(\frac{\pi j}{d} + \pi b\right) \\ &= -\sum \mathrm{i}^{\mu+\nu+1} 2^{\mu+\nu} \frac{m^\mu}{\mu!} \frac{d^{\nu+1}}{\nu!} \Big(t_1 A_\nu(t_2) - (-1)^{\mu+\nu} t_1' A_\nu(t_2')\Big) \\ &\quad\; D(j_1, j_2, \ldots, j_n). \end{aligned} \tag{3.25}$$

Here the sum is over all nonnegative integers $j_1,\ldots,j_n$, μ and ν such that $2j_1 + \cdots + 2j_n + \mu + \nu = n-1$. We also have $t_1 = \mathrm{e}^{-2\pi \mathrm{i} m b}$, $t_2 = \mathrm{e}^{-2\pi \mathrm{i} d b}$, $t_1' = \mathrm{e}^{2\pi \mathrm{i} m b}$ and $t_2' = \mathrm{e}^{2\pi \mathrm{i} d b}$; here $b \notin \mathbb{Z}/d$ so that the trigonometric sum is well defined. $\mathbb{Z}$ represents the set of integers. Furthermore,

$$D(j_1, j_2, \ldots, j_n) = \prod_{r=1}^{n} C_{j_r}. \tag{3.26}$$

Proof : We choose contour C_R as a positively oriented indented rectangle with vertices at $\pm \mathrm{i}R$ and $1 \pm \mathrm{i}R$. The contour has two semicircular indentations of radius ϵ $(R > \epsilon)$ to the left of both 0 and 1 [143]. Let us take the complex function as

$$g_1(z) = \frac{\mathrm{e}^{2\pi \mathrm{i} m z} \cot^n(\pi z + \pi b)}{\mathrm{e}^{2\pi \mathrm{i} d z} - 1} - \frac{\mathrm{e}^{-2\pi \mathrm{i} m z} \cot^n(\pi z + \pi b)}{\mathrm{e}^{-2\pi \mathrm{i} d z} - 1} \tag{3.27}$$

and consider $\frac{1}{2\pi \mathrm{i}} \int_C g_1(z) dz$. Since $g_1(z)$ has period 1, the integrals along the indented vertical sides of C_R cancel. Since we have taken $m < d$, $g_1(z)$ tends to zero uniformly for $0 \leqslant x \leqslant 1$ as $|y| \to \infty$. Hence, $\frac{1}{2\pi \mathrm{i}} \int_C g_1(z) dz = 0$. We can now calculate the contour integral using Cauchy's residue theorem. The function $g_1(z)$ has poles at a number of points. To start with, $g_1(z)$ has a simple pole at $z = 0$, with residue

$$\mathrm{Res}(g_1, 0) = \frac{1}{\pi \mathrm{i} d} \cot^n(b\pi). \tag{3.28}$$

The function $g_1(z)$ also has simple poles at $z = \frac{j}{d}$, with $1 \leqslant j \leqslant d-1$. The corresponding residues at these points are

$$\mathrm{Res}\left(g_1, \frac{j}{d}\right) = \frac{1}{\pi \mathrm{i} d} \cos\left(\frac{2\pi m j}{d}\right) \cot^n\left(\frac{\pi j}{d} + \pi b\right). \tag{3.29}$$

In addition the function $g_1(z)$ has a pole of order n at $z=-b+1$. Using equations (3.20) and (3.24), we can write

$$\begin{aligned} g_1(z) &= t_1\sum_{\mu=0}^{\infty}\frac{(2\pi\mathrm{i}m)^{\mu}}{\mu!}(z+b-1)^{\mu}\left(\sum_{j=0}^{\infty}C_j\pi^{2j-1}(z-1+b)^{2j-1}\right)^n \\ &\quad\times\sum_{\nu=0}^{\infty}\frac{(2\pi\mathrm{i}d)^{\nu}}{\nu!}A_{\nu}(t_2)(z+b-1)^{\nu} \\ &\quad -t_1'\sum_{\mu=0}^{\infty}\frac{(-2\pi\mathrm{i}m)^{\mu}}{\mu!}(z+b-1)^{\mu}\left(\sum_{j=0}^{\infty}C_j\pi^{2j-1}(z-1+b)^{2j-1}\right)^n \\ &\quad\times\sum_{\nu=0}^{\infty}\frac{(-2\pi\mathrm{i}d)^{\nu}}{\nu!}A_{\nu}(t_2')(z+b-1)^{\nu}. \end{aligned} \tag{3.30}$$

Then after few steps of straightforward calculation, one can show that,

$$\mathrm{Res}(g_1,-b+1)=\sum \mathrm{i}^{\mu+\nu}2^{\mu+\nu}\frac{m^{\mu}}{\mu!}\frac{d^{\nu}}{\nu!}\big(\frac{t_1}{\pi}A_{\nu}(t_2)-(-1)^{\mu+\nu}\frac{t_1'}{\pi}A_{\nu}(t_2')\big)D(j_1,j_2,\ldots,j_n). \tag{3.31}$$

Here the sum is over all nonnegative integers $j_1,\ldots,j_n$, μ and ν such that $2j_1+\cdots+2j_n+\mu+\nu=n-1$. Using (3.28), (3.29), (3.31) and applying residue theorem we can obtain the sum (3.25).

Corollary 1: Let m and d be positive integers such that $m<d$ and $b\notin\mathbb{Z}/d$. Then

$$e_1(d,m)=\sum_{j=0}^{d-1}\cos\left(\frac{2\pi mj}{d}\right)\cot\left(\frac{\pi j}{d}+\pi b\right)=d\cos[(2m-d)b\pi]\operatorname{cosec}(bd\pi). \tag{3.32}$$

Proof : Put $n=1$ in Theorem 1. Using the values $A_0(t)$ and C_0, one can easily find this.

Theorem 2: Let m,n and d denote positive integers with $m<d$ and $b\notin\mathbb{Z}/d$. Then

$$\begin{aligned} h_n(d,m) &= -\sum \mathrm{i}^{\mu+\nu}2^{\mu+\nu}\frac{m^{\mu}}{\mu!}\frac{d^{\nu+1}}{\nu!}\Big(t_1A_{\nu}(t_2)+(-1)^{\mu+\nu}t_1'A_{\nu}(t_2')\Big) \\ &\quad D(j_1,j_2,\ldots,j_n). \end{aligned} \tag{3.33}$$

We have already defined all the terms and conditions in Theorem 1. Here

$$h_n(d,m)=\sum_{j=1}^{d-1}\sin\left(\frac{2\pi mj}{d}\right)\cot^n\left(\frac{\pi j}{d}+\pi b\right). \tag{3.34}$$

Proof : Our contour will be the same as in Theorem 1. Let us take the complex function as

$$g_2(z) = \frac{\mathrm{e}^{2\pi\mathrm{i}mz}\cot^n(\pi z + \pi b)}{\mathrm{e}^{2\pi\mathrm{i}dz} - 1} + \frac{\mathrm{e}^{-2\pi\mathrm{i}mz}\cot^n(\pi z + \pi b)}{\mathrm{e}^{-2\pi\mathrm{i}dz} - 1} \tag{3.35}$$

and consider $\frac{1}{2\pi\mathrm{i}}\int_C g_2(z)dz$. As before, $\int_C g_2(z)dz = 0$. The pole structure of this function is same as in Theorem 1. However, this time residue is zero at $z = 0$, so we take the sum from $j = 1$. Since, $\sin x$ vanishes at $x = 0$, we can take the sum from $j = 0$. The function $g_2(z)$ has simple poles at $z = \frac{j}{d}$, with $1 \leqslant j \leqslant d - 1$. The corresponding residues at these points are

$$\mathrm{Res}\left(g_2, \frac{j}{d}\right) = \frac{1}{\pi d}\sin\left(\frac{2\pi mj}{d}\right)\cot^n\left(\frac{\pi j}{d} + \pi b\right). \tag{3.36}$$

The function $g_2(z)$ also has a pole of order n at $z = -b + 1$. Using (3.20) and (3.24), as in the case of last theorem, we can obtain after a few steps of straight forward calculation,

$$\mathrm{Res}(g_2, -b+1) = \sum \mathrm{i}^{\mu+\nu}2^{\mu+\nu}\frac{m^\mu}{\mu!}\frac{d^\nu}{\nu!}\Big(\frac{t_1}{\pi}A_\nu(t_2) + (-1)^{\mu+\nu}\frac{t_1'}{\pi}A_\nu(t_2')\Big)D(j_1, j_2, \ldots, j_n). \tag{3.37}$$

Using (3.36), (3.37) and applying residue theorem we can easily obtain (3.33).

Corollary 2: Let m and d be positive integers such that $m < d$ and $b \notin \mathbb{Z}/d$. Then

$$h_1(d,m) = \sum_{j=1}^{d-1}\sin\left(\frac{2\pi mj}{d}\right)\cot\left(\frac{\pi j}{d} + \pi b\right) = -d\sin[(2m-d)b\pi]\,\mathrm{cosec}(bd\pi). \tag{3.38}$$

Proof : Put $n = 1$ in Theorem 2. Using the values $A_0(t)$ and C_0, we can obtain this.

Using above two corollaries and sum and difference formula for cosines, we find.

$$\sum_{\alpha=0}^{d-1}\cos\Big(\frac{2\pi m}{d}(\alpha + \frac{1}{4})\Big)\cot\Big(\frac{\pi}{d}(\alpha + \frac{1}{4})\Big) = d. \tag{3.39}$$

This sum is remarkably simple. We note that the value of this sum is independent of m. This is crucial in relating the value of the Bell-SLK function and entanglement. Eqs. (3.7), (3.16), (3.19) and (3.39) together imply

$$I_{SLK} = 4\sqrt{2}\sum_{\substack{p\neq q\\ p>q}} c_p c_q. \tag{3.40}$$

This sum is proportional to the negativity of the state. The negativity, $\mathcal{N}$, for a two-qudit pure state is defined as [52, 53]

$$\mathcal{N} = \sum_{\substack{p \neq q \\ p > q}} c_p c_q \frac{2}{d-1}. \tag{3.41}$$

Using this, we finally get

$$I_{SLK} = 2\sqrt{2}(d-1)\mathcal{N}. \tag{3.42}$$

Thus, we obtain an interesting relation between negativity and the value of the Bell-SLK function for a particular measurement setting. Value of this function is zero for product states whereas it increases linearly with the negativity for pure entangled states (In $d = 2$, the Bell-SLK inequality reduces to familiar Bell-CHSH inequality [78], so this relation holds for CHSH inequality also). This gives a way to measure the entanglement of a pure two-qudit entangled state. Hence, the entanglement of a pure two-qudit state can be calculated by measuring the Bell-SLK function for the measurement setting given in (3.8–3.9).

3.2 Case of Mixed States

For bipartite mixed states the situation is more complicated, as we have already seen in the case of two-qubit mixed states in the second chapter. In general, it is a formidable task to find a relation between Bell-SLK function and negativity for a two-qudit mixed state. However, here we will describe a relation between Bell-SLK function and negativity for some special classes of mixed states.

3.2.1 Isotropic States

For a two-qudit system, isotropic states are convex mixtures of the maximally entangled state,

$$|\Psi^+\rangle = \frac{1}{\sqrt{d}} \sum_{j=0}^{d-1} |jj\rangle, \tag{3.43}$$

with a maximally mixed state $\mathbb{I} = \mathbb{I}_A \otimes \mathbb{I}_B / d^2$, where $\mathbb{I}$ is a identity matrix. These states can be written as

$$\rho_F = \frac{1-F}{d^2-1}\big(\mathbb{I} - |\Psi^+\rangle\langle\Psi^+|\big) + F|\Psi^+\rangle\langle\Psi^+|, \tag{3.44}$$

where F is the fidelity of ρ_F and $|\Psi^+\rangle$ satisfying $0 \leqslant F \leqslant 1$. These states are separable for $F \leqslant 1/d$ [23, 144].

In the following, we calculate the Bell-SLK function for these states. The Bell-SLK function I_{SLK} (given in Eq. (3.6)) consists of four probabilities. Here, we calculate one of the probabilities, $P(A_1 = B_1 + \alpha)$, other probabilities can be calculated similarly.

$$\begin{aligned} P(A_1 = B_1 + \alpha) &= \mathrm{Tr}\big[\hat{P}(A_1 = B_1 + \alpha)\rho_F\big] \\ &= \frac{1-F}{d^2-1}\mathrm{Tr}\big[\hat{P}(A_1 = B_1 + \alpha)\mathbb{I}\big] \\ &\quad + \frac{d^2F-1}{d^2-1}\mathrm{Tr}\big[\hat{P}(A_1 = B_1 + \alpha)|\Psi^+\rangle\langle\Psi^+|\big], \end{aligned} \tag{3.45}$$

where $\hat{P}(A_1 = B_1 + \alpha)$ stands for appropriate projector. The first part of the above sum can be calculated as

$$\begin{aligned} \mathrm{Tr}\big[\hat{P}(A_1 = B_1 + \alpha)\mathbb{I}\big] &= \frac{1}{d^2}\sum_{i,j,p,q,l,m,n} \omega^{(l+\alpha)(i-j)}\omega^{(-l+1/4)(p-q)} \\ &\qquad \times \langle m|i\rangle\langle j|m\rangle\langle n|p\rangle\langle q|n\rangle \\ &= d, \end{aligned} \tag{3.46}$$

whereas the second part as

$$\begin{aligned} \mathrm{Tr}\big[\hat{P}(A_1 = B_1 + \alpha)|\Psi^+\rangle\langle\Psi^+|\big] &= \langle\Psi^+|\hat{P}(A_1 = B_1 + \alpha)|\Psi^+\rangle \\ &= \frac{1}{d^3}\sum_{i,j,l,r,s,p,q} \omega^{(l+\alpha)(r-s)}\omega^{(-l+1/4)(p-q)} \\ &\qquad \times \langle i|r\rangle\langle i|p\rangle\langle s|j\rangle\langle q|j\rangle \\ &= \frac{1}{d^2}\sum_{i,j}\omega^{(\alpha+1/4)(i-j)}. \end{aligned} \tag{3.47}$$

The other three joint probabilities when calculated, come out to be equal to the probability calculated above. The Bell-SLK function, I_{SLK} can now be obtained, by putting for these probabilities in Eq. (3.6), as:

$$I_{SLK} = \left(\frac{1-F}{d^2-1}\right)4d\sum_{\alpha=0}^{d-1} f(\alpha) + \left(\frac{d^2F-1}{d^2-1}\right)\frac{4}{d^2}\sum_{i,j,\alpha=0}^{d-1} f(\alpha)\omega^{(\alpha+1/4)(i-j)}. \tag{3.48}$$

Using the fact that $\sum_{\alpha=0}^{d-1} f(\alpha) = 0$, the Bell-SLK function reads

$$I_{SLK} = \left(\frac{d^2F-1}{d^2-1}\right)\frac{4}{d^2}\sum_{i,j,\alpha=0}^{d-1} f(\alpha)\omega^{(\alpha+1/4)(i-j)}. \tag{3.49}$$

Proceeding now in a manner similar as in the previous section, we get the Bell-SLK function as

$$I_{SLK} = \frac{2\sqrt{2}}{d+1}(d^2F-1). \tag{3.50}$$

The negativity $\mathcal{N}(\rho_F)$ for isotropic states (with some normalization) can be calculated as

$$\mathcal{N}(\rho_F) = \begin{cases} 0, & F \leqslant 1/d, \\ \frac{dF-1}{d-1}, & 1/d \leqslant F \leqslant 1. \end{cases} \tag{3.51}$$

Using Eq.(3.51) in Eq. (3.50), we can be rewrite the later equation to read as

$$I_{SLK} = \begin{cases} \frac{2\sqrt{2}}{d+1}(d^2F-1), & F \leqslant 1/d, \\ \frac{2\sqrt{2}}{d+1}\big((d-1)(d\mathcal{N}(\rho_F)+1)\big), & 1/d \leqslant F \leqslant 1. \end{cases} \tag{3.52}$$

Thus, we get an interesting relation between the Bell-SLK function and the negativity for isotropic states. It can easily be checked that for $F \leqslant 1/d$, i.e. for the separable isotropic states, the value of the Bell-SLK function is upper bounded by the $\frac{2\sqrt{2}}{d+1}(d-1)$. A value larger than this bound, immediately suggests that the isotropic states undergoing the said Bell-SLK measurements are entangled and their value of the Bell-SLK function increases with entanglement.

3.2.2 Maximally Entangled state through a noisy channel

In this subsection, we will consider another class of mixed states that are obtained when particles in a maximally entangled state pass through noisy channels. This is often a real laboratory situation. Let's say a party prepares a maximally entangled state and sends it to two distant parties by some noisy channels. The state will no longer be a pure state. Since we can compute negativity for a mixed state, we can explore the relationship between negativity and the value of the Bell-SLK function. We can also find how robust is the measure of entanglement of a pure state using the Bell-SLK function. We will study this situation in $d = 3$ taking two well known channels – the amplitude damping and the phase damping channels.

A. Amplitude damping Let us consider a maximally entangled state $|\psi\rangle = \frac{1}{\sqrt{3}}(|00\rangle + |11\rangle + |22\rangle)$. Two qutrits are sent to distant parties through amplitude damping channels. For a qutrit, amplitude damping channel can be represented in terms of Kraus operators as [145]

$$K_0 = \begin{pmatrix} 1 & 0 & 0 \\ 0 & \sqrt{1-p} & 0 \\ 0 & 0 & \sqrt{1-p} \end{pmatrix}, K_1 = \begin{pmatrix} 0 & \sqrt{p} & 0 \\ 0 & 0 & 0 \\ 0 & 0 & 0 \end{pmatrix} \text{ and } K_2 = \begin{pmatrix} 0 & 0 & \sqrt{p} \\ 0 & 0 & 0 \\ 0 & 0 & 0 \end{pmatrix},$$

where p is the channel parameter. For simplicity we take same channel on both sides. We find that, without noise, the value of I_{SLK} is 5.657 and negativity is $\mathcal{N} = 1$. At 90% purity (purity varies with the channel parameter, p) $I_{SLK} = 5.359$ and negativity is $\mathcal{N} = 0.922$. So the value of negativity is about 8% lower. However, it turns out that there is still a relationship between the value of the Bell-SLK function and entanglement for such states. From the value of the Bell-SLK function we can infer the entanglement of the state in terms of negativity. This is clear from Figure3.1 that looking at the I_{SLK} curve, we can find state's negativity at any purity.

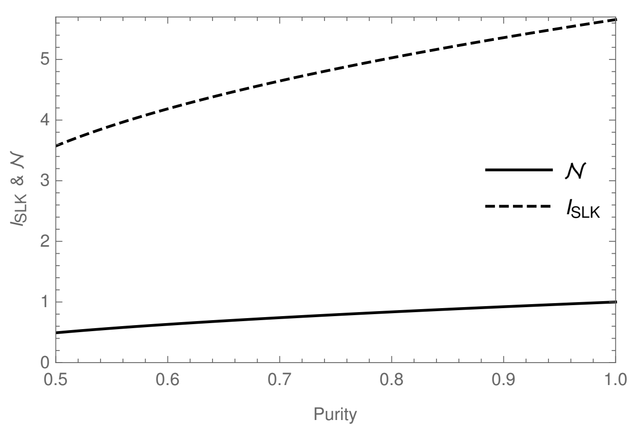

Figure 3.1: Change in the Bell-SLK function and negativity with purity for a maximally entangled two-qutrit state passed through the amplitude damping channel.

B. Phase damping Let us now consider the case when the two qutrits in a maximally entangled state pass through phase damping channels separately. The Kraus operators for the phase damping channel are [145]

$$K_0 = \sqrt{1-p}\begin{pmatrix}1 & 0 & 0\\ 0 & 1 & 0\\ 0 & 0 & 1\end{pmatrix} \text{ and } K_1 = \sqrt{p}\begin{pmatrix}1 & 0 & 0\\ 0 & \omega & 0\\ 0 & 0 & \omega^2\end{pmatrix},$$

where $\omega = e^{\frac{2\pi i}{3}}$ and p is the channel parameter. We do the same analysis as for the amplitude damping channel. At 90% purity $I_{SLK} = 5.209$ and $\mathcal{N} = 0.922$. Both values decrease by about 8%, as compared to the starting pure state. However, as before, from Figure3.2, we notice an interesting relationship between entanglement and the value of the Bell-SLK function. If we measure the I_{SLK} value for the state, we can easily determine the entanglement of the state in terms of negativity.

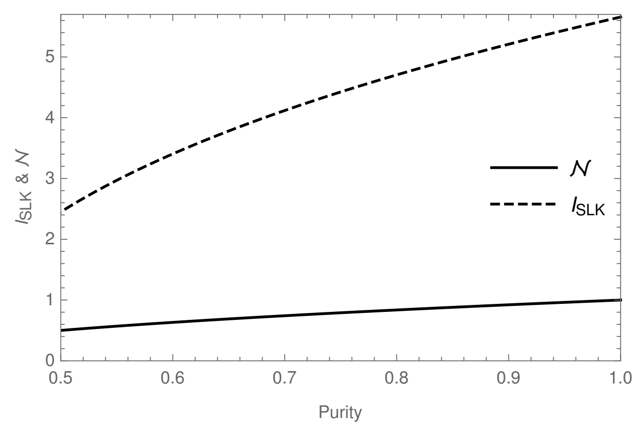

Figure 3.2: Change in the Bell-SLK function and negativity with purity for a maximally entangled two-qutrit state passed through the phase damping channel.

3.3 An Experimental scheme

Interestingly, this Bell-SLK test can be performed in laboratories with the present day's technology [134, 135]. One technique to encode a state of a qudit is to use the orbital angular momentum (OAM) states of photons [146]. Higher dimensional bipartite entanglement is generated through spontaneous parametric down conversion (SPDC) [134, 147]. In [134], Dada *et al.* have employed the same measurement setting as in Eq. (3.8) to obtain the violation of CGLMP inequality for bipartite qudit systems with dimensions up to twelve. One can use the same experimental set up to measure the Bell-SLK function (instead of the CGLMP function as done in [134]) in order to find the amount of entanglement present in a pure bipartite state. In this case, four observables are to be measured. However, in this experimental set up, the measurement of each observable requires $(d-1)$ experimental settings. The number of settings varies linearly with respect to the dimension d. In principle, it might be possible to reduce the number of settings to measure an observable with d outcomes. In [135], Lo *et al.* employ a different experimental set up. They simulate qudits using multiple pairs of polarization-entangled photons. They also measure four observables with $(d-1)$ experimental settings for each observable and demonstrate the violation of CGLMP inequality up to $d = 16$. Though violation of the CGLMP inequality can detect the presence of entanglement, but this violation cannot be used to measure the amount of entanglement present in the bipartite state, at least, for the employed setting. This is because, for these settings, CGLMP inequality is not maximally violated for a maximally entangled state of two qudits [89]. It is also known [89] that CGLMP inequality is violated maximally by a partially entangled state. Therefore, it is unlikely that CGLMP function measurement can help in measuring the amount of entanglement in a two-qudit state. As is known, the choice of measurement setting is important. There are measurement settings, for which even maximally entangled state may not violate an inequality. One of the key mathematical reason for the relation (3.42) to exist is that the sum (3.39) is independent of m. In the case of CGLMP inequality, the function $f(\alpha)$ is different, therefore a different sum occurs. That sum is not independent of m. Therefore, such a relation does not exist for the CGLMP inequality. However, the measurement of the Bell-SLK function can help us in finding the amount of entanglement in a pure two-qudit state.

3.4 Advantage of Bell-SLK test

The widely adopted method for measuring entanglement of a state is the quantum state tomographic reconstruction [148]. In this method, a complete set of observables is measured on the system to reconstruct its state and thus to calculate the entanglement. Though, successfully implemented for lower-dimensional systems [149], this method is not suitable for systems of higher dimension. This is because the number of observables to be measured increases dramatically with the dimension of the system [150]. However, there are suggestions to characterize the state with less number of observables, but most of these methods are for two-qubit systems [151]. For higher dimensional systems, the alternative suggestions, though reduces the number of observables (in comparison to the traditional tomography), but the number is still high and increases with the dimension of the subsystems [152]. In case of bipartite systems, the number of measurements needed is of the order of d^4 (d is dimension of each subsystem). If a priori, it is known that the state is pure, then we need only $2(d^2 - 1)$ measurements to reconstruct the state [153]. Moreover, the implementation of these observables in an experiment is also an issue to be taken proper consideration [154]. The measurement of the Bell-SLK function can be a method to measure entanglement of a pure bipartite state. Unlike the earlier schemes where number of observables needed depends on dimension of subsystems, this scheme needs measurement of only four observables to calculate the entanglement of any pure bipartite state. Moreover, this new scheme can be implemented in laboratories with the existing technology.

3.5 Discussion

Bell-SLK inequality can be useful in measuring the entanglement present in two-qudit systems. This also addresses an important question in entanglement theory: How to measure amount of entanglement in a bipartite state experimentally? In the earlier methods for measuring entanglement, the required number of observables increases with dimension of the subsystems. In contrast, the scheme presented here requires only four observables to be measured to find the amount of entanglement present in a bipartite pure state. The scheme also works for a class of bipartite mixed qudit states – isotropic states. Furthermore, for the case of mixed states which are obtained after applying phase or amplitude damping channels on maximally entangled two qutrits, one can also measure entanglement, as characterized by negativity. Most importantly, Bell-SLK test can be easily performed with the current day technology.

Chapter 4

Three-qubit pure state and SLOCC classes

Quantification and characterization of entanglement is unambiguous for pure bipartite state, but not for mixed bipartite states [17, 37]. In the spirit of resource theory of entanglement [37, 39], two entangled states are said to be equivalent if they can be obtained from each other with certainty with respect to LOCC (local operation and classical communication). Entanglement of any pure bipartite state is uniquely captured by the entropy of entanglement in the asymptotic limit [155]. But this is not true for mixed states. There is no unique quantification of entanglement for this case and a number of entanglement measures and monotones [17] have been proposed over the years. Situation gets worse for multipartite scenario, both for pure and mixed states. One can straightforwardly extend some of the entanglement measures and monotones constructed for bipartite systems to multipartite scenario, but there is no unique quantification of entanglement in multipartite scenario even for pure states. We can not even define a unique maximally entangled multipartite state and there are many inequivalent forms of entanglement [76, 156]. As an example, for a three-qubit pure state, there exist six SLOCC inequivalent classes of entanglement: separable, three bi-separable and two genuinely entangled (GHZ and W) [57]. In general it is very difficult to characterize and distinguish different classes from each other. For three-qubit pure states analytical characterization is present in literature using local entropies and the concept of tangle [57]. But from an experimental point of view these are not realizable. In a very recent work [157], a proposed set of Bell inequalities can distinguish separable, biseparable and genuine entanglement for pure three-qubit states by the pattern of violations of the Bell inequalities within the set. In another work, Zhao et.al. [158] have provided the necessary and sufficient conditions to classify the separable, biseparable and genuine entangled state. But both these work did not succeed in distinguishing the GHZ-type and W-type states, which fall under the category of genuinely entangled states. In this chapter, we will construct some operators, which can distinguish six classes of entanglement for pure three-qubit states. Moreover, they are easily implementable in an experiment.

4.1 Tangle and its observable measure

Any three-qubit pure state can be written in the canonical form [159, 160],

$$|\psi\rangle = \lambda_0|000\rangle + \lambda_1 e^{i\theta}|100\rangle + \lambda_2|101\rangle + \lambda_3|110\rangle + \lambda_4|111\rangle, \tag{4.1}$$

where $\lambda_i \geqslant 0$, $\sum_i \lambda_i^2 = 1$, $\theta \in [0, \pi]$ and $\{|0\rangle, |1\rangle\}$ denote the basis of Alice's, Bob's and Charlie's Hilbert space. The tangle for the state $|\psi\rangle$ given in (4.1) is found to be

$$\tau_\psi = 4\lambda_0^2\lambda_4^2. \tag{4.2}$$

The tangle as given in (4.2) may be measured experimentally, since we can write it as the expectation value of the operator

$$O = 2(\sigma_x \otimes \sigma_x \otimes \sigma_x), \tag{4.3}$$

with respect to the state $|\psi\rangle$. The operator O, given in (4.3), can be obtained by suitably choosing the unit vectors in Mermin operator, which is defined as [161, 162]

$$\begin{aligned} B_M \;=\; & \hat{a}_1.\vec{\sigma} \otimes \hat{a}_2.\vec{\sigma} \otimes \hat{a}_3.\vec{\sigma} - \hat{a}_1.\vec{\sigma} \otimes \hat{b}_2.\vec{\sigma} \otimes \hat{b}_3.\vec{\sigma} - \\ & \hat{b}_1.\vec{\sigma} \otimes \hat{a}_2.\vec{\sigma} \otimes \hat{b}_3.\vec{\sigma} - \hat{b}_1.\vec{\sigma} \otimes \hat{b}_2.\vec{\sigma} \otimes \hat{a}_3.\vec{\sigma}, \end{aligned} \tag{4.4}$$

where $\hat{a}_j$, b_j $(j = 1, 2, 3)$ are the measurement direction for the jth party and $\vec{\sigma} = (\sigma_x, \sigma_y, \sigma_z)$ are the usual Pauli matrices. By choosing the unit vectors as $\hat{a}_1 = (1, 0, 0)$, $\hat{a}_2 = (1, 0, 0)$, $\hat{a}_3 = (1, 0, 0)$, $\hat{b}_1 = (-1, 0, 0)$, $\hat{b}_2 = (1, 0, 0)$ and $\hat{b}_3 = (1, 0, 0)$, we can construct the operator O. The expectation value of the operator O in the state $|\psi\rangle$ is given by

$$\langle O\rangle_\psi = \langle\psi|O|\psi\rangle = 4\lambda_0\lambda_4 = 2\sqrt{\tau_\psi}. \tag{4.5}$$

From this, it is clear that by measuring the expectation value of O, one can easily calculate the value of the tangle.

4.2 Classification of three-qubit pure states

In this section, we will show how to classify six different classes of three-qubit pure states. It is known that tangle is nonzero only for GHZ class [57]; it is zero for other five classes. So using (4.5) one can separate GHZ class from other five classes. Since it is not possible to distinguish zero tangle classes of three-qubit pure states with a single quantity τ_ψ, so we need to define other observables. To fulfill our aim, let us consider two quantities P and Q, which can be defined as

$$P = \langle\psi|O_1|\psi\rangle\langle\psi|O_2|\psi\rangle = \langle O_1\rangle_\psi\langle O_2\rangle_\psi, \tag{4.6}$$

and

$$Q = \langle O_1\rangle_\psi + \langle O_2\rangle_\psi + \langle O_3\rangle_\psi. \tag{4.7}$$

The operators O_1, O_2 and O_3 are given by

$$O_1 = 2(\sigma_x \otimes \sigma_x \otimes \sigma_z), \tag{4.8}$$

$$O_2 = 2(\sigma_x \otimes \sigma_z \otimes \sigma_x) \tag{4.9}$$

and

$$O_3 = 2(\sigma_z \otimes \sigma_x \otimes \sigma_x). \tag{4.10}$$

The operator O_1 given in (4.8) can be obtained from the Mermin operator (4.4) by choosing the unit vectors as $\hat{a}_1 = (1,0,0)$, $\hat{a}_2 = (1,0,0)$, $\hat{a}_3 = (0,0,1)$, $\hat{b}_1 = (-1,0,0)$, $\hat{b}_2 = (1,0,0)$ and $\hat{b}_3 = (0,0,1)$. One can find operator O_2 given in (4.9) by choosing the unit vectors as $\hat{a}_1 = (1,0,0)$, $\hat{a}_2 = (0,0,1)$, $\hat{a}_3 = (1,0,0)$, $\hat{b}_1 = (-1,0,0)$, $\hat{b}_2 = (0,0,1)$ and $\hat{b}_3 = (1,0,0)$. Similarly operator O_3 given in (4.10) can be obtained by choosing the unit vectors as $\hat{a}_1 = (0,0,1)$, $\hat{a}_2 = (1,0,0)$, $\hat{a}_3 = (1,0,0)$, $\hat{b}_1 = (0,0,-1)$, $\hat{b}_2 = (1,0,0)$ and $\hat{b}_3 = (1,0,0)$. The expectation value of the operators O_1, O_2 and O_3 with respect to the state $|\psi\rangle$ are as follows,

$$\begin{aligned}
\langle O_1\rangle_\psi &= 4\lambda_0\lambda_3, \\
\langle O_2\rangle_\psi &= 4\lambda_0\lambda_2 \quad \text{and} \\
\langle O_3\rangle_\psi &= -4(\lambda_2\lambda_3 + \lambda_1\lambda_4\cos\theta).
\end{aligned} \tag{4.11}$$

Therefore, using (4.11), we can obtain P and Q as

$$\begin{aligned}
P &= 16\lambda_0^2\lambda_2\lambda_3 \quad \text{and} \\
Q &= 4\Big(\lambda_0\lambda_3 + \lambda_0\lambda_2 - (\lambda_2\lambda_3 + \lambda_1\lambda_4\cos\theta)\Big).
\end{aligned} \tag{4.12}$$

We are now in a position to classify zero tangle three-qubit pure states based on the expectation values of the operators O_1,O_2,O_3 and the two quantities P and Q.

Theorem 1: Any three-qubit state belongs to the W class if,

$$\begin{aligned}
&(i)\tau_\psi = 0, \\
&(ii)P \neq 0.
\end{aligned} \tag{4.13}$$

Proof : Using parametrization (4.1), any three-qubit pure state, which is in W class can be written as [57, 160],

$$|\psi\rangle_W = \lambda_0|000\rangle + \lambda_1|100\rangle + \lambda_2|101\rangle + \lambda_3|110\rangle. \tag{4.14}$$

As there is no λ_4, so from (4.2) it is clear that $\tau_{\psi_W} = 0$. From (4.12) one can find $P = 16\lambda_0^2\lambda_2\lambda_3 \neq 0$ and $Q = 4(\lambda_0\lambda_3 + \lambda_0\lambda_2 - \lambda_2\lambda_3) \neq 0$.

We will deduce the conditions by which it is possible to distinguish three biseparable classes.

Lemma 1 : Any three-qubit state is biseparable in 1 and 23 bipartition if

$$
\begin{aligned}
&(i)\tau_\psi = 0,\\
&(ii)\langle O_1\rangle_\psi = 0,\\
&(iii)\langle O_2\rangle_\psi = 0 \quad \text{and}\\
&(iv)\langle O_3\rangle_\psi \neq 0.
\end{aligned}
\tag{4.15}
$$

Proof : Any pure three-qubit state which is biseparable in 1 and 23 bipartition, can be written as $|0\rangle(\alpha|00\rangle + \beta|11\rangle)$, upto some local unitary transformation []. Canonical form of three-qubit pure states as written in (4.1) will have the aforesaid biseparable form if all the λ_i's except λ_1 and λ_4 are zero. Hence, the state belonging to 1 and 23 bipartition can be written in terms of λ_i's as

$$|\psi\rangle_{1|23} = |1\rangle(\lambda_1|00\rangle + \lambda_4|11\rangle). \tag{4.16}$$

As $\lambda_0 = 0$, the tangle is zero for this class of state. From (4.11) we notice that, $\langle O_1\rangle_\psi = 0$, $\langle O_2\rangle_\psi = 0$ and $\langle O_3\rangle_\psi = -4\lambda_1\lambda_4$. Hence, $P = 0$ and $Q \neq 0$.

Lemma 2 : Any three-qubit state is biseparable in 12 and 3 bipartition if,

$$
\begin{aligned}
&(i)\tau_\psi = 0,\\
&(ii)\langle O_1\rangle_\psi \neq 0,\\
&(iii)\langle O_2\rangle_\psi = 0 \quad \text{and}\\
&(iv)\langle O_3\rangle_\psi = 0.
\end{aligned}
\tag{4.17}
$$

Proof : The state, which belongs to 12 and 3 bipartition can be written as

$$|\psi\rangle_{12|3} = (\lambda_0|00\rangle + \lambda_3|11\rangle)|0\rangle. \tag{4.18}$$

The tangle is zero as $\lambda_4 = 0$. Using (4.11) we can infer that $\langle O_1\rangle_\psi = 4\lambda_0\lambda_3$, $\langle O_2\rangle_\psi = 0$ and $\langle O_3\rangle_\psi = 0$. Therefore, $P = 0$ and $Q \neq 0$.

Lemma 3 : Any three-qubit state is biseparable in 13 and 2 bipartition if

$$\begin{aligned}
&(i)\tau_\psi = 0,\\
&(ii)\langle O_1\rangle_\psi = 0,\\
&(iii)\langle O_2\rangle_\psi \neq 0 \quad \text{and}\\
&(iv)\langle O_3\rangle_\psi = 0.
\end{aligned} \tag{4.19}$$

Proof : The state belongs to 13 and 2 bipartition can be written as

$$|\psi\rangle_{13|2} = \lambda_0|000\rangle + \lambda_2|101\rangle. \tag{4.20}$$

The tangle is zero as $\lambda_4 = 0$. The expectation values of the operators O_1, O_2 and O_3 in this state are as follows $\langle O_1\rangle_\psi = 0$, $\langle O_2\rangle_\psi = 4\lambda_0\lambda_2$ and $\langle O_3\rangle_\psi = 0$. Therefore, $P = 0$ and $Q \neq 0$.

We can now use these lemmas to prove the following theorem.

Theorem 2: Any three-qubit pure state is biseparable if,

$$\begin{aligned}
&(i)\tau_\psi = 0,\\
&(ii)P = 0 \quad \text{and}\\
&(iii)Q \neq 0.
\end{aligned} \tag{4.21}$$

Proof : From the above lemmas, it is clear that for a biseparable state, either $\langle O_1\rangle_\psi = 0$, or $\langle O_2\rangle_\psi = 0$. As P is the product of these two expectation values, therefore $P = 0$ for any biseparable three-qubit pure state. The quantity Q is the sum of the expectation values of the operators O_1, O_2 and O_3, and according to the above three lemmas, at least one is nonzero. Therefore $Q \neq 0$. This proves the theorem.

Theorem 3: Any three-qubit state is separable if

$$\begin{aligned}
&(i)\tau_\psi = 0,\\
&(ii)P = 0 \quad \text{and}\\
&(iii)Q = 0.
\end{aligned} \tag{4.22}$$

Proof : Any separable three-qubit pure state can be written as $|0\rangle|0\rangle|0\rangle$, after applying some appropriate local unitary operation. For this state τ_ψ, P and Q all are zero. That completes the proof.

From the above theorems and lemmas we can classify all the classes of three-qubit pure states. Moreover, as these observables only contain Pauli matrices, they can be measured in experiments. We note that there is some arbitrariness in the definition of P. Above proofs will go through, even if we would have have defined P as a product of the expectation values of operators "O_2 and O_3", or "O_1 and O_3", instead of operators "O_1 and O_2". A pictorial depiction of this characterization has been given in the Fig. 4.1.

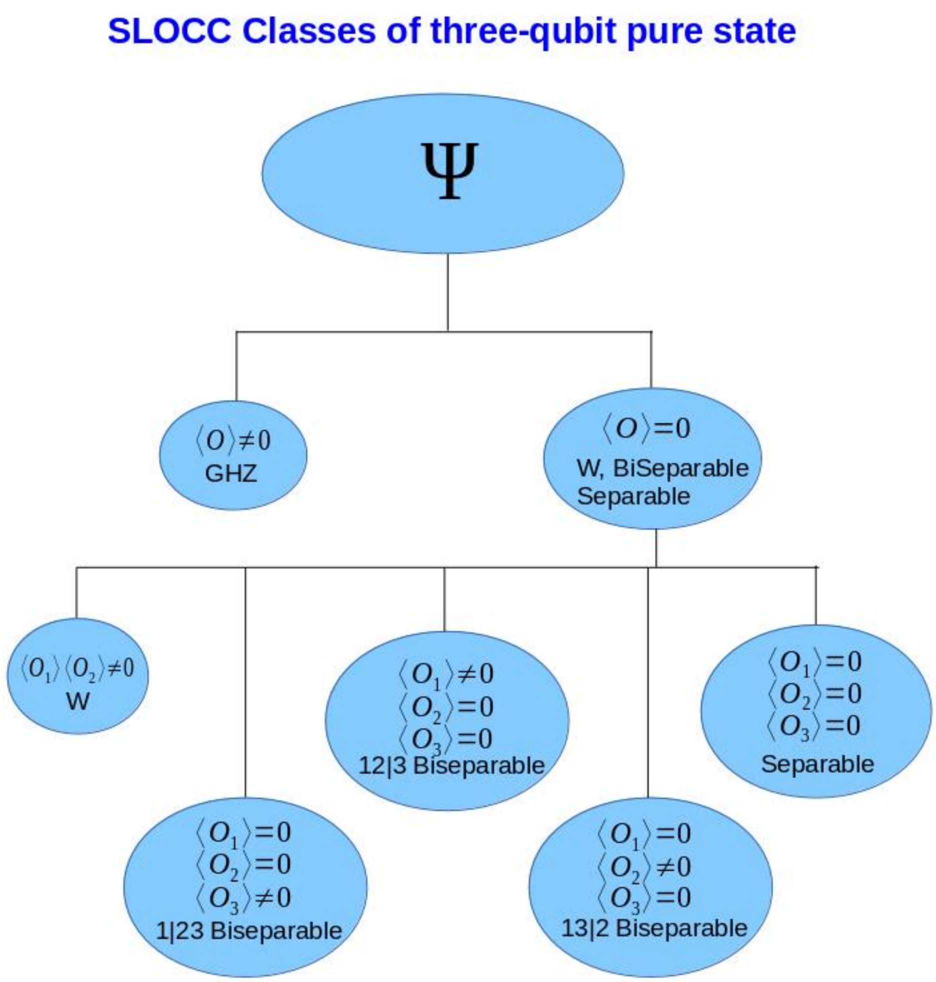

Figure 4.1: Pictorial depiction of the classification of three-qubit pure state.

4.3 Local unitary equivalence with computational basis

In the previous section the entire characterization has been carried out by writing the state in the canonical form and the corresponding operators in the corresponding basis. So, if we are given a state in any other basis, will the analysis still hold? The fact, that any three-qubit pure state can be written down in the canonical form is an existence proof that in principle one can always apply some local unitary operators to convert a state from any basis, in particular computational basis, to canonical-form basis and vice-versa. We will now argue that these theorems will hold in any basis with suitably transformed operators. We have to find the particular local unitary operation that connect two sets of basis vectors and write those operator in that basis. Let us consider that we are given a three-qubit pure state : $|\psi\rangle = \sum_{i,j,k=0}^{1} t_{ijk}|ijk\rangle$ in computational basis. Now, given this state, we can in principle always transform it to the canonical form [163]. Only requirement is that one has to judiciously choose the local unitary operators. Following two examples will clarify this issue. Suppose, we have been given a state in computational basis:

$$|\psi\rangle_c = \frac{1}{2}(|000\rangle_c + |011\rangle_c + |100\rangle_c + |111\rangle_c), \tag{4.23}$$

where c represents that the state is in computational basis. Clearly the given state is not in canonical form. But it can be converted to one having the canonical form using local unitaries. For that we have to follow the prescription mentioned by Acín *et. al.* in [163]. Doing the necessary calculations we have found that the unitary operators that have to act on the first, second and third qubits are,

$$U1 = \frac{1}{\sqrt{2}}\begin{pmatrix} -1 & 1 \\ 1 & 1 \end{pmatrix},\ U2 = \begin{pmatrix} 1 & 0 \\ 0 & 1 \end{pmatrix} \text{ and } U3 = \begin{pmatrix} 1 & 0 \\ 0 & 1 \end{pmatrix}. \tag{4.24}$$

Then by applying the operator $U = U1 \otimes U2 \otimes U3$ on $|\psi\rangle_c$, we get the state in the canonical-form basis as

$$|\psi\rangle_a = \frac{1}{\sqrt{2}}(|100\rangle_a + |111\rangle_a), \tag{4.25}$$

where, a denotes that the state is in the canonical-form basis Now we can calculate the expectation values of those operators given in the previous sections. We will find that $\langle O\rangle_{\psi_a} = 0$, $\langle O_1\rangle_{\psi_a} = 0$, $\langle O_2\rangle_{\psi_a} = 0$ and $\langle O_3\rangle_{\psi_a} = -2$. So the state is biseparable in

1 and 23 bipartition. Now to verify this result in computational basis we have to rotate these observables by inverse of U. $U^{-1} = U^\dagger = U1 \otimes U2 \otimes U3 = U$. The transformed observables are $O_t = UOU^\dagger$, $O_{1t} = UO_1U^\dagger$, $O_{2t} = UO_2U^\dagger$ and $O_{3t} = UO_3U^\dagger$. If we calculate the expectation values of thees operator on state $|\psi\rangle_c$, we find $\langle O_t\rangle_{\psi_c} = 0$, $\langle O_{1t}\rangle_{\psi_c} = 0$, $\langle O_{2t}\rangle_{\psi_c} = 0$ and $\langle O_{3t}\rangle_{\psi_c} = -2$. Hence, the state is $1|23$ biseparable.

Let us consider another state in computational basis :

$$|\phi\rangle_c = \frac{1}{\sqrt{3}}(e^{i\theta}|000\rangle_c + |011\rangle_c - |100\rangle_c). \tag{4.26}$$

To transform it in Acín's canonical form following local unitaries are required

$$U1 = \begin{pmatrix} 0 & -1 \\ 1 & 0 \end{pmatrix},\ U2 = \begin{pmatrix} 1 & 0 \\ 0 & 1 \end{pmatrix} \text{ and } U3 = \begin{pmatrix} 1 & 0 \\ 0 & 1 \end{pmatrix}. \tag{4.27}$$

Hence, $U = U1 \otimes U2 \otimes U3$. Applying this operator to the state, we can get the final state as,

$$|\phi\rangle_a = \frac{1}{\sqrt{3}}(|000\rangle_a + e^{i\theta}|100\rangle_a + |111\rangle_a). \tag{4.28}$$

For this state, we find that $\langle O\rangle_{\phi_a} = \frac{4}{3}$, $\langle O_1\rangle_{\phi_a} = 0$, $\langle O_2\rangle_{\phi_a} = 0$ and $\langle O_3\rangle_{\phi_a} = -\frac{4\cos\theta}{3}$. So the state is in GHZ class. Now to get these results in computational basis we rotate these observables by $U^{-1} = U^\dagger = U1^\dagger \otimes U2 \otimes U3 = U_I$. Similarly, we transform these observables by U_I, as shown in previous example. Now we find that $\langle O_t\rangle_{\phi_c} = \frac{4}{3}$, $\langle O_{1t}\rangle_{\phi_c} = 0$, $\langle O_{2t}\rangle_{\phi_c} = 0$ and $\langle O_{3t}\rangle_{\phi_c} = -\frac{4\cos\theta}{3}$. Hence, the results are consistent. In the examples above, it was important to know the state to determine suitable unitary transformations.

4.4 Case of mixed states

The case of mixed states is more involved. There is no closed from of tangle. But one can find a lower bound on the tangle for a three-qubit mixed state. For a mixed state $C^2_{A(BC)} = 2(1 - \text{Tr}\rho_A^2)$ is no longer valid. Here ρ_A is the density matrix of a subsystem of the three-qubit state ρ. Instead we have to consider the convex roof optimization of all the pure states as follows

$$C^2_{A(BC)}(\rho) = \inf_{p_i,|\psi_i\rangle} \sum_i p_i C^2_{A(BC)}(|\psi_i\rangle), \tag{4.29}$$

where $\rho = \sum_i p_i|\psi_i\rangle\langle\psi_i|$. But it is a formidable task. Instead of finding this, one can find a lower bound on $C^2_{A(BC)}(\rho)$ easily. It has been shown in [164] that this lower bound is given as – $C^2_{A(BC)}(\rho)|_{LB} = 2(\mathrm{Tr}\rho^2 - \mathrm{Tr}\rho_A^2)$. By substituting this in the expression of tangle in Eq. (1.27), one can find the lower bound on tangle. However, this $\tau^{LB}(\rho)$ is not always invariant under the permutation of A, B and C. Hence, for the case of mixed states, it is reasonable to use the average over all the permutations of A, B and C and calculate $\tau^{LB}(\rho)$ as follows [164, 165]

$$\bar{\tau}^{LB} = \frac{1}{6}\sum_{\{ABC\}}\Big(C^2_{A(BC)}|_{LB} - C^2_{AB} - C^2_{AC}\Big). \tag{4.30}$$

Let's take an example of a mixed state which is a mixture of a GHZ state and a W state

$$\rho = p|GHZ\rangle\langle GHZ| + (1-p)|W\rangle\langle W|. \tag{4.31}$$

For this state we compare graphically the observable measure of tangle for pure state, i.e. $\frac{\langle O\rangle^2}{4}$ with the lower bound of tangle as given in Eq. (4.30). As p increases, the state becomes

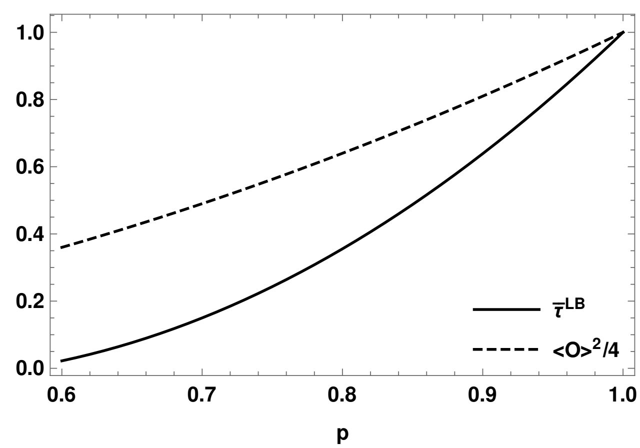

Figure 4.2: Comparison between lower bound of tangle ($\bar{\tau}^{LB}$) and $\frac{\langle O\rangle^2}{4}$ with the variation of p for the state given in Eq. (4.31).

more pure and the values of ($\bar{\tau}^{LB}$) and $\frac{\langle O\rangle^2}{4}$ approach each other. In [165], Farías et. al. considered a very interesting class of three-qubit mixed states which can be obtained as follows. First they prepare a two-qubit Bell state $|\phi^+\rangle_{AB} = \frac{1}{\sqrt{2}}(|00\rangle + |11\rangle)$. Then they let the second qubit interact with the environment. The interaction can be described by a phase damping channel

$$|0\rangle_B|0\rangle_E \rightarrow |0\rangle_B|0\rangle_E \tag{4.32}$$

$$|1\rangle_B|0\rangle_E \rightarrow \sqrt{1-p}|1\rangle_B|0\rangle_E + \sqrt{p}|0\rangle_B|1\rangle_E, \tag{4.33}$$

where p is the channel parameter. This phase damping interaction prepares a tripartite state,

$$|\phi\rangle_{ABE} = \frac{1}{\sqrt{2}}\Big(|000\rangle + \sqrt{1-p}|110\rangle + \sqrt{p}|111\rangle\Big), \tag{4.34}$$

where initially the environment state is $|0\rangle$. In [165], authors experimentally prepared this kind of state with some purity. We can represent it by adding some white noise with $|\phi\rangle_{ABE}$ as

$$\rho = m|\phi\rangle_{ABE}\langle\phi| + \frac{1-m}{8}\mathbb{I}, \tag{4.35}$$

where $\mathbb{I}$ is the eight dimensional identity matrix. For purity equals to 0.92 or $m \approx 0.95$, we compare numerically the tangle measure for pure state, i.e., $\frac{\langle O\rangle^2}{4}$ with the lower bound of tangle. From the FIG. 4.3, we see that $\frac{\langle O\rangle^2}{4}$, i.e., the measure of tangle is just above the value of lower bound of tangle. Similar results can be obtained for any other class of mixed state as well.

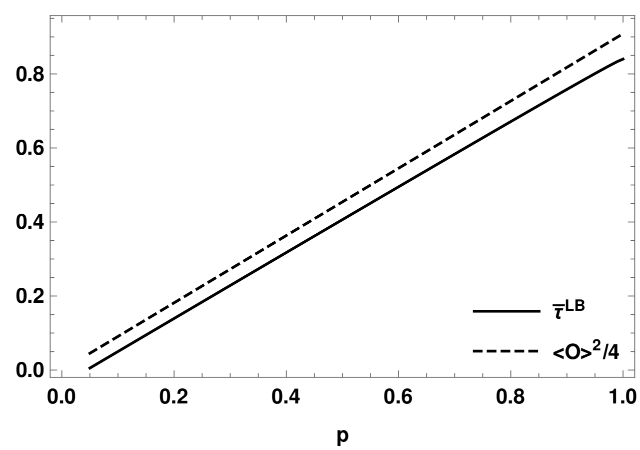

Figure 4.3: Comparison between lower bound of tangle ($\bar{\tau}^{LB}$) and $\frac{\langle O\rangle^2}{4}$ with the variation of p.

4.5 Experimental measure of fidelity for a teleportation scheme

In this section, we will discuss a teleportation scheme using a three-qubit pure state as studied earlier in [166]. The teleportation scheme is as follows: Let us consider a three-qubit pure entangled state shared by three parties i, j and k. We make an orthogonal measurement on the k^{th} qubit and consider the joint state of the system i and j. Using this joint state as a resource state, one can teleport a single qubit state. The faithfulness of this teleportation scheme depends on the single qubit measurement on k^{th} qubit and the compound state of the system i and j. In [166], authors introduced a new quantity called partial tangle, which is defined as,

$$\tau_{ij} = \sqrt{C^2_{i(jk)} - C^2_{ik}}, \quad i \neq j \neq k \quad \text{and} \quad i, j, k = 1, 2, 3. \tag{4.36}$$

The partial tangles for the state given in (4.1) are

$$\begin{aligned} \tau_{12} &= 2\lambda_0\sqrt{\lambda_3^2 + \lambda_4^2}, \\ \tau_{23} &= 2\sqrt{\lambda_0^2\lambda_4^2 + \lambda_1^2\lambda_4^2 + \lambda_2^2\lambda_3^2 - 2\lambda_1\lambda_2\lambda_3\lambda_4\cos\theta}, \\ \tau_{31} &= 2\lambda_0\sqrt{\lambda_2^2 + \lambda_4^2}. \end{aligned} \tag{4.37}$$

They showed that these partial tangles are related to singlet fraction f_k and maximum teleportation fidelity F_k. Here index k just indicates that the measurement is done on the k^{th} qubit. The relation is as follows,

$$\tau_{ij} = 3F_k - 2 = 2f_k - 1. \tag{4.38}$$

We will now provide the explicit relationship between the partial tangles and the expectation value of the operators O, O_1, O_2, O_4 and O_5. The operators O_4 and O_5 will be defined in this section. Since partial tangle is related with singlet fraction and teleportation fidelity, we may measure the teleportation fidelity experimentally for the teleportation scheme given in [166].

Let us define two new operators as

$$\begin{aligned} O_4 &= 2(\sigma_z \otimes \sigma_y \otimes \sigma_y), \\ O_5 &= 2(\sigma_z \otimes \sigma_y \otimes \sigma_x). \end{aligned} \tag{4.39}$$

Operator O_4 given in (4.39) can be obtained from the Mermin operator (4.4) by choosing the unit vectors as $\hat{a}_1 = (0,0,1)$, $\hat{a}_2 = (0,1,0)$, $\hat{a}_3 = (0,1,0)$, $\hat{b}_1 = (0,0,-1)$, $\hat{b}_2 = (0,1,0)$ and $\hat{b}_3 = (0,1,0)$. Similarly O_5 can be obtained by choosing the unit vectors as $\hat{a}_1 = (0,0,1)$, $\hat{a}_2 = (0,1,0)$, $\hat{a}_3 = (1,0,0)$, $\hat{b}_1 = (0,0,-1)$, $\hat{b}_2 = (0,1,0)$ and $\hat{b}_3 = (1,0,0)$.

The expectation value of the above observables for the state in (4.1) are

$$\begin{aligned} \langle O_4 \rangle_\psi &= -4(\lambda_2\lambda_3 - \lambda_1\lambda_4 \cos\theta), \\ \langle O_5 \rangle_\psi &= 4\lambda_1\lambda_4 \sin\theta. \end{aligned} \tag{4.40}$$

After a few steps of calculation, we can show that,

$$\begin{aligned} \tau_{12} &= \frac{1}{2}\sqrt{\langle O\rangle_\psi^2 + \langle O_1\rangle_\psi^2} = 3F_3 - 2, \\ \tau_{23} &= \frac{1}{2}\sqrt{\langle O\rangle_\psi^2 + \langle O_4\rangle_\psi^2 + \langle O_5\rangle_\psi^2} = 3F_1 - 2, \\ \tau_{31} &= \frac{1}{2}\sqrt{\langle O\rangle_\psi^2 + \langle O_2\rangle_\psi^2} = 3F_2 - 2. \end{aligned} \tag{4.41}$$

We note that the operators O, O_1, O_2, O_4 and O_5 are observables and hence their expectation values are measurable quantities. Since the teleportation fidelities are related with some functions of these expectation values as shown in (4.41), so we can say that the teleportation fidelities for the teleportation scheme described in [166] may be measured experimentally.

From (4.40) and (4.41), we can draw following conclusions:

1. If all the partial tangles are equal to zero then the state is a separable one. This is because the expectation value of O_4 and O_5 are also zero for a separable state.

2. If at least one partial tangle is equal to zero, then the three-qubit state is a biseparable state.

3. If each partial tangle is not equal to zero then the state is a three-qubit genuine entangled state.

Lemma 4: Any pure three-qubit genuinely entangled state is useful in the teleportation scheme of [166].

Proof : Three-qubit genuinely entangled states consist of GHZ-class and W-class. We will prove the proposition by taking these two classes separately. The relation in (4.38) can be written as

$$F_k = \frac{2}{3} + \frac{\tau_{ij}}{3}. \tag{4.42}$$

Case-I: For GHZ-class states, $\tau_{ij} > 0$.This can be compared for If $\tau_{ij} > 0$, $F_k > \frac{2}{3}$ [167]. Therefore the resource state consisting of qubits i and j is suitable for teleportation. In this case, the partial tangle is nonzero and so $\langle O \rangle_\psi$ is also nonzero. Hence, from (4.41), it is clear that $\tau_{ij} > 0$. Therefore, F_k is always greater than $\frac{2}{3}$.

Case-II: For W-class states, $\tau_{ij} = 0$ and hence $\langle O \rangle_\psi = 0$. Therefore, for these class of states, the equations (4.41) reduces to

$$\begin{aligned}
\tau_{12} &= \frac{1}{2}\langle O_1 \rangle_\psi, \\
\tau_{23} &= \frac{1}{2}\sqrt{\langle O_4 \rangle_\psi^2 + \langle O_5 \rangle_\psi^2}, \\
\tau_{31} &= \frac{1}{2}\langle O_2 \rangle_\psi.
\end{aligned} \tag{4.43}$$

From (4.6) it can be seen that $4\tau_{12}\tau_{31} = P$. For W-class states, $\tau_{12} \neq 0$ and $\tau_{31} \neq 0$ as $P \neq 0$. Hence, F_3 and F_2 are greater than $\frac{2}{3}$. Thus it remains to see the remaining partial tangle τ_{23}, which is related with $\langle O_4 \rangle_\psi$ and $\langle O_5 \rangle_\psi$. From equation (4.12), for W-class states, λ_0, λ_2 and λ_3 can not be zero simultaneously. Equation (4.39) ensures that $\langle O_4 \rangle_\psi$ is nonzero. Therefore, $\tau_{23} \neq 0$ and F_1 is greater than $\frac{2}{3}$. Thus for the teleportation scheme of [166], all states in W-class are useful for teleportation. This completes the proof.

4.6 Discussion

For a three-qubit pure state, there exist six SLOCC incomparable classes of entanglement. In general it is very difficult to distinguish them from each other. In this chapter, we have discussed a feasible way to distinguish them from one another. Employing Pauli matrices, we have constructed observables which are useful to distinguish these classes from each other. Most importantly these operators can be easily measured in an experiment. Recently, there has been an experiment [168] which distinguishes these six SLOCC classes based on the proposals in this chapter. Although theses operators are constructed in the canonical-form basis, a suitably transformed set of operators will work in any basis. In this sense, results in this chapter are independent of the choice of the basis. However, the construction of suitable transformations may require the knowledge about the state. We have also considered a few mixed states and showed graphically that the measure of tangle for pure states approaches minimum value of the tangle as the state becomes more pure. In the one class of mixed states, that we considered, the measure of tangle is just above the lower bound on tangle. This is because the purity of the states is quite high. In another case, the measure of tangle approaches the lower bound, as the state becomes more pure. This shows that the measure of tangle works quite well for some classes of mixed state. Also we have shown that the operators defined here can be used to measure the fidelity of a teleportation scheme introduced in [166].

Chapter 5

Polygamous nature of quantum steering in three-qubit

Quantum mechanical correlations offer many surprises whenever one digs into the theory to understand its nature and differences from the classical world. Some examples include correlations arising from entanglement [17], Bell non-locality [1,3,80], contextuality [169, 170], coherence [106] and steering [92]. Such correlations have the unique and surprising property of being monogamous [171–174]. Correlations between certain parties are said to be monogamous if they diminish when shared among more additional parties. A simple example is illustrated by Bell-CHSH inequality [173]: Two parties Alice and Bob share non-local correlations and are able to violate the Bell inequality. If the state of Alice is also entangled with a third party Charlie, the non-local correlations between Alice and Bob diminish as the correlations between Alice and Charlie increase. It is therefore implied that the Bell-CHSH correlations are monogamous. Monogamy of correlations has been extensively studied and has found widespread applications in information theoretic tasks like key distribution [175, 176]. While it is well known that steering is monogamous [177, 178], a major aspect of it has not been addressed yet. Steering at its core is asymmetric and although it's monogamous from one side, the nature of correlations from the other side is yet to be studied.

Consider a scenario, where three parties Alice, Bob and Charlie share an entangled state ρ_{abc}. From monogamy of steerability [177, 178], if Alice can steer Bob, she cannot steer

Charlie and vice-versa. The idea originates from the resource theory of quantum correlations like entanglement [17, 179]. However, the question we will address in this chapter is to check whether there exist states for which a particular party (say Alice) cannot be steered independently either by Bob or Charlie but only if they steer together. The scenario is opposite of what is generally considered to show monogamous nature of quantum steering. In this chapter, we provide a detailed analysis of quantum steering in such a scenario. We identify a set of states for which Alice can share a polygamous relationship with Bob and Charlie and also lay down the foundation for identifying the complete set of such states.

5.1 Two-qubit steering criteria and coherence

Recently, a steering criteria for a two-qubit system has been derived using the coherence of the steered party [180, 181]. In this section we provide a very brief summary of that. Let's consider a single qubit system in the state $\rho = \frac{1}{2}(\mathbb{I} + \vec{n} \cdot \vec{\sigma})$, where $\vec{\sigma} = (\sigma_x, \sigma_y, \sigma_z)$ and $\vec{n}$ is a vector in $\mathbb{R}^3$. The coherence (quantified by l_1-norm) of ρ in the basis of Pauli matrix σ_i (the basis in which σ_i is diagonal) is

$$C_i(\rho) = \sqrt{n_j^2 + n_k^2}, \tag{5.1}$$

where $i \neq j \neq k$ and $i, j, k \in \{x, y, z\}$. Mondal et. al. have shown that the sum of the coherence calculated in three different basis is upper bounded by $\sqrt{6}$ [180], i.e.,

$$C_x(\rho) + C_y(\rho) + C_z(\rho) = \sum_{i=x,y,z} C_i(\rho) \leqslant \sqrt{6}. \tag{5.2}$$

Hence, for a single qubit system this inequality can be treated as a coherence complementarity relation.

Now let's consider a bipartite steering scenario. Bob prepares an entangled state ρ_{AB} of joint systems A and B. He keeps the system B with himself and transmits the system A to Alice. Bob's task is to convince Alice that he can steer her system. To do that Bob performs some projective measurement in the eigenbasis of $\{\sigma_x, \sigma_y, \sigma_z\}$. After the measurement Bob sends the measurement basis (σ_i) and the outcome $(a \in \{0, 1\})$ to Alice. As a result Alice's state will collapse to the conditional state $\rho_{A|\Pi_i^a}$ with probability

$p(\rho_{A|\Pi_i^a}) = \mathrm{Tr}[(\mathbb{I} \otimes \Pi_i^a)\rho_{AB}]$. Now Alice will measure coherence in two other basis on his conditional state. Using this one can derive a following coherence steerability criteria [180]

$$\frac{1}{2}\sum_{i,j,a} p(\rho_{A|\Pi^a_{j\neq i}})C(\rho_{A|\Pi^a_{j\neq i}}) > \sqrt{6}, \tag{5.3}$$

which states that if $\frac{1}{2}\sum_{i,j,a} p(\rho_{A|\Pi^a_{j\neq i}})C(\rho_{A|\Pi^a_{j\neq i}})$ is more than $\sqrt{6}$, then Alice's qubit state is steerable by Bob. Therefore, the violation of the inequality given in Eq. (5.2) by the conditional states of Alice suggests that no single system description is possible for Alice and hence, the state ρ_{AB} is steerable from Bob to Alice.

5.2 Polygamous steering

Since we are solely interested in a subset of states for which Alice cannot be steered individually by Bob or Charlie but only by their joint efforts in a tripartite scenario, we start with a tripartite state ρ_{abc} prepared by Bob (or Charlie). Bob sends the subsystem A to Alice and C to Charlie. Since Alice does not believe Bob or Charlie, she asks them to perform a set of measurements and send her the outcomes. Based on the measurement outcomes, she computes the coherence of her conditional states. We show that there exist states ρ_{abc} for which Alice is steerable if and only if Bob and Charlie make an effort together but not otherwise. To find such a set of states $\{S(A \leftarrow B : C)\}$, we first find out a set of states $\{S(A \leftarrow B, C)\}$ for which Alice is steerable by Bob and Charlie together as well as individually. We then compute the union of set of states $\{S(A \leftarrow B)\} \cup \{S(A \leftarrow C)\}$ for which Alice is steerable by Bob and Charlie individually. Our set of interest is the difference of the above two sets, i.e., $S_i \equiv S(A \leftarrow B, C) \setminus \{S(A \leftarrow B) \cup S(A \leftarrow C)\}$.

We now explicitly find out a set of states, which exhibit polygamous nature of quantum steering. First, we focus on to single out the first set $\{S(A \leftarrow B, C)\}$ (set I). Alice will be convinced that her state is entangled if her system A cannot be written by a local hidden state (LHS) model

$$\rho_{bc}^{BC} = \sum_{\lambda} \mathcal{P}(\lambda)\mathcal{P}(b,c|B,C,\lambda)\rho_A^Q(\lambda), \tag{5.4}$$

where $\{\mathcal{P}(\lambda), \rho_A^Q(\lambda)\}$ represents an ensemble of pre-existing local hidden states of Alice and $\mathcal{P}(b, c|B, C, \lambda)$ is Bob and Charlie's joint stochastic map to convince Alice by preparing a state ρ_{bc}^{BC}. $\mathcal{P}(\lambda)$ forms a valid probability distribution such that $\sum_{\lambda} \mathcal{P}(\lambda) = 1$. The joint probability distribution on such states can be written as,

$$\mathcal{P}(a_i, b_j, c_k) = \sum_{\lambda} \mathcal{P}(\lambda)\mathcal{P}(b_j, c_k|\lambda)\mathcal{P}^{Q}(a_i|\lambda), \tag{5.5}$$

where $\mathcal{P}(a_i, b_j, c_k)$ represents the probability to obtain outcome a for the measurement of observables chosen from the set $\{\mathcal{A}_i\}$ by Alice, outcome b for the measurement of observables chosen from the set $\{\mathcal{B}_j\}$ by Bob and outcome c for the measurement of observables chosen from the set $\{\mathcal{C}_k\}$ by Charlie.

We consider a tripartite state ρ_{abc} distributed between Alice (A), Bob (B) and Charlie (C). Alice asks Bob and Charlie to perform projective measurements on their respective systems (B) and (C) on stated bases. We consider Bob and Charlie to perform projective measurements in Pauli eigenbases (or in general on a set of mutually unbiased bases) and communicate the results to Alice. Upon receiving the results, Alice measures coherences on her conditional states with respect to her Pauli eigenbases (or a mutually unbiased bases). The choice of basis will be based on the measurement results from Bob and Charlie. It can be seen that Bob, together with Charlie can steer the state of Alice if at least one of the following steering inequality is violated –

$$\sum_{i\neq k,j,b,c} p(\rho_{A|\Pi_i^b\Pi_j^c})C_k(\rho_{A|\Pi_i^b\Pi_j^c}) \leqslant 6\epsilon, \tag{5.6}$$

$$\sum_{i,j\neq k,b,c} p(\rho_{A|\Pi_i^b\Pi_j^c})C_k(\rho_{A|\Pi_i^b\Pi_j^c}) \leqslant 6\epsilon, \tag{5.7}$$

$$\sum_{i=j=k,b,c} p(\rho_{A|\Pi_i^b\Pi_j^c})C_k(\rho_{A|\Pi_i^b\Pi_j^c}) \leqslant \epsilon, \tag{5.8}$$

$$\sum_{i=j\neq k,b,c} p(\rho_{A|\Pi_i^b\Pi_j^c})C_k(\rho_{A|\Pi_i^b\Pi_j^c}) \leqslant 2\epsilon, \tag{5.9}$$

$$\sum_{i\neq j=k,b,c} p(\rho_{A|\Pi_i^b\Pi_j^c})C_k(\rho_{A|\Pi_i^b\Pi_j^c}) \leqslant 2\epsilon, \tag{5.10}$$

$$\sum_{i=k\neq j,b,c} p(\rho_{A|\Pi_i^b\Pi_j^c})C_k(\rho_{A|\Pi_i^b\Pi_j^c}) \leqslant 2\epsilon, \tag{5.11}$$

where $\epsilon = \sqrt{6}$.

Now, to prove the criteria (5.6), we consider that the conditional states of Alice have a local hidden state model as given in Eq. (5.4), i.e., $\rho_{A|\Pi_i^b\Pi_j^c} \equiv \frac{\rho^{BC}_{\Pi_i^b\Pi_j^c}}{p(\rho^{BC}_{\Pi_i^b\Pi_j^c})}$. Thus,

$$\begin{aligned}
& \sum_{i\neq k,j,b,c} p\Big(\rho^{BC}_{\Pi_i^b\Pi_j^c}\Big) C_k\bigg(\frac{\rho^{BC}_{\Pi_i^b\Pi_j^c}}{p(\rho^{BC}_{\Pi_i^b\Pi_j^c})}\bigg) \\
= & \sum_{i\neq k,j,b,c} p\Big(\rho^{BC}_{\Pi_i^b\Pi_j^c}\Big) C_k\bigg(\frac{\sum_\lambda \mathcal{P}(\lambda)\mathcal{P}(b,c|\Pi_i^b\Pi_j^c,\lambda)\rho_A^Q(\lambda)}{p(\rho^{BC}_{\Pi_i^b\Pi_j^c})}\bigg) \\
\leqslant & \sum_{i\neq k,j,b,c,\lambda} p\Big(\rho^{BC}_{\Pi_i^b\Pi_j^c}\Big) \frac{\mathcal{P}(\lambda)\mathcal{P}(b,c|\Pi_i^b\Pi_j^c,\lambda)}{p(\rho^{BC}_{\Pi_i^b\Pi_j^c})} C_k\Big(\rho_A^Q(\lambda)\Big) \\
= & \sum_{i\neq k,j,b,c,\lambda} \mathcal{P}(\lambda)\mathcal{P}(b,c|\Pi_i^b\Pi_j^c,\lambda) C_k\Big(\rho_A^Q(\lambda)\Big) \\
= & \sum_{k,j,c,\lambda} 2\mathcal{P}(\lambda)\mathcal{P}(c|\Pi_j^c,\lambda) C_k\Big(\rho_A^Q(\lambda)\Big) \\
\leqslant & \sum_{j,c,\lambda} 2\mathcal{P}(\lambda)\mathcal{P}(c|\Pi_j^c,\lambda)\epsilon = 6\epsilon.
\end{aligned}$$

Now we focus on to single out the second set (set II), i.e., $S(A \leftarrow B) \cup S(A \leftarrow C)\}$. This is the union of sets of states for which Alice (A) can be steered individually by Bob (B) and Charlie (C). In this case, Alice ignores the results sent by one party while acknowledging the other. A set of steering inequalities in this two-qubit scenario, where Alice ignores the results of Charlie, can be constructed as [180, 181]

$$\sum_{i=k,b} p(\rho_{A|\Pi_i^b}) C_k(\rho_{A|\Pi_i^b}) \leqslant \epsilon, \tag{5.12}$$

$$\sum_{i\neq k,b} p(\rho_{A|\Pi_i^b}) C_k(\rho_{A|\Pi_i^b}) \leqslant 2\epsilon \tag{5.13}$$

and similarly, when Alice ignores the results of Bob, can be expressed as

$$\sum_{j=k,c} p(\rho_{A|\Pi_j^c}) C_k(\rho_{A|\Pi_j^c}) \leqslant \epsilon, \text{ and} \tag{5.14}$$

$$\sum_{j\neq k,c} p(\rho_{A|\Pi_j^c}) C_k(\rho_{A|\Pi_j^c}) \leqslant 2\epsilon. \tag{5.15}$$

We denote all local unitary equivalent inequalities of Eqs. (5.8) as the first set and Eqs. (5.12)-(5.15) as the second set of inequalities. It is our aim to look for a set of states which violate at least one of the first set but not the second set of inequalities. This would ensure that the state of Alice can only be steered by Bob and Charlie together but not individually.

It is well known fact that a state is deemed steerable if a steering inequality is violated. However, the converse is not always true. Thus, there is no definite way to single out the set of such unsteerable states as is required in the two-qubit scenario to define the set of our interest (S_i). To overcome this issue, we need to use the tightest steering inequalities with semi-definite programming and the free will to choose the bases. However, one may start with the set of states for which bi-partite entanglements i.e., E_{AB} and E_{AC} are zero. For such states, by definition, Alice cannot be steered in the two-qubit scenarios.

For example, we consider a genuine entangled state such as a generalized GHZ state

$$|\psi\rangle = \alpha|000\rangle + \sqrt{1-\alpha^2}|111\rangle, \tag{5.16}$$

where $0 \leq \alpha \leq 1$. For the state, it can be shown that no inequality from the second set is violated. This is due to the fact that the entanglement between Alice-Bob (E_{AB}) and Alice-Charlie (E_{AC}) are zero for GHZ states. On the other hand, all the inequalities in the first set are violated for a certain range of α. Inequality given in Eq.(5.8) gives violation for the maximum range of α than the others. Therefore, we have only shown its variation in Fig. 5.1.

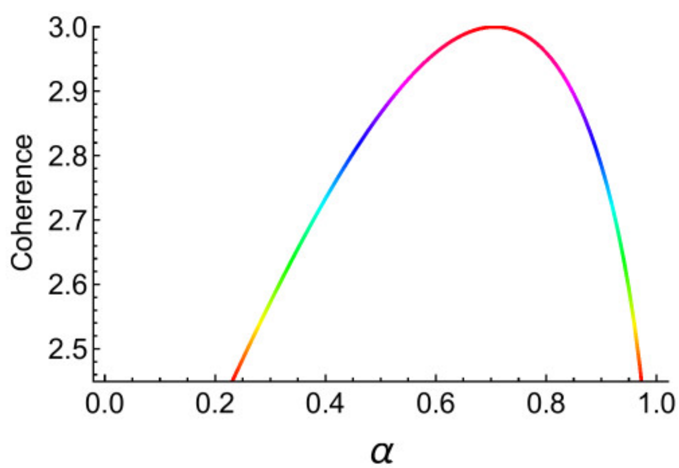

Figure 5.1: Plot of left hand side of Eq. (5.8) considering Pauli bases with respect to arbitrary reference frame vs α for generalized GHZ state in Eq. (5.16). For this range of α, inequality (5.8) shows violation.

In this regard, a non-trivial example would be W state, i.e., $|\psi\rangle_W = \frac{1}{\sqrt{3}}(|001\rangle + |010\rangle + |100\rangle)$, for which (E_{AB}) and (E_{AC}) are non-zero. For this state inequalities of the set I are violated but not of set II. In set I first inequality gives a value of 15.6835, which is greater than $6\sqrt{6} \approx 14.6969$. Second one gives 15.6835 which is also greater than $6\sqrt{6} \approx 14.6969$. Third one is violated by 2.86603 which is greater than $\sqrt{6} \approx 2.4495$. Fourth one give 5.4664 which is again more than $2\sqrt{6} \approx 4.8989$. Fifth and sixth one give 5.69936 which is also more than $2\sqrt{6} \approx 4.8989$. Now we examine the second set for W state. After tracing out Charlie, the concurrence of the reduced density matrix of Alice and Bob is $\frac{2}{3}$. First one give 1.84424, which is less than $\sqrt{6} \approx 2.4495$. For second one we get 3.54606 which is again less than $2\sqrt{6} \approx 4.8989$. Now after tracing out Bob, the concurrence of reduced density matrix of Alice and Charlie is again $\frac{2}{3}$. Third one give 1.84424 which is less than $\sqrt{6} \approx 2.4495$. The final one give 3.54606 which is again less than $2\sqrt{6} \approx 4.8989$. Therefore, we see that W state does not violate the inequalities in the second set, though the reduced density matrix possesses some entanglement after tracing out one party. However, if we consider a generalized W state of the form $|\psi\rangle_{GW} = \frac{1}{5}|001\rangle + \sqrt{\frac{3}{5}}|010\rangle + \frac{3}{5}|100\rangle$, then this state gives violation for set I and set II both. In set I, first inequality gives a value of 17.4464, which is greater than $6\sqrt{6} \approx 14.6969$. Second one gives 14.5289 which is less than $6\sqrt{6} \approx 14.6969$. Third one is violated by 2.92952 which is greater than $\sqrt{6} \approx 2.4495$. Fourth one gives 5.79661 which is more than $2\sqrt{6} \approx 4.8989$. Fifth and sixth one give 5.88952 which is also more than $2\sqrt{6} \approx 4.8989$. Now we will see what happens for the second set for this generalized W state. After tracing out Charlie, the concurrence between Alice and Bob is 0.93. In the second set, first one gives 2.82029, which is greater than $\sqrt{6} \approx 2.4495$. For second one, we get 5.64058 which is more than $2\sqrt{6} \approx 4.8989$. Now tracing out Bob, the concurrence between Alice and Charlie is $\frac{6}{25}$. Third one gives 0.893575 which is less than $\sqrt{6} \approx 2.4495$. The final one gives 1.77809 which is again less than $2\sqrt{6} \approx 4.8989$. Hence, using these two examples, we can emphasize that to violate inequality from the second set, the concurrence of the reduced density matrix has to be more than some specific value.

5.3 Discussion

In this chapter, we have exploited the asymmetric nature of quantum steering and shown the existence of polygamous nature of quantum non-locality, a unique property observed so far only in quantum steering. A recipe has been provided to find the set of polygamous steering states for three-qubit systems. We find that GHZ and W states are good examples of polygamous states.

Chapter 6

Coherence of quantum channels

The quantum coherence like other quantum resources is also fragile in the presence of noisy environment. The interaction of quantum systems with environment have been extensively studied using different models, in particular using noisy channels [16]. Characterizing all these channels and their effect on various physical resources are vital [16, 105]. These channels are also important to construct resource theoretic aspect of coherence. Here, in this chapter, we consider a reverse question. Can we associate coherence with a quantum channel? We define the coherence of quantum channels using the Choi-Jamiołkowski (C-J) isomorphism [60–62]. In this chapter, we consider the unital as well as non-unital qubit channels [62, 104, 105]. We compute their coherence and purity analytically. Using the coherence-purity (CoPu) diagrams, we find that it may be possible to distinguish unital channels and non-unital channels. The resource theory of coherence require two important elements – free states and free operations [10, 106]. Free states are those which have no coherence in a given reference basis. Free operations do not create any coherence and are known as incoherent operations. Depending on the restrictions (physical requirement), there exist different types of incoherent operations. The largest set of incoherent operations contains Maximally Incoherent Operations (MIO) [9]. The other candidates are Incoherent Operations (IO) [106], Strictly Incoherent Operations (SIO) [114, 117], Physical Incoherent Operations (PIO) [107] etc. There are many other free operations in the literature like Fully Incoherent Operations (FIO), Genuine Incoherent Operations (GIO) etc [10, 109]. It is an important task to understand these operations and distinguish them. In this chapter, we aim to distinguish these operations using CoPu diagrams. Furthermore, we also consider the class of coherence non-generating qubit channels (CNC) as well as the channels to create maximal coherence (CMC). CNC is the bigger set in comparison to all incoherent operations [109]. We also consider other known qubit channels like the class of Pauli channels, degradable and anti-degradable channels, amplitude damping channels, depolarizing channels, and homogenization channels and show that they might be distinguished using CoPu diagrams.

6.1 C-J Isomorphism and coherence of a channel

C-J isomorphism or channel state duality can be represented as [60–62]

$$\rho_{AB} = \Phi \otimes \mathbb{I}_B(|\Psi\rangle_{AB}\langle\Psi|), \tag{6.1}$$

where $|\Psi\rangle_{AB}$ is a maximally entangled state and Φ corresponds to a quantum channel. As there is one to one map between the state and the channel, the coherence of the final state ρ_{AB} can represent the coherence of the quantum channel. Hence, coherence of the channel Φ is

$$C_{l_1}(\Phi) = C_{l_1}(\rho_{AB}). \tag{6.2}$$

In this chapter we will only consider qubit channels. For qubit channels, without loss of generality, we will consider the singlet state as the two-qubit maximally entangled state. The canonical form of singlet state is

$$|\Psi\rangle_{AB}\langle\Psi| = \frac{1}{4}(\mathbb{I} \otimes \mathbb{I} - \sum_{i=1}^{3} \sigma_i \otimes \sigma_i), \tag{6.3}$$

where σ_i ($i = 1, 2, 3$) are the Pauli matrices. Coherence of a state depends on the reference basis used to write it. Here throughout the chapter, we will use computational basis as the reference basis.

6.2 Coherence of the channels

Here we investigate the coherence of the unital as well as non-unital channels. According to C-J isomorphism, the coherence of the channels is equivalent to the coherence of the transformed singlet state. Hence, the channel coherence and its other properties can easily be evaluated. In this section, we will mainly follow the affine representation of the channel (AROC) as described in Sec. 1.4, chapter 1.

6.2.1 Coherence of Unital Channels

Unital qubit channels are those which do not change the maximally mixed state, $\mathbb{I}/2$. They satisfy, $\sum_i K_i^\dagger K_i = \mathbb{I} = \sum_i K_i K_i^\dagger$. From the section 1.4 in chapter 1, it is clear that the set of unital channels can be represented as a three-parametric family of completely positive maps. Now if we apply the C-J map on the state given in (6.3), then the final state will be

$$\rho_{AB} = \frac{1}{4}\Big(\mathbb{I}\otimes\mathbb{I} - \vec{\lambda}\cdot(\vec{\sigma}\otimes\vec{\sigma})\Big). \tag{6.4}$$

The positivity of the eigenvalues of ρ_{AB} will ensure the complete positivity of the unital map. Let us define $q_{ij} = 1 + (-1)^i\lambda_x + (-1)^{i+j}\lambda_y + (-1)^j\lambda_z$ with $i, j = 0, 1$, where q_{ij} are the four eigenvalues of the density matrix ρ_{AB}. Therefore, the positivity constraints on the unital channels are [105]

$$q_{ij} \geq 0. \tag{6.5}$$

Using the l_1-norm, the coherence of the unital channel is given by

$$C_{l_1} = \frac{1}{2}\big(|\lambda_x + \lambda_y| + |\lambda_x - \lambda_y|\big). \tag{6.6}$$

Note that the coherence does not depend on λ_z. It implies that many isocoherence planes will lie along λ_z axis. This is the consequence of the choice of reference basis. The coherence of unital channel will reach its maximum value 1 when we have $\lambda_x = \lambda_y = \pm 1$ or $\lambda_x = -\lambda_y = \pm 1$. The purity, as defined by $\mathcal{P} = \mathrm{Tr}[\rho^2]$, of the unital channel is given by

$$\mathcal{P} = \frac{1}{4}(1 + |\vec{\lambda}|^2). \tag{6.7}$$

It is well known that the unital channels form a tetrahedron with unitary operators in its vertices [182]. The state ρ_{AB} has the same geometrical picture. Bell states sits on the four extremal points of the tetrahedron [182]. From eq. (6.7) it is clear that $|\vec{\lambda}|^2 = 4\mathcal{P} - 1$. Values of λ_i lie on the surface of sphere with the radius $4\mathcal{P} - 1$ centered at the point $\lambda_x = \lambda_y = \lambda_z = 0$. The channels with the same purity form a sphere. Therefore, there may exist quantum channels with different coherence but the same purity (see Fig.6.1).

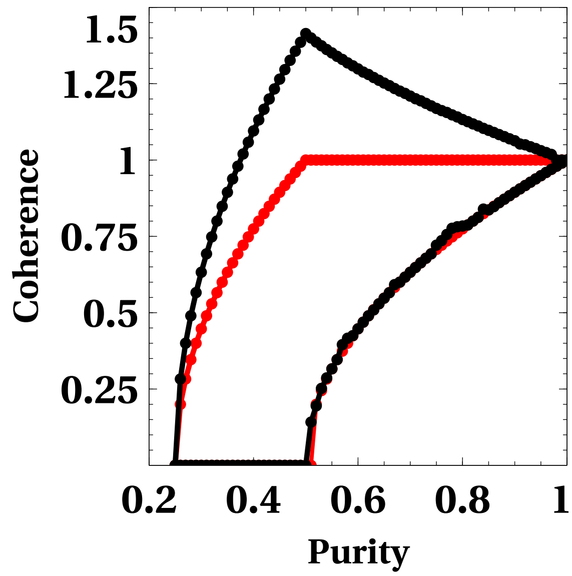

Figure 6.1: The figure depicts the allowed region of coherence as measured by the l_1-norm for unital (region inside red curve) and non-unital (region inside black curve) channels, respectively for the allowed purity range. The CoPu diagram shows that the channels outside the overlap region are non-unital and can be exactly distinguished from unital ones. The purity for these channels, $\mathcal{P} \in [\frac{1}{4}, 1]$.

6.2.2 Coherence of Non-unital Channels

The non-unital qubit channels are characterized by six parameters as shown in the section 1.4 in chapter 1. The Choi matrix corresponding to the non-unital channels is given by

$$\rho_{AB} = \frac{1}{4}\Big((\mathbb{I} + \vec{\tau}\cdot\vec{\sigma}) \otimes \mathbb{I} - \vec{\lambda}\cdot(\vec{\sigma}\otimes\vec{\sigma})\Big). \tag{6.8}$$

The positivity of the non-unital channel is guaranteed by $\rho_{AB} \geq 0$. Let us define $\tau = \parallel \vec{\tau} \parallel$ and $\hat{n} = \frac{\vec{\tau}}{\tau}$. Then the non-unital map is positive iff

$$q_{ij} \geq 0 \text{ and } \tau^2 \leq u - \sqrt{u^2 - q}, \tag{6.9}$$

where $u = 1 - \sum \lambda_i^2 + 2\sum \lambda_i^2 n_i^2$ and $q = \prod q_{ij}$ [105].

The coherence of the non-unital channel is given by

$$C_{l_1} = \frac{1}{2}\Big(|\lambda_x + \lambda_y| + |\lambda_x - \lambda_y| + 2\sqrt{\tau_x^2 + \tau_y^2}\Big). \tag{6.10}$$

Note that the coherence is independent of both λ_z and τ_z. Hence, some isocoherence planes will lie on the λ_z and τ_z planes. The purity for the channel is given by

$$\mathcal{P} = \frac{1}{4}(1 + |\vec{\lambda}|^2 + |\vec{\tau}|^2). \tag{6.11}$$

Eq. (6.11) can be written as $|\vec{\lambda}|^2 + |\vec{\tau}|^2 = 4\mathcal{P} - 1$. It is clear, as before, that for a fixed purity, the values of parameters characterizing non-unital channels lie on the surface of a sphere. By fixing purity we can get the allowed regions of coherence as is shown in the Fig.6.1.

Observation 1: If the coherence of the channel is more than 1, then it is non unital. One can easily see this from Fig. 6.1. Hence, CoPu diagrams can help us distinguishing between unital and non unital channels for some region.

Observation 2: Unital channel cannot create coherence in the subsystem A whereas the non-unital channel can.

It can be easily checked by looking at the density matrix of the subsystem A after the operation of the channel on the state (6.3). For unital and non-unital channel density matrices of subsystem A are respectively

$$\rho_A^u = \frac{1}{2}\mathbb{I} \quad \text{and} \quad \rho_A^{nu} = \frac{1}{2}\begin{pmatrix} 1+\tau_z & \tau_x - i\tau_y \\ \tau_x + i\tau_y & 1-\tau_z \end{pmatrix}. \tag{6.12}$$

where $\rho_A^u = \text{Tr}[\Phi_A^u \otimes \mathbb{I}_B(|\Psi\rangle_{AB}\langle\Psi|)]$ and $\rho_A^{nu} = \text{Tr}[\Phi_A^{nu} \otimes \mathbb{I}_B(|\Psi\rangle_{AB}\langle\Psi|)]$. Note that the non-unital channels with $\vec{\tau} = (0, 0, \tau_z)$, cannot create coherence in subsystem A.

If we look closely at Eq.(6.10) and Eq.(6.12), it is clear that the coherence of the nonunital channel can exactly be decomposed into the coherence of unital channel plus the coherence induced in the subsystem A by the nonunital channel, i.e.,

$$C_{l_1}(\Phi^{nu}) = C_{l_1}(\Phi^u) + C_{l_1}(\rho_A^{nu}). \tag{6.13}$$

Also the Eq.(6.13) tells that $C_{l_1}(\Phi^{nu}) \geq C_{l_1}(\Phi^u)$. The Eq.(6.13) has been depicted in Fig.6.2. Plot shows that the minimum coherence of nonunital channels are exactly equal to the coherence induced in the subsystem A.

Proposition 1: All coherence breaking channels have zero coherence.

Proof. A quantum channel is called coherence breaking channel if it maps any state to an

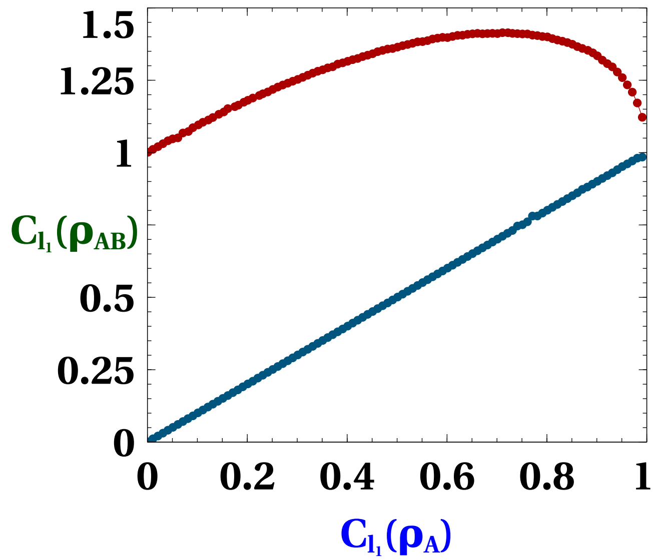

Figure 6.2: The channel coherence ($C_{l_1}(\rho_{AB})$) vs coherence induced in the subsystem A ($C_{l_1}(\rho_A)$) plot for nonunital qubit channels. The red curve depicts the nonunital channels which has maximum coherence for a given subsystem coherence whereas blue one represents the nonunital channels with minimum coherence. Plot shows that the minimum channel coherence is exactly equal to the coherence induced in the subsystem A.

incoherent state [183]. This fact directly imply the above proposition.1. As an example, one can consider the case of qubit channels. For coherence breaking qubit channels, the Λ_Φ should take the following form [183]

$$\Lambda_\Phi = \begin{pmatrix} 1 & 0 & 0 & 0 \\ 0 & 0 & 0 & 0 \\ 0 & 0 & 0 & 0 \\ \tau_z & 0 & 0 & \lambda_z \end{pmatrix}.$$

Applying this channel on the state (6.3), one can show that Choi matrix is

$$\frac{1}{4}\begin{pmatrix} 1+\tau_z-\lambda_z & 0 & 0 & 0 \\ 0 & 1+\tau_z+\lambda_z & 0 & 0 \\ 0 & 0 & 1-\tau_z+\lambda_z & 0 \\ 0 & 0 & 0 & 1-\tau_z-\lambda_z \end{pmatrix}.$$

Clearly, we get an incoherent Choi matrix.

6.3 Coherence of incoherent channels

Like entanglement the concept of free operations or incoherent operations in resource theory of coherence is not unique. There exists many concepts of incoherent operations from the resource theory perspective of coherence. We have already discussed about different incoherent operations in chapter 1. Here we will discuss about the coherence of the incoherent channels using C-J isomorphism.

The following Kraus representations are the possible FIOs for single qubits [109]

$$\left\{\begin{pmatrix} a_1 & b_1 \\ 0 & 0 \end{pmatrix}, \begin{pmatrix} a_2 & b_2 \\ 0 & 0 \end{pmatrix}\right\}; \left\{\begin{pmatrix} 0 & 0 \\ a_1 & b_1 \end{pmatrix}, \begin{pmatrix} 0 & 0 \\ a_2 & b_2 \end{pmatrix}\right\};$$
$$\left\{\begin{pmatrix} 0 & d_1 \\ c_1 & 0 \end{pmatrix}, \begin{pmatrix} 0 & d_2 \\ c_2 & 0 \end{pmatrix}\right\}; \left\{\begin{pmatrix} c_1 & 0 \\ 0 & d_1 \end{pmatrix}, \begin{pmatrix} c_2 & 0 \\ 0 & d_2 \end{pmatrix}\right\}; \tag{6.14}$$

where $|a_1|^2 + |b_1|^2 = 1 = |a_2|^2 + |b_2|^2$ and $a_1 b_1^* + a_2 b_2^* = 0 = b_1 a_1^* + b_2 a_2^*$, and $|c_1|^2 + |c_2|^2 = 1 = |d_1|^2 + |d_2|^2$. From Eq. (6.14) one can easily check that all the matrices of a Kraus representations have the same form. As an example, the first two matrices have nonzero entries only in the first row. The last one is the GIO for the qubit case. Note that first two FIOs have zero coherence. The coherence and purity of last two FIOs are $C_{l_1} = |d_1 c_1^* + d_2 c_2^*|$ and $\mathcal{P} = \frac{1}{2}(1 + C_{l_1}^2)$. Hence, we have the relation $2\mathcal{P} - C_{l_1}^2 = 1$ with $\mathcal{P} \in [\frac{1}{2}, 1]$.

According to the Ref. [184], any qubit incoherent operation (IO) admits a decomposition with at most five Kraus operators. A canonical choice of Kraus operators for IO is

$$\left\{\begin{pmatrix} a_1 & b_1 \\ 0 & 0 \end{pmatrix}, \begin{pmatrix} 0 & 0 \\ a_2 & b_2 \end{pmatrix}, \begin{pmatrix} a_3 & 0 \\ 0 & b_3 \end{pmatrix}, \begin{pmatrix} 0 & b_4 \\ a_4 & 0 \end{pmatrix}, \begin{pmatrix} a_5 & 0 \\ 0 & 0 \end{pmatrix}\right\}, \tag{6.15}$$

where one can choose $a_i \in \mathbb{R}$ while $b_i \in \mathbb{C}$. Further, $\sum_{i=1}^{5} a_i^2 = \sum_{j=1}^{4} |b_j|^2 = 1$ and $a_1 b_1 + a_2 b_2 = 0$ holds. The coherence and purity of IOs are $C_{l_1} = \sum_{i=1}^{4} a_i |b_i|$ and $\mathcal{P} = \frac{1}{2}[1 - \mu(1-\mu) - \kappa(1-\kappa) + \sum_{i=1}^{4} a_i^2 |b_i|^2]$, respectively, where $\mu = (a_2^2 + a_4^2)$ and $\kappa = (|b_1|^2 + |b_4|^2)$.

Similarly, Ref. [184] shows that the canonical set of Kraus operators for SIO is

$$\left\{ \begin{pmatrix} a_1 & 0 \\ 0 & b_1 \end{pmatrix}, \begin{pmatrix} 0 & b_2 \\ a_2 & 0 \end{pmatrix}, \begin{pmatrix} a_3 & 0 \\ 0 & 0 \end{pmatrix}, \begin{pmatrix} 0 & 0 \\ a_4 & 0 \end{pmatrix} \right\}, \tag{6.16}$$

where $a_i \in \mathbb{R}$ and $\sum_{i=1}^{4} a_i^2 = \sum_{j=1}^{2} |b_j|^2 = 1$ holds. The coherence and purity of SIOs are $C_{l_1} = a_1|b_1| + a_2|b_2|$ and $\mathcal{P} = \frac{1}{2}[1 - \nu(1-\nu) + |b_1|^2|b_2|^2 + \sum_{i=1}^{2} a_i^2|b_i|^2]$, respectively, with $\nu = (a_1^2 + a_3^2)$.

The CoPu diagrams in Fig.(6.3) show that SIOs are subset of IOs. Note that all of the purity range is not allowed for both SIOs and IOs.

Observtion 3: It is possible to distinguish between SIO and IO for some regions of CoPu diagram in Fig. 6.3. According to the Ref. [184, 185], if one considers state transformation by incoherent operations, qubit SIOs and IOs are equivalent. However, the above observation tells us the opposite behavior.

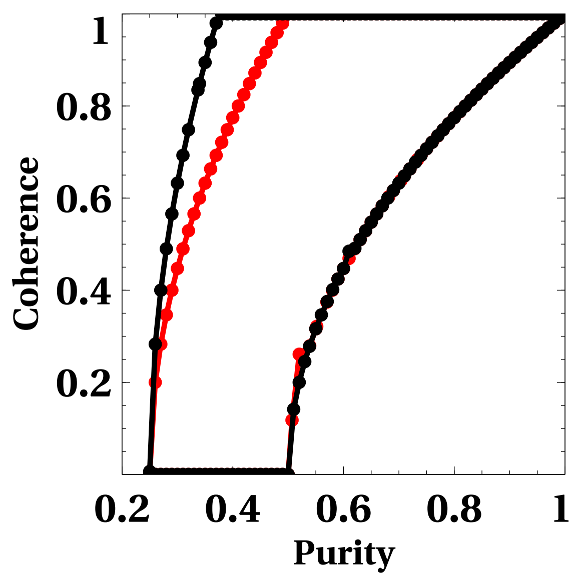

Figure 6.3: The allowed coherence-vs-purity region for IO (region inside black curve) and SIO (region inside red curve) respectively. Coherence of the channels is measured by l_1-norm. The figure depicts the well known phenomenon that $SIO \subset IO$. Moreover, channels outside the overlap region are IO and can be easily distinguished from the SIO.

The Kraus representation of all possible single qubit PIOs are given by [185]

$$\left\{\begin{pmatrix} e^{i\theta_1} & 0 \\ 0 & 0 \end{pmatrix}, \begin{pmatrix} 0 & 0 \\ 0 & e^{i\theta_2} \end{pmatrix}\right\}; \left\{\begin{pmatrix} 0 & 0 \\ e^{i\phi_2} & 0 \end{pmatrix}, \begin{pmatrix} 0 & e^{i\phi_1} \\ 0 & 0 \end{pmatrix}\right\};$$
$$\left\{\begin{pmatrix} e^{i\theta_1} & 0 \\ 0 & 0 \end{pmatrix}, \begin{pmatrix} 0 & e^{i\phi_1} \\ 0 & 0 \end{pmatrix}\right\}; \left\{\begin{pmatrix} 0 & 0 \\ e^{i\phi_2} & 0 \end{pmatrix}, \begin{pmatrix} 0 & 0 \\ 0 & e^{i\theta_2} \end{pmatrix}\right\}; \tag{6.17}$$
$$\left\{\begin{pmatrix} e^{i\theta_1} & 0 \\ 0 & e^{i\theta_2} \end{pmatrix}\right\}; \left\{\begin{pmatrix} 0 & e^{i\phi_1} \\ e^{i\phi_2} & 0 \end{pmatrix}\right\}, \tag{6.18}$$

where first four PIOs are the coherence breaking channels and have zero coherence in both KROC and AROC, and the last two PIOs are the all possible single qubit CPOs and have unit coherence and unit purity in KROC. As the coherence of PIO is either zero or one hence, we establish a well known fact that $PIO \subset SIO \subset IO$.

Although we have expected that the coherence of the incoherent channels will be zero, it turns out to be not so. However, we draw the following observation from the incoherent channels considered in this section.

Observation 4: All qubit incoherent channels which are either unital or nonunital, cannot create coherence in the subsystem 'A' of its Choi matrix. It can easily be verified from the Table 6.1.

Proof. Here we will try to prove the Observation.4 for IO, SIO and PIO. If we consider the Kraus decomposition of IO as given in Eq.(1.49), then its Choi matrix will be

$$\begin{aligned}
\rho_{AB} &= \frac{1}{d}\sum_i K_i \otimes \mathbb{I}\left(\sum_{lm} |ll\rangle\langle mm|\right) K_i^\dagger \otimes \mathbb{I}, \\
&= \frac{1}{d}\sum c_{ij}c_{it}^* |f_i(j)\rangle\langle j|l\rangle\langle m|t\rangle\langle f_i(t)| \otimes |l\rangle\langle m|, \\
&= \frac{1}{d}\sum c_{ij}c_{it}^* |f_i(j)\rangle\langle f_i(t)| \otimes |l\rangle\langle m|\delta_{jl}\delta_{mt}, \\
&= \frac{1}{d}\sum c_{il}c_{it}^* |f_i(l)l\rangle\langle f_i(t)t|.
\end{aligned}$$

Now the reduced density matrix of the subsystem A is

$$\begin{aligned}
\rho_A &= \frac{1}{d}\sum c_{il}c_{it}^* |f_i(l)\rangle\langle f_i(t)| \otimes \langle n|l\rangle\langle t|n\rangle, \\
&= \frac{1}{d}\sum c_{il}c_{il}^* |f_i(l)\rangle\langle f_i(l)|.
\end{aligned} \tag{6.19}$$

Therefore, ρ_A is incoherent for IO. This also guarantees that ρ_A will be incoherent for SIO and PIO. Although we do not have direct proof for other type of incoherent operations, the following Table. 6.1 confirms that the Observation.4 is also true at least for single qubit FIO and GIO. $\square$

This observation says that the nonunital channels which has $\vec{\tau} = \{0, 0, \tau_z\}$ qualifies as potential candidates for incoherent operations (see Table 6.1).

Channels	Coherence of ρ_{AB}	ρ_A	τ_z
IO	$[0, 1]$	0	$*$
SIO	$[0, 1]$	0	$*$
PIO (CPO)	0 (1)	0	$*$
FIO (GIO)	#($[0, 1]$)	0	# (0)

Table 6.1: Table shows that all qubit incoherent operations have zero coherence in $\rho_A(= \text{Tr}_A[\rho_{AB}])$. The $*$ denotes that the corresponding channels are in general nonunital. The # for FIOs indicates that the channels which have zero coherence (in Choi matrix) are nonunital otherwise they are unital.

6.3.1 Coherence Non-Generating Channel (CNC)

A CPTP map, Φ which does not generate quantum coherence from an incoherent state is known as the coherence non-generating channel [186], i.e., $\Phi[\mathcal{I}] \subset \mathcal{I}$. The incoherent operations are strict subset of these channels. These channels are different from the set of incoherent operations in the sense that the monotonicity of coherence may break under these operations while acting on one subsystem [186].

Proposition 2: For general qubit CNC channels, $0 \leq C_{l_1} \leq \sqrt{2}$.

Proof. A full rank qubit channel is CNC iff it admits following two Kraus decompositions

[186]. The first one is

$$K_1 = \begin{pmatrix} \mathrm{e}^{\mathrm{i}\eta}\cos\theta\cos\phi & 0 \\ -\sin\theta\sin\phi & \mathrm{e}^{\mathrm{i}\xi}\cos\phi \end{pmatrix},$$

$$K_2 = \begin{pmatrix} \sin\theta\cos\phi & \mathrm{e}^{\mathrm{i}\xi}\sin\phi \\ \mathrm{e}^{-\mathrm{i}\eta}\cos\theta\sin\phi & 0 \end{pmatrix},$$

where $\theta, \phi, \xi, \eta \in \mathbb{R}$. Notice that K_1 and K_2 may not individually be incoherent but $K_1(\cdot)K_1^\dagger + K_2(\cdot)K_2^\dagger$ can be if $\sin\phi\cos\phi\sin\theta\cos\theta = 0$. Therefore, CNC channels may not be incoherent.

The coherence and purity of the above channel are given by $C_{l_1} = \cos\theta + |\sin\theta\sin 2\phi|$ and $\mathcal{P} = \frac{1}{8}(5+\cos 2\theta + 2\cos^2\theta\cos 4\phi)$, respectively. The incoherent condition will always guarantee that the coherence will be less than or equal to 1. Otherwise, the coherence of CNC can be $0 \leq C_{l_1} \leq \sqrt{2}$. The coherence will reach its maximum at $\theta = \frac{\pi}{4} = \phi$.

The other CNC channel is given by

$$K_1 = \begin{pmatrix} \cos\theta & 0 \\ 0 & \mathrm{e}^{\mathrm{i}\chi}\cos\phi \end{pmatrix} \quad \text{and} \quad K_2 = \begin{pmatrix} 0 & \sin\phi \\ \mathrm{e}^{\mathrm{i}\chi}\sin\theta & 0 \end{pmatrix}.$$

This channel is an incoherent channel. The coherence and purity of this CNC channel is $C_{l_1} = \cos\theta\cos\phi + |\sin\theta\sin\phi|$ and $\mathcal{P} = \frac{1}{16}(10 + \cos 4\theta + 4\cos 2\theta\cos 2\phi + \cos 4\phi)$, respectively and $0 \leq C_{l_1} \leq 1$.

The Fig. (6.4) shows allowed range of all CNC channels. It is clear that allowed region of incoherent CNCs is inside the region of all CNCs. From the CoPu diagrams it is clear that for these channels, purity ranges from $\frac{1}{2}$ to 1.

6.4 Coherence of other known qubit channels

In this section we will consider some known qubit channels and find its l_1-norm coherence. We will investigate whether these channels can be characterized by its coherence and purity.

Channel to obtain maximum coherence (CMC): The maximum value of the l_1-norm coherence for two qubit system is 3. This value is achieved by the state $|++\rangle$, where

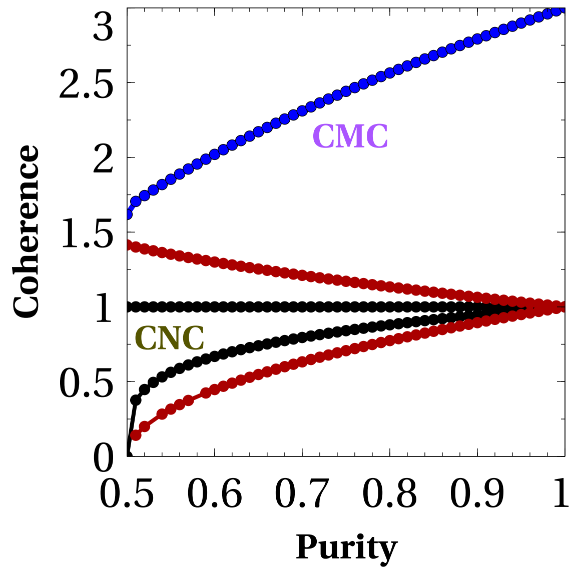

Figure 6.4: The allowed coherence-vs-purity region for CMC and CNC. The region inside the red curve is for CNC and if the CNCs are incoherent then its coherence lie in the region between black curves. The region between upper black line ($y = 1$ -line) and blue curves is for CMCs. Note that for all these channels $\mathcal{P} \in [\frac{1}{2}, 1]$.

$|+\rangle = \frac{1}{\sqrt{2}}(|0\rangle + |1\rangle)$. Hence, its obvious to search for a qubit channel which will reach this value.

Proposition 3: For general two qubit CMC channels, $1 \leqslant C_{l_1} \leqslant 3$.

Proof. The channel which may reach this value admits the following Kraus decomposition

$$K_1 = \frac{1}{\sqrt{2}} \begin{pmatrix} \cos\theta_1 & \mathrm{e}^{-\mathrm{i}\phi_1}\sin\theta_1 \\ \mathrm{e}^{\mathrm{i}\phi_1}\sin\theta_1 & -\cos\theta_1 \end{pmatrix},$$

$$K_2 = \frac{1}{\sqrt{2}} \begin{pmatrix} \cos\theta_2 & \mathrm{e}^{-\mathrm{i}\phi_2}\sin\theta_2 \\ \mathrm{e}^{\mathrm{i}\phi_2}\sin\theta_2 & -\cos\theta_2 \end{pmatrix}.$$

The coherence and purity of the channel is

$$\begin{aligned} C_{l_1} &= \frac{1}{4}\Big(2 + \varsigma + \sum_{j=\pm} g_j + f_j\Big), \\ \mathcal{P} &= \frac{1}{16}(11 + 3\cos 2\theta_1 \cos 2\theta_2 + \varsigma + \ell_{21} + \ell_{12}), \end{aligned} \tag{6.20}$$

where $g_\pm = |\mathrm{e}^{\pm 2\mathrm{i}\phi_1}\sin^2\theta_1 + \mathrm{e}^{\pm 2\mathrm{i}\phi_2}\sin^2\theta_2|$, $f_\pm = 2|\mathrm{e}^{\pm\mathrm{i}\phi_1}\sin 2\theta_1 + \mathrm{e}^{\pm\mathrm{i}\phi_2}\sin 2\theta_2|$, $\varsigma = \cos 2\theta_1 + \cos 2\theta_2$ and $\ell_{mn} = 4\cos m(\phi_1 - \phi_1)\sin^m n\theta_1 \sin^m n\theta_2$. The coherence of the channel will reach its maximum, i.e., $C_{l_1} = 3$ for $\theta_1 = \frac{\pi}{4} = \theta_2$ and $\phi_1 = \phi_2$. In fact, the coherence of this channel obeys $1 \leq C_{l_1} \leq 3$ which is confirmed by the CoPu diagram (see Fig. (6.4)). Therefore, CMC channel either increases or unalters the coherence of the state. Moreover, this channel can be considered as coherence generating channel.

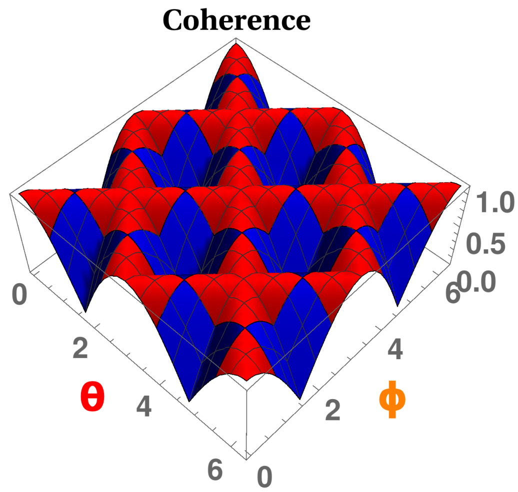

Figure 6.5: Plot of the l_1-norm coherence of degradable (red regions) and anti-degradable channels (blue regions) with the parameters θ and ϕ. It depicts that the whole region is completely covered and degradable channels lie in the range $\frac{1}{\sqrt{2}} \leq C_{l_1} \leq 1$.

A family of qubit channels: A family of qubit channels can be described by two Kraus operators in σ_z basis as [187]

$$K_1 = \begin{pmatrix} \cos\theta & 0 \\ 0 & \cos\phi \end{pmatrix} \quad \text{and} \quad K_2 = \begin{pmatrix} 0 & \sin\phi \\ \sin\theta & 0 \end{pmatrix}, \tag{6.21}$$

where $\theta, \phi \in [0, \pi]$. In AROC, the channel is described by $\lambda_x = \cos(\phi - \theta)$, $\lambda_y = \cos(\phi + \theta)$, $\lambda_z = (\cos 2\phi + \cos 2\theta)/2$, $\tau_x = \tau_y = 0$ and $\tau_z = (\cos 2\theta - \cos 2\phi)/2$. The coherence and purity of the channel are $C_{l_1} = \cos\theta\cos\phi + |\sin\theta\sin\phi|$ and $\mathcal{P} = \frac{1}{2} + \frac{1}{8}(\cos 2\phi + \cos 2\theta)^2$.

We know that a CPTP map can be described as a unitary coupling with the external environment. If a CPTP map Φ changes a state ρ_S to ρ'_S, then it can be represented as

$$\rho'_S = \Phi(\rho_S) = \text{Tr}_E[U_{SE}(\rho_S \otimes \omega_E)U^\dagger_{SE}], \tag{6.22}$$

where U_{SE} is the unitary coupling between the system and the environment E and ω_E is a fixed state of E. In this process environment state also changes to ω'_E. A CPTP map can also be represented as operator sum representation as in Eq. (1.43). The final environment state can be found from the initial system state ρ by using the complementary channel Φ' of Φ as

$$\omega'_E = \Phi'(\rho_S) = \text{Tr}_S[U_{SE}(\rho_S \otimes \omega_E)U^\dagger_{SE}]. \tag{6.23}$$

A map Φ is called degradable if there exists a third map Ω such that $\Phi' = \Omega\Phi$ and Ω takes the state ρ'_S to ω'_E [187]. Similarly a map is antidegradable if there exist a Ω such that $\Phi = \Omega\Phi'$ and which take the final environment state ω'_E to ρ'_S [187]. More details can be found in the reference [187]. The channel represented in Eq. (6.21) is degradable for $\frac{\cos 2\theta}{\cos 2\phi} \geq 0$, otherwise anti-degradable [187], see Fig.(6.5). The Fig.(6.5) shows that the coherence of degradable channel satisfies $\frac{1}{\sqrt{2}} \leq C_{l_1} \leq 1$. The CoPu diagram in Fig.(6.7) also confirms this observation.

Observation 5: If the channel in Eq.(6.21) is anti-degradable then its coherence be always less than $\frac{1}{\sqrt{2}}$.

For $\cos 2\theta = 1$ and $\cos 2\phi = 2\eta - 1$, it describes the amplitude damping (AD) channels with damping rate η. The coherence and purity of AD channels are $C_{l_1} = \sqrt{\eta}$ and $\mathcal{P} = \frac{1}{2}(1 + C^4_{l_1})$ respectively. Equivalently, $C_{l_1} = \sqrt[4]{2\mathcal{P} - 1}$. As it is a non-unital channel, the CoPu diagram for this channel is shown in Fig.(6.7).

If $\sin\theta = \pm\sin\phi$, the above channel becomes unital. Specifically, for $\theta = \phi$, the channel becomes a bit flip channel but for $\theta = -\phi$, it is a bit-phase flip channel. The coherence and purity of both bit flip and bit-phase flip channels are $C_{l_1} = \cos(2\theta)$ and $\mathcal{P} = \frac{1}{4}(1 + 2C^2_{l_1})$ respectively or equivalently, $2\mathcal{P} - C^2_{l_1} = \frac{1}{2}$, with $\mathcal{P} \in [\frac{1}{4}, \frac{3}{4}]$. The above channel will unitarily transform to a phase flip channel (decoherence channel) if we multiply the Kraus operators with Hadamard gate [187]. All the Pauli channels are unital channels. Thus, the CoPu diagrams of these channels can be depicted inside the CoPu diagram of general unital channels (see Fig. (6.6)).

Qubit Decoherence, Depolarization and Homogenization channels: The decoherence, depolarization and homogenization are nonunitary channels and form Markovian semigroup [182].

The decoherence is a process in which the off-diagonal terms of the density matrix of a quantum system are continuously suppressed in time, i.e., $\rho \to \rho_{t\to\infty} = \text{diag}(\rho)$. The

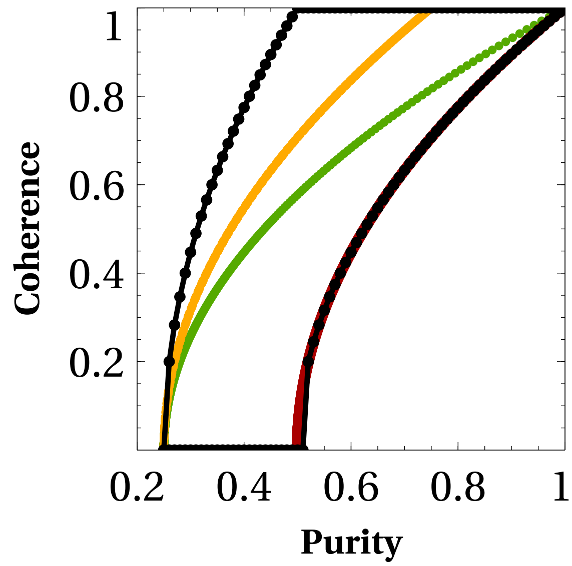

Figure 6.6: Figure depicts the coherence vs purity curve for unital channels. The red curve depicts the decoherence channels which coincides with the lower boundary of CoPu curve of unital channels. The green curve represents the depolarizing channels and the orange one is for the bit flip as well as bit-phase flip channels.

decoherence channel is described by $\lambda_x = \lambda_y = \mathrm{e}^{-\frac{t}{T}}$ and $\lambda_z = 1$. This channel is a unital channel. The coherence and purity of this channel are given by

$$C_{l_1} = \mathrm{e}^{-\frac{t}{T}} \text{ and } \mathcal{P} = \frac{1}{2}(1 + C_{l_1}^2) \tag{6.24}$$

respectively. Now we have $2\mathcal{P} - C_{l_1}^2 = 1$. As $\mathcal{P} \in [\frac{1}{2}, 1]$, the decoherence channels will represent the minimum coherence boundary of unital channels. The CoPu diagram for this channel is in Fig.(6.6).

Observation 6: For the qubit decoherence channels, the concurrence and the l_1-norm coherence are same.

The above observation can be easily verified as the concurrence of the decoherence channel is $\mathrm{e}^{-\frac{t}{T}}$ [182].

The depolarizing channel with noise parameter p transmits an input qubit perfectly with probability $1-p$ and outputs the completely mixed state with probability p, i.e., $\rho \to \rho_f = (1-p)\rho + p\mathbb{I}/2$. The depolarization channel is described as $\lambda_x = \lambda_y = \lambda_z = \mathrm{e}^{-\frac{t}{T}}$. This channel is also a unital channel. The coherence and purity of this channel are

$$C_{l_1} = \mathrm{e}^{-\frac{t}{T}} \text{ and } \mathcal{P} = \frac{1}{4}(1 + 3C_{l_1}^2), \tag{6.25}$$

respectively. Therefore, $4\mathcal{P} - 3C_{l_1}^2 = 1$, with $\mathcal{P} \in [\frac{1}{4}, 1]$. This restriction is represented in CoPu diagram (see Fig.(6.6)).

The homogenization is an evolution that transforms the whole Bloch sphere into a single point, i.e., it is a contractive map with the fixed point (the stationary state of the dynamics). This map is described by $\lambda_x = \lambda_y = \mathrm{e}^{-\frac{t}{T_2}}$, $\lambda_z = \mathrm{e}^{-\frac{t}{T_1}}$, $\tau_x = \tau_y = 0$ and $\tau_z = \omega(1 - \mathrm{e}^{-\frac{t}{T_1}})$, where the parameters, ω is the purity of the final state, T_1 is the decay time, T_2 is the decoherence time. It is a non-unital process. The coherence and the purity of this channel are

$$C_{l_1} = \mathrm{e}^{-\frac{t}{T_2}} \text{ and } \mathcal{P} = \frac{1}{4}[1 + \mathrm{e}^{-\frac{2t}{T_1}} + 2\mathrm{e}^{-\frac{2t}{T_2}} + \omega^2(1 - \mathrm{e}^{-\frac{t}{T_1}})^2], \tag{6.26}$$

respectively. For $\omega = 1$ and $T_2 = 2T_1$, we have the relation between the coherence and purity as given by $C_{l_1} = \sqrt[4]{2\mathcal{P} - 1}$. Some CoPu diagrams of this channel are shown in Fig. (6.7).

6.5 Relative Entropy of Coherence and Holevo quantity

Here, we find a complimentarity relation between the relative entropy of coherence and the Holevo quantity of the channel. Recently, there has been an attempt to find such relation involving quantum coherence and the information processing quantities like superdense coding capacity, teleportation fidelity etc [188]. In fact, in Ref. [189], authors try to relate the Holevo quantity with the loss of coherence due to the projective measurement in one of the subsystems of an arbitrary bipartite density matrix.

The Holevo quantity is lower bound to the classical capacity of the quantum channel. In fact, the Holevo quantity is exactly equal to the classical capacity for all entanglement breaking channels, depolarizing channels and qubit unital channels. Let us define the Holevo quantity, χ. Let Alice encode the information of an random variable X in an quantum ensemble $\{p_x, \rho_x\}$ and sends it to Bob through a quantum channel. In order to extract the information about X, Bob will perform positive operator valued measurement

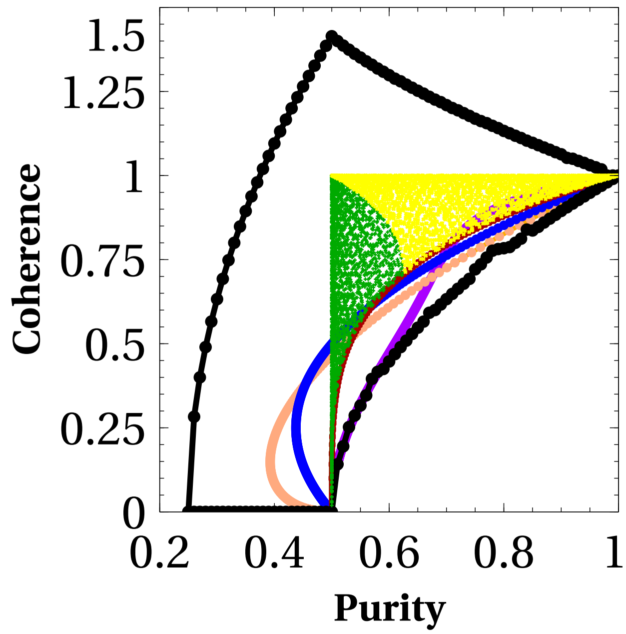

Figure 6.7: Figure depicts the coherence vs purity curve for non-unital channels. The green region represents the anti-degradable channels whereas the yellow region shows the degradable ones. The lower boundary of these two channels coincides with the red curve which represents the amplitude damping channels. The blue, orange, red and the purple curve represents the homogenization channels for $T_2 = T_1$, $2T_2 = T_1$, $T_2 = 2T_1$ and $T_2 = 5T_1$ respectively with $\omega = 1$. Note that the $T_2 = 2T_1$ curve coincides with AD curve.

(POVM) on the received state and record the outcomes which is another random variable Y. Then we have the following inequality

$$I(X : Y) \leq S(\sum_x p_x \rho_x) - \sum_x p_x S(\rho_x), \tag{6.27}$$

where $S(\rho_X) - \sum_x p_x S(\rho_x) = \chi$, the Holevo quantity []. It gives the upper bound to the accessible information about X by Bob.

The classical correlations [190] and the Holevo quantity are related concepts [191]. *A bipartite state will have classical correlations if after application of rank one POVM (i.e., entanglement breaking operation) on one of the parties will transform the state to either classical-quantum (CQ) or quantum classical (QC) states* [191]. The classical correlations

[190] of a quantum state ρ_{SA} is given by,

$$J = \sup_{\Pi_j} \left[S(\rho_S) - \sum_j p_j S(\rho_{S|\Pi_j^A}) \right], \tag{6.28}$$

where $\rho_{S|\Pi_j^A}$ are the post measurement states with probability p_i due to the application of projective measurements ($\{\Pi_j\}$) on the part A of the Choi matrix ρ_{SA}. Application of projective measurements on the A, the average post measurement state will be of the form of QC state, i.e.,

$$\rho_{QC} = \sum_i p_i \rho_Q^i \otimes |i\rangle\langle i|_C, \tag{6.29}$$

where ρ^i are not orthogonal. Therefore, the classical correlations of the state ρ_{SA} should be equivalent to the maximum possible mutual information of ρ_{QC}, i.e., $J = I(\rho_{QC}) = S(\sum_i p_i \rho_i) - \sum_i p_i S(\rho_i)$, therefore, the classical correlations is nothing but the Holevo quantity. Hence, the Holevo quantity of a channel is equal to the classical correlations of its Choi matrix [191].

The classical correlation, i.e., the Holevo quantity is bounded by the relation $\chi(\Phi) \leqslant \log d$. This observation leads us to derive a complementarity between the relative entropy of coherence and the Holevo quantity of a channel.

Theorem – The complementarity relation between the Holevo quantity and the channel coherence is given by

$$C_r(\Phi) + \chi(\Phi) \leqslant 2 \log d, \tag{6.30}$$

where d is the dimension of the system $B(A)$.

Proof. Under state-channel duality, we have [60–62]

$$\rho_{AB} = (\Phi \otimes \mathbb{I})|\Psi\rangle_{AB}\langle\Psi| \equiv \Phi(|\Psi\rangle_{AB}). \tag{6.31}$$

The relative entropy of coherence for ρ_{AB} is defined in the basis $\{|\mu_i\rangle|i\rangle\}$, where $\{|\mu\rangle\}$ is eigen basis of ρ_A and $\{|i\rangle\}$ is the basis in which a rank one projective measurement is performed on B. Therefore, we have

$$C_r(\rho_{AB}) = S(\rho_{AB}^D) - S(\rho_{AB}). \tag{6.32}$$

The Holevo quantity or the classical correlation is given by

$$\chi(\Phi) = J(\rho_{AB}) = S(\rho_A) + S(\rho_B^D) - S(\rho_{AB}^D), \tag{6.33}$$

where $S(\rho_{AB}^D) = \sum_i (\mathbb{I} \otimes \Pi_i)\rho_{AB}(\mathbb{I} \otimes \Pi_i)$ with $\Pi_i = |i\rangle\langle i|$. Thus we have

$$C_r(\rho_{AB}) + \chi(\Phi) = S(\rho_A) + S(\rho_B^D) - S(\rho_{AB}). \tag{6.34}$$

Using the triangle inequality for $S(\rho_{AB})$, i.e., $S(\rho_{AB}) \geq S(\rho_A) - S(\rho_B)$, and the fact that $S(\rho_B) \leq \log d$ and $S(\rho_B^D) \leq \log d$, we have

$$C_r(\rho_{AB}) + \chi(\Phi) \leq 2 \log d. \tag{6.35}$$

Hence the proof. □

The above relation shows that the more coherence a channel has, the less will be its Holevo quantity.

6.6 Discussion

The significance of this chapter is three fold: Choi-Jamiołkowski isomorphism allows us to associate a density matrix with a channel. The purity and coherence of this density matrix can be fruitfully associated with the channel. Using CoPu diagrams it may be possible to distinguish different qubit channels. Distinguishing the channels using CoPu diagrams depicts the inter-relation between purity and the coherence of the channels. It has a broader meaning also, e.g., given a purity one may not find a channel which has certain amount of coherence. These relations between coherence and purity show deeper restriction on available coherent channel.

If we look closely, we find that the purity and coherence satisfy the following equation in some of the cases, i.e.,

$$\varpi\mathcal{P} - \varphi C_{l1}^2 = 1, \tag{6.36}$$

where $\varpi, \varphi \in \mathbb{R}$.

We can rewrite this as,

$$\left(\sqrt{\frac{\varpi}{\varphi}}\sqrt{\mathcal{P}}\right)^2 - (C_{l1})^2 = \left(\frac{1}{\sqrt{\varphi}}\right)^2. \tag{6.37}$$

This expression can have an interesting interpretation. We can think of scaled $\sqrt{\mathcal{P}}$ as time component, and coherence as the spatial component of a vector in two-dimensional Minkowski space. This vector is timelike.

Boundaries of light cone are given by the following relation

$$\left(\frac{C_{l1}}{\sqrt{\mathcal{P}}}\right)^2 = \frac{\varpi}{\varphi}. \tag{6.38}$$

In general, $\frac{C_{l1}}{\sqrt{\mathcal{P}}} \leq \pm\sqrt{\frac{\varpi}{\varphi}}$. Physically, this means that the allowed regions in CoPu diagrams are restricted by the above relation. The values are further constrained by (6.37) and lie inside hyperbolas within the above light cone boundaries.

Secondly, the CoPu diagram can help us in distinguishing different qubit channels, e.g., the unital and nonunital, the incoherent channels, degradable and antidegradable, Pauli channels, etc. These studies unveil very interesting properties of these channels. For example, we find that the qubit incoherent channels can either be unital or nonunital with $\vec{\tau} = \{0, 0, \tau_z\}$. We also find that all coherence breaking channels has zero coherence. However, this is not usually true for entanglement breaking channels. We observe that the coherence preserving qubit channels have unit coherence.

Thirdly, we find a complimentarity relation between relative entropy of coherence and the Holevo quantity of the channel. It says that if channel has more coherence, the Holevo quantity of the channel will be restricted. Naturally, this relation is very much important in quantum information processing tasks.

Although the main focus of this chapter is to study the single qubit coherence, it will be interesting to extend these results to higher dimensional systems. There are many indications in this chapter how one might be able to do it.

Summary

In this thesis, we have studied characterization and quantification of entanglement and coherence in a bipartite and multipartite scenario. Here we give a brief summary of each chapter.

In the introduction chapter, we have briefly surveyed the existing literature about the characterization and quantification of entanglement and coherence.

For a two-qubit pure state characterization and quantification of entanglement is well understood. However, this is not the case for a two-qubit mixed state. The violation of Bell inequality guarantees the presence of entanglement in a system. Optimal Bell-CHSH value for a two-qubit pure state only depends on entanglement. However, this is not the case for a two-qubit mixed state. It is a common consensus that optimal Bell-CHSH value for a two-qubit mixed state can be characterized by purity and entanglement. In the second chapter we have illustrated that purity and concurrence (a measure of entanglement) are not good enough to characterize optimal Bell-CHSH value. We required other functions of state parameters to completely characterize optimal Bell-CHSH value.

In the third chapter, we have proposed a possible way to quantify entanglement in a two-qudit system. To do this we have used Bell-SLK inequality. For a two-qudit pure state we have found a nice relation between Bell-SLK function and entanglement as characterized by negativity. This relation provides an operational way to detect and measure entanglement. Moreover, we have shown that this scheme can be useful to quantify and measure entanglement of some classes of mixed states. The proposed scheme is not only experimentally feasible but is also superior to the conventional schemes like state tomography.

In the next chapter, we have discussed the classification of six SLOCC classes of three-qubit pure states. Using Pauli matrices we have constructed a few observables which can completely distinguish these classes from each other. As these operators are constructed from Pauli matrices and have a very simple structure, they are easily implementable in an experiment. Moreover, we have provided a method to construct these observables in any

basis. We have also discussed the usefulness of these observables for some classes of three-qubit mixed states. By considering the teleportaion scheme of Lee et. al [166], we have also shown that the teleportation fidelity can be measured using these observables.

In the fifth chapter, we have explored the possible connection between coherence and steering in a three-qubit state. We have discussed a three-qubit steering scenario where Alice cannot be steered independently either by Bob or Charlie but rather only if they steer together. Using coherence of steered party, we have constructed some coherence steerability criterias which are useful to identify such set of states.

In the final chapter, we have defined coherence of a quantum channel using Choi-Jamiołlkowski isomorphism. For a fixed purity we find out the allowed range of coherence and plotted them in coherence-purity diagram. Using coherence-purity diagram, one can distinguish quiet a few qubit channels. Moreover, we have also discussed coherence of different incoherent channels. From coherence purity diagram we can verify a well-known fact about different incoherent operations, i.e., $PIO \subset SIO \subset IO$. Furthermore, we have derived a complementarity relation between relative entropy of coherence and Holevo quantity of the channel.

Bibliography

[1] A. Einstein, B. Podolsky, and N. Rosen, *Phys. Rev.* **47**, 777 (1935).

[2] E. Schrödinger, in *Mathematical Proceedings of the Cambridge Philosophical Society*, Vol. **31** (Cambridge University Press, 1935) pp. 555.

[3] J. S. Bell, *Physics* **1**, 195 (1964); J. S. Bell, *Rev. Mod. Phys.* **38**, 447 (1966).

[4] A. K. Ekert, *Phys. Rev. Lett.* **67**, 661, (1991).

[5] C. H. Bennett, G. Brassard, C. Crépeau, R. Jozsa, A. Peres, and W. K. Wootters, *Phys. Rev. Lett.* **70**, 1895 (1993).

[6] C. H. Bennett, and S. J. Wiesner, *Phys. Rev. Lett.* **69**, 2881 (1992).

[7] A. Ekert and C. Macchiavello, *Phys. Rev. Lett.* **77**, 2585 (1996).

[8] C. H. Bennett, D. P. DiVincenzo, J. A. Smolin, and W. K. Wootters, *Phys. Rev. A* **54**, 3824 (1996).

[9] J. Åberg, *arXiv:*quant-ph/0612146 (2006).

[10] A. Streltsov, G. Adesso, and M. B. Plenio, *Rev. Mod. Phys.* **89**, 041003 (2017).

[11] E. Biham, G. Brassard, D. Kenigsberg, and T. Mor, *Theo. Com. Sci.* **320**, 15 (2004).

[12] H.-L. Shi, S.-Y. Liu, X.-H. Wang, W.-L. Yang, Z.-Y. Yang, and H. Fan, *Phys. Rev. A* **95**, 032307 (2017); M. Hillery, *Phys. Rev. A* **93**, 012111 (2016).

[13] V. Giovannetti, S. Lloyd, and L. Maccone, *Nat. Photonics* **5**, 222 (2011).

[14] M. Lostaglio, D. Jennings, and T. Rudolph, *Nat. Commun.* **6**, 6383 (2015); V. Narasimhachar and G. Gour, *Nat. Commun.* **6**, 7689 (2015); P. Ćwikliński, M. Studziński, M. Horodecki, and J. Oppenheim, *Phys. Rev. Lett.* **115**, 210403 (2015); M. Lostaglio, D. Jennings, and T. Rudolph, *New J. Phys.* **19**, 043008 (2017).

[15] M. B. Plenio and S. F. Huelga, *New J. Phys.* **10**, 113019 (2008); S. Lloyd, *J. Phys.: Conf. Ser.* **302**, 012037 (2011); F. Levi and F. Mintert, *New J. Phys.* **16**, 033007 (2014).

[16] M. A. Nielsen, and I. L. Chuang, *Quantum Computation and Quantum Information*, Cambridge University Press, Cambridge, England (2000).

[17] R. Horodecki, P. Horodecki, M. Horodecki, and K. Horodecki, *Rev. Mod. Phys.* **81**, 865 (2009).

[18] A. Peres, *Phys. Rev. Lett.* **77**, 1413 (1996).

[19] M. Horodecki, P. Horodecki, and R. Horodecki, *Phys. Lett. A* **223**, 1 (1996).

[20] P. Horodecki, *Phys. Lett. A* **232**, 333 (1997).

[21] M. Horodecki, P. Horodecki, and R. Horodecki, *Phys. Rev. Lett.* **80**, 5239 (1998).

[22] N. J. Cerf, C. Adami, and R. M. Gingrich, *Phys. Rev. A* **60**, 898 (1999).

[23] M. Horodecki, and P. Horodecki, *Phys. Rev. A* **59**, 4206 (1999).

[24] H.-P. Breuer, *Phys. Rev. Lett.* **97**, 080501 (2006).

[25] W. Hall, *arXiv:*quant-ph/0607035 (2006).

[26] H.-P. Breuer, *J. Phys. A* **39**, 11847 (2006).

[27] C. H. Bennett, D. P. DiVincenzo, T. Mor, P. W. Shor, J. A. Smolin, and B. M. Terhal, *Phys. Rev. Lett.* **82**, 5385 (1999).

[28] D. P. DiVincenzo, T. Mor, P. W. Shor, J. A. Smolin, and B. M. Terhal, *Commun. Math. Phys.* **238**, 379 (2003).

[29] K. Chen, and L.-A. Wu, *Quantum Inf. Comput.***3**, 193 (2003).

[30] O. Rudolph, *J. Phys. A* **36**, 5825 (2003).

[31] M. Horodecki, P. Horodecki, and R. Horodecki, *Open Syst. Inf. Dyn.* **13**, 103 (2006).

[32] B. M. Terhal, *Phys. Lett. A* **271**, 319 (2000).

[33] B. M. Terhal, and P. Horodecki, *Phys. Rev. A* **61**, 040301 (2000).

[34] G. Vidal, W. Dür, and J. I. Cirac, *Phys. Rev.Lett.* **89**, 027901 (2002).

[35] K. Audenaert, M. B. Plenio, and J. Eisert, *Phys. Rev. Lett.* **90** 027901 (2003).

[36] E. M. Rains, *arXiv:*quant-ph/9809078 (1998).

[37] M. B. Plenio, and S. Virmani,*Quantum Inf. Comput.* **7**, 1 (2006).

[38] V. Vedral, M. B. Plenio, M. A Rippin, and P. L. Knight, *Phys. Rev. Lett.* **78**, 2275 (1997).

[39] V. Vedral, and M. B. Plenio, *Phys. Rev. A* **57**, 1619 (1998).

[40] M. Horodecki, P. Horodecki, and R. Horodecki, *Phys. Rev. Lett.* **84**, 2014 (2000).

[41] G. Vidal, *J. Mod. Opt.* **47**, 355 (2000).

[42] A. Uhlmann, *Rep. Math. Phys.* **9**, 273 (1976).

[43] R. Jozsa, *J. Mod. Opt.* **41**, 2315 (1994).

[44] C. H. Bennett, D. P. DiVincenzo, J. A. Smolin, and W. K. Wootters, *Phys. Rev. A* **54**, 3824 (1996).

[45] A. Uhlmann, *Open Syst. Inf. Dyn.* **5**, 209 (1998).

[46] A. Sanpera, D. Bruß, and M. Lewenstein, *Phys. Rev. A* **63**, 050301 (2001).

[47] S. Hill, and W. K. Wootters, *Phys. Rev. Lett.* **78**, 5022 (1997).

[48] W. K. Wootters, *Phys. Rev. Lett.* **80**, 2245 (1998).

[49] K. Audenaert, F. Verstraete, and B. De Moor, *Phys. Rev. A* **64**, 052304 (2001).

[50] P. Rungta, V. Buzek, C. M. Caves, M. Hillery, and G. J. Milburn, *Phys. Rev. A* **64**, 042315 (2001).

[51] F. Mintert, M. Kuś, and A. Buchleitner, *Phys. Rev. Lett.* **92**, 167902 (2004).

[52] K. Życzkowski, P. Horodecki, A. Sanpera, and M. Lewenstein, *Phys. Rev. A* **58**, 883 (1998).

[53] G. Vidal, and R. F. Werner, *Phys. Rev. A* **65**, 032314 (2002).

[54] W. Dür and J. I. Cirac, *Phys. Rev. A* **61**, 042314 (2000).

[55] V. Vedral, M. B. Plenio, K. Jacobs, and P. L. Knight, *Phys. Rev. A* **56**, 4452 (1997).

[56] A. V. Thapliyal, *Phys. Rev. A* **59**, 3336 (1999).

[57] W. Dür, G. Vidal, and J. I. Cirac, *Phys. Rev. A* **62**, 062314 (2000).

[58] F. Verstraete, J. Dehaene, B. De Moor, and H. Verschelde, *Phys. Rev. A* **65**, 052112 (2002).

[59] M. Horodecki, P. Horodecki, and R. Horodecki, *Phys. Lett. A* **283**, 1 (2001).

[60] A. Jamiołlkowski, *Rep. Math. Phys.* **3**, 275 (1972); M.-D. Choi, *Proc. Symp. Pure Math.* **38**, 583 (1982).

[61] A. S. Holevo, *Russ. Math. Surv.* **53**, 1295 (1998).

[62] M. B. Ruskai, S. Szarek, and E. Werner, *Lin. Alg. Appl.* **347**, 159 (2002).

[63] V. Coffman, J. Kundu, and W. K. Wootters, *Phys. Rev. A* **61**, 052306 (2000).

[64] A. Miyake, *Phys. Rev. A* **67**, 012108 (2003).

[65] R. Lohmayer, A. Osterloh, J. Siewert, and A. Uhlmann, *Phys. Rev. Lett.* **97**, 260502 (2006).

[66] J. Eisert, and H. J. Briegel, *Phys. Rev. A* **64**, 022306 (2001).

[67] F. Verstraete, J. Dehaene, and B. De Moor, *Phys. Rev. A* **68**, 012103 (2003).

[68] A. Miyake, *Int. J. Quantum Inf.* **2**, 65 (2004).

[69] P. Levay, *J. Phys. A* **39**, 9533 (2006).

[70] H. Barnum, and N. Linden, *J. Phys. A* **34**, 6787 (2001).

[71] A. Wong, and N. Christensen, *Phys. Rev. A* **63**, 044301 (2001).

[72] A. Osterloh, and J. Siewert, *Phys. Rev. A* **72**, 012337 (2005); A. Osterloh, and J. Siewert, *Int. J. Quantum Inf.* **4**, 531 (2006).

[73] H.-K. Lo, and S. Popescu, *Phys. Rev. A* **63**, 022301 (2001).

[74] M. A. Nielsen, *Phys. Rev. Lett.* **83**, 436 (1999).

[75] G Vidal, *J. Mod. Opt*. **47**, 355 (2000).

[76] C. H. Bennett, S. Popescu, D. Rohrlich, J. A. Smolin, and A. V. Thapliyal, *Phys. Rev. A* **63**, 012307 (2000).

[77] N. Brunner, D. Cavalcanti, S. Pironio, V. Scarani, and S. Wehner, *Rev. Mod. Phys.* **86**, 419 (2014).

[78] J. F. Clauser, M. A. Horne, A. Shimony, and R. A. Holt, *Phys. Rev. Lett.* **23**, 880 (1969).

[79] S. J. Freedman , and J. F. Clauser, *Phys. Rev. Lett.* **28**, 938 (1972).

[80] J. F. Clauser, and M. A. Horne, *Phys. Rev. D* **10**, 526 (1974).

[81] A. Aspect, P. Grangier, and G. Roger, *Phys. Rev. Lett.* **49**, 91 (1982).

[82] W. Tittel, J. Brendel, H. Zbinden, and N. Gisin, *Phys. Rev. Lett.* **81**, 3563 (1998).

[83] B. Hensen et al., *Nature* **526**, 682 (2015).

[84] M. Giustina et al., *Phys. Rev. Lett.* **115**, 250401 (2015).

[85] L. K. Shalm et al., *Phys. Rev. Lett.* **115**, 250402 (2015).

[86] I. Pitowsky, Quantum Probability — Quantum Logic, *Lecture Notes in Physics* **321**, (1989).

[87] D. Collins, N. Gisin, N. Linden, S. Massar, and S. Popescu, *Phys. Rev. Lett.* **88**, 040404 (2002).

[88] L. Masanes, *Quantum Inf. Comput.* Vol. **3**, No. 4, 345 (2003).

[89] A. Acín, T. Durt, N. Gisin and J. I. Latorre, *Phys. Rev. A* **65**, 052325 (2002).

[90] W. Son, J. Lee, and M. S. Kim, *Phys. Rev. Lett.* **96**, 060406 (2006).

[91] S.-W. Lee, Y. W. Cheong, and J. Lee, *Phys. Rev. A* **76**, 032108 (2007).

[92] H. M. Wiseman, S. J. Jones, and A. C. Doherty, *Phys. Rev. Lett.* **98**, 140402 (2007).

[93] J. Bowles, T. Vértesi, M. T. Quintino, and N. Brunner, *Phys. Rev. Lett.* **112**, 200402 (2014).

[94] M. T. Quintino, T Vértesi, D. Cavalcanti, R. Augusiak, M. Demianowicz, A. Acín, and N. Brunner, *Phys. Rev. A* **92**, 032107 (2015).

[95] E. G. Cavalcanti, S. J. Jones, H. M. Wiseman, and M. D. Reid, *Phys. Rev. A* **80**, 032112 (2009).

[96] S. P. Walborn, A. Salles, R. M. Gomes, F. Toscano, and P. H. Souto Ribeiro, *Phys. Rev. Lett.* **106**, 130402 (2011).

[97] E. G. Cavalcanti, C. J. Foster, M. Fuwa, and H. M. Wiseman, *J. Opt. Soc. Am. B* **32**, A74 (2015).

[98] D. J. Saunders, S. J. Jones, H. M. Wiseman, and G. J. Pryde, *Nat. Phys.* **6**, 845 (2010).

[99] P. Skrzypczyk, and D. Cavalcanti, *Phys. Rev. A* **92** 022354 (2015).

[100] D. Cavalcanti, and P. Skrzypczyk, *Rep. Prog. Phys.* **80** 024001 (2017).

[101] Q. Y. He, and M. D. Reid *Phys. Rev. Lett.* **111**, 250403 (2013).

[102] D. Cavalcanti, P. Skrzypczyk, G. H. Aguilar, R. V. Nery, P. H. S. Ribeiro, and S. P. Walborn, *Nat. Commun.* **6** 7941 (2015).

[103] K. Kraus, *States, Effects and Operations: Fundamental Notions of Quantum Theory* (Springer-Verlag, Berlin) 1983.

[104] C. King and M. B. Ruskai, *IEEE Trans. Info. Theory* **47**, 192 (2001).

[105] D. Braun, O. Giraud, I. Nechita1, C. Pellegrini, and M. Žnidarič, *J. of Phys. A: Math. and Theo.* **47**, 135302 (2014).

[106] T. Baumgratz, M. Cramer, and M. B. Plenio, *Phys. Rev. Lett.* **113**, 140401 (2014).

[107] E. Chitambar and G. Gour, Phys. Rev. Lett. **117**, 030401 (2016).

[108] I. Marvian and R. W. Spekkens, Phys. Rev. A **90**, 062110 (2014).

[109] J. I. de Vicente and A. Streltsov, J. Phys. A **50**, 045301 (2017).

[110] T. R. Bromley, M. Cianciaruso, and G. Adesso, *Phys. Rev. Lett.* **114**, 210401 (2015).

[111] A. Streltsov, U. Singh, H. S. Dhar,M. N. Bera, and G. Adesso, *Phys. Rev. Lett.* **115**, 020403 (2015).

[112] F. Levi, and F. Mintert, *New J. Phys.* **16**, 033007 (2014).

[113] X. Yuan, H. Zhou, Z. Cao, and X. Ma, *Phys. Rev. A* **92**, 022124 (2015).

[114] A. Winter, and D. Yang, *Phys. Rev. Lett.* **116**, 120404 (2016).

[115] G. Gour, I. Marvian, and R.W. Spekkens, *Phys. Rev. A* **80**, 012307 (2009).

[116] X. Qi, T. Gao, and F. Yan, *J. Phys. A: Math. Theor.* **50**, 285301 (2017).

[117] B. Yadin, J. Ma, D. Girolami, M. Gu, and V. Vedral, *Phys. Rev. X* **6**, 041028 (2016).

[118] E. Chitambar and G. Gour, *Phys. Rev. A* **94**, 052336 (2016).

[119] E. Chitambar and G. Gour, *Phys. Rev. A* **95**, 019902(E) (2017).

[120] Y. Peng, Y. Jiang, and H. Fan, *Phys. Rev. A* **93**, 032326 (2016).

[121] N. Gisin, *Phys. Lett. A* **154**, 201 (1991).

[122] K. Fukuda, cdd/cdd+ Reference Manual, Swiss Federal Institute of Technology Institute, ETH-Zentrum.

[123] B. S. Tsirelson, *Lett. Math. Phys.* **4**, 93 (1980).

[124] S. Popescu, and D. Rohrlich, *Found. Phys.* **24**, 379 (1994).

[125] V. Scarani, *Acta Physica Slovaca* **62**, 347 (2012).

[126] R. Horodecki, M. Horodecki, and P. Horodecki, *Phys. Lett. A* **200**, 340 (1995).

[127] P. E. M. F. Mendonça, M. A. Marchiolli, and D. Galetti, *Ann. Phys* **351**, 79 (2014).

[128] Sumit Nandi, Chandan Datta, Arpan Das, and Pankaj Agrawal, Submitted to *European Physics Journal D*.

[129] H. Bechmann-Pasquinucci, and A. Peres, *Phys. Rev. Lett.* **85**, 3313 (2000); D. Bruß, and C. Macchiavello, *Phys. Rev. Lett.* **88**, 127901 (2002); T. Durt, N. J. Cerf, N. Gisin, and M. Zukowski, *Phys. Rev. A* **67**, 012311 (2003); T. Durt, D. Kaszlikowski, J. L. Chen, and L. C. Kwek, *Phys. Rev. A* **69**, 032313 (2004).

[130] C. Wang, F.-G. Deng, Y.-S. Li, X.-S. Liu, and G. L. Long, *Phys. Rev. A* **71**, 044305 (2005).

[131] M. L. Almeida, S. Pironio, J. Barrett, G. Toth, and A. Acin, *Phys. Rev. Lett.* **99**, 040403 (2007); L. Sheridan, and V. Scarani, *Phys. Rev. A* **82**, 030301 (2010).

[132] N. Gisin, and A. Peres, *Phys. Lett. A* **162**, 15 (1992).

[133] S.-W. Lee, J. Ryu, and J. Lee, *Journal of the Korean Physical Society*, Vol. **48**, No. 6, 1307 (2006).

[134] A. C. Dada, J. Leach, G. S. Buller, M. J. Padgett, and E. Andersson, *Nature Physics* **7**, 677 (2011).

[135] H.-P. Lo *et al.*, *Sci. Rep.* **6**, 22088 (2016).

[136] C. Bernhard, B. Bessire, A. Montina, M. Pfaffhauser, A. Stefanov, and S. Wolf, *J. Phys A: Math. Theor.* **47**, 424013 (15pp) (2014).

[137] J.-L. Chen, D.-L. Deng, and M.-G. Hu, *Phys. Rev. A* **77**, 060306(R) (2008).

[138] N. J. Cerf, S. Massar and S. Pironio, *Phys. Rev. Lett.* **89**, 080402 (2002).

[139] T. Durt, D. Kaszlikowski, and M. Zukowski, *Phys. Rev. A* **64**, 024101 (2001).

[140] H. A. Hassan, *J. Math. Anal. Appl.* **339**, 811 (2008).

[141] I. S. Gradshteyn, and I. M. Ryzhik, *Table of integrals, series, and products.* 7th ed. Academic Press, page 36.

[142] T. M. Apostol, On the Lerch Zeta Function. *Pacific J. Math.* **1951**, 1, 161-167.

[143] B. C. Berndt, and B. P. Yeap, *Adv. Appl. Math.* **29**, 358 (2002).

[144] P. Rungta, W.J. Munro, K. Nemoto, P. Deuar, G.J. Milburn, and C.M. Caves, in *Directions in Quantum Optics: A Collection of Papers Dedicated to the Memory of Dan Walls*, edited by H.J. Carmichael, R.J. Glauber, and M.O. Scully (Springer, Berlin, 2001), p. 149.

[145] M. Ramzan, and M. K. Khan, *Quant. Inf. Process.* **11**, 443 (2012); G. Jaeger, and K. Ann, *J. Mod. Opt.* **54**, 2327 (2007).

[146] A.Vaziri, G.Weihs, and A. Zeilinger, *J. Opt. B Quantum Semiclassical Opt.* Vol. **4**, 47 (2002).

[147] A. Mair, A. Vaziri, G. Weihs, and A. Zeilinger, *Nature*(London) **412**, 313 (2001).

[148] D. F. V. James, P. G. Kwiat, W. J. Munro, and A. G. White, *Phys. Rev. A* **64**, 052312 (2001); M. Cramer et al., *Nat. Commun.* **1**, 149 (2010); M. Mohammadi, A. M. Brańczyk, and D. F. V. James, *Phys. Rev. A* **87**, 012117 (2013); T. Jullien et al., *Nat. Lett.* **514**, 603 (2014).

[149] A. G. White, D. F. V. James, P. H. Eberhard, and P. G. Kwiat, *Phys. Rev. Lett* **83**, 3103 (1999); J. M. G. Sancho and S. F. Huelga, *Phys. Rev. A* **61**, 042303 (2000); W. Laskowski, D. Richart, C. Schwemmer, T. Paterek, and H. Weinfurter, *Phys. Rev. Lett* **108**, 240501 (2012).

[150] J. T. Barreiro et al., *Nat. Phys.* **9**, 559 (2013).

[151] P. Horodecki, *Phys. Rev. Lett* **90**, 167901 (2003); F. Mintert, M. Kuś, and A. Buchleitner, *Phys. Rev. Lett* **95**, 260502 (2005); S. P. Walborn, P. H. Souto Ribeiro, L. Davidovich, F. Mintert and A. Buchleitner, *Nat. Lett.* **440**, 1022 (2006).

[152] D. Giovannini, J. Romero, J. Leach, A. Dudley, A. Forbes, and M. J. Padgett, *Phys. Rev. Lett* **110**, 143601 (2013); J. Chen, H. Dawkins, Z. Ji, N. Johnston, D. Kribs, F. Shultz, and B. Zeng, *Phys. Rev. A* **88**, 012109 (2013); F. Tonolini, S. Chan, M. Agnew, A. Lindsay and J. Leach, *Sci. Rep.* **4**, 6542 (2014).

[153] R. T. Thew, K. Nemoto, A. G. White, and W. J. Munro, *Phys. Rev. A* **66**, 012303 (2002).

[154] D. Gross, Y.-K. Liu, S. T. Flammia, S. Becker, J. Eisert, *Phys. Rev. Lett.* **105**, 150401 (2010); S. T Flammia, D. Gross, Y. -K. Liu, J. Eisert, *New J. Phys.* **14**, 095022 (2012); T. B. Jackson, M. Sc. Thesis, Univ. of Guelph, Chap. 2, (2013).

[155] C. H. Bennett, H. J. Bernstein, S. Popescu, and B. Schumacher, *Phys. Rev. A* **53**, 2046 (1996).

[156] N. Linden, S. Popescu, B. Schumacher, and M. Westmoreland, e-print quant-ph/**9912039** unpublished; G. Vidal, W. Dür,and J. I. Cirac, *Phys. Rev. Lett.* **85**, 658 (2000); S.Wu and Y. Zhang, *Phys. Rev. A* **63**, 012308 (2000).

[157] A. Das, C. Datta, and P. Agrawal, *Phys. Lett. A* **381**, 3928 (2017).

[158] M.-J. Zhao, T.-G. Zhang, X. Li-Jost and S.- M. Fei, *Phys. Rev. A* **87**, 012316 (2013).

[159] A. Acín, A. Andrianov, E. Jané, and R. Tarrach, *J. Phys. A: Math. Gen.* **34**, 6725 (2001).

[160] A. Acín, D. Bruss, M. Lewenstein, and A. Sanpera, *Phys. Rev. Lett.* **87**, 040401 (2001).

[161] D. P. Chi, K. Jeong, T. Kim, K. Lee, and S. Lee, *Phys. Rev. A* **81**, 044302 (2010).

[162] S. Adhikari, and A. S. Majumdar, *arXiv:*1602.02619, (2016).

[163] A. Acín, A. Andrianov, L. Costa, E. Jané, J. I. Latorre, and R. Tarrach, *Phys. Rev. Lett.* **85**, 1560 (2000).

[164] F. Mintert, and A. Buchleitner, *Phys. Rev. Lett.* **98**, 140505 (2007).

[165] O. J. Farías, G. H. Aguilar, A. V.-Hernández, P. H. S. Ribeiro, L. Davidovich, and S. P. Walborn, *Phys. Rev. Lett.* **109**, 150403 (2012).

[166] S. Lee, J. Joo, and J. Kim, *Phys. Rev. A* **72**, 024302 (2005).

[167] S. Popescu, *Phys. Rev. Lett.* **72**, 797 (1994); S. Massar and S. Popescu, *Phys. Rev. Lett.* **74**, 1259 (1995).

[168] A. Singh, H. Singh, K. Dorai, and Arvind, *arXiv:*1804.09320, (2018).

[169] S. Kochen and E. P. Specker, *Journal of Mathematics and Mechanics* **17**, 59 (1967).

[170] A. Cabello, S. Severini, and A. Winter, *Phys. Rev. Lett.* **112**, 040401 (2014).

[171] M. Koashi and A. Winter, *Phys. Rev. A* **69**, 022309 (2004).

[172] M. P. Seevinck, *Quant. Inf. Proc.* **9**, 273 (2010).

[173] M. Pawłowski and C. Brukner, *Phys. Rev. Lett.* **102**, 030403 (2009).

[174] P. Kurzyński, T. Paterek, R. Ramanathan, W. Laskowski, and D. Kaszlikowski, *Phys. Rev. Lett.* **106**, 180402 (2011).

[175] M. Pawłowski, *Phys. Rev. A* **82**, 032313 (2010).

[176] J. Singh, K. Bharti, and Arvind, *Phys. Rev. A* **95**, 062333 (2017).

[177] M. D. Reid, *Phys. Rev. A* **88**, 062108 (2013).

[178] A. Milne, S. Jevtic, D. Jennings, H. Wiseman, and T. Rudolph, *New J. of Phys.* **16**, 083017 (2014).

[179] M. B. Plenio and S. S. Virmani, An Introduction to Entanglement Theory Springer International Publishing, Cham, 173 (2014).

[180] D. Mondal, T. Pramanik, and A. K. Pati, *Phys. Rev. A* **95**, 010301 (2017).

[181] D. Mondal and D. Kaszlikowski, *arXiv*:1711.02612 (2017).

[182] M. Ziman and V. Bužek, *Phys. Rev. A* **72**, 052325 (2005).

[183] K. Bu, Swati, U. Singh, and J. Wu, *Phys. Rev. A* **94**, 052335 (2016).

[184] A. Streltsov, S. Rana, P. Boes, and J. Eisert, *Phys. Rev. Lett.* **119**, 140402 (2017).

[185] H.-L. Shi, X.-H. Wang, S.-Y. Liu, W.-L. Yang, Z.-Y. Yang, and H. Fan, *Sci. Rep.* **7**, 14806 (2017).

[186] X. Hu, *Phys. Rev. A* **94**, 012326 (2016).

[187] F. Caruso, V. Giovannetti, C. Lupo, and S. Mancini, *Rev. Mod. Phys.* **86**, 1203 (2014).

[188] F. Pan, L. Qiu, and Z. Liu, *Sci. Rep.* **7**, 43919 (2016).

[189] A. K. Goswami and P. K. Panigrahi, *arXiv*:1703.08700 (2017).

[190] L. Henderson and V. Vedral, *J. Phys. A: Math. Gen.* **34**, 6899 (2001).

[191] M. Zwolak and W. H. Zurek, *Sci. Rep.* **3**, 1729 (2013).